AD_____

Award Number: DAMD17-98-1-8223

TITLE: Developing Strategies to Block Beta-Catenin Action in Signaling and Cell Adhesion During Carcinogenesis

PRINCIPAL INVESTIGATOR: Mark A. Peifer, Ph.D.

CONTRACTING ORGANIZATION: University of North Carolina
Chapel Hill, North Carolina 27599-1350

REPORT DATE: July 2002

TYPE OF REPORT: Final

PREPARED FOR: U.S. Army Medical Research and Materiel Command
Fort Detrick, Maryland 21702-5012

REPORT DOCUMENTATION PAGE

Form Approved
OMB No. 074-0188

1. AGENCY USE ONLY (Leave blank)	2. REPORT DATE	3. REPORT TYPE AND DATES COVERED
	July 2002	Final (1 Jul 98 - 30 Jun 02)

4. TITLE AND SUBTITLE
Developing Strategies to Block Beta-Catenin Action in Signaling and Cell Adhesion During Carcinogenesis

5. FUNDING NUMBERS
DAMD17-98-1-8223

6. AUTHOR(S)
Mark A. Peifer, Ph.D.

7. PERFORMING ORGANIZATION NAME(S) AND ADDRESS(ES)
University of North Carolina
Chapel Hill, North Carolina 27599-1350

E-MAIL:
peifer@unc.edu

8. PERFORMING ORGANIZATION REPORT NUMBER

9. SPONSORING / MONITORING AGENCY NAME(S) AND ADDRESS(ES)
U.S. Army Medical Research and Materiel Command
Fort Detrick, Maryland 21702-5012

10. SPONSORING / MONITORING AGENCY REPORT NUMBER

11. SUPPLEMENTARY NOTES
report contains color

12a. DISTRIBUTION / AVAILABILITY STATEMENT
Approved for Public Release; Distribution Unlimited

12b. DISTRIBUTION CODE

13. ABSTRACT ***(Maximum 200 Words)***

To understand cancer, we must first understand normal cell behavior. *Drosophila* Armadillo (Arm) and its human homolog ß-catenin are key players in adhesive junctions and in transduction of Wingless (Wg)/Wnt signals. Our working hypotheses are: 1) Several protein partners compete to bind Arm, and 2) Arm:dTCF activates Wg-responsive genes, while dTCF alone represses the same genes. Aim 1 is to understand how different partners compete with one another for binding Arm. Aim 2 focuses on how Arm and dTCF positively and negatively regulate Wg-responsive genes. We made significant progress on both Aims. We used the two-hybrid system to further define the Arm binding site on DE-cadherin and extended our analysis of the effect of point mutations on binding. Our collaborators at the Weizmann Institute completed a parallel analysis in mammalian cells, assessing the ability of cadherin-derived peptides to compete ß-catenin from its endogenous partners. This work was published in Molecular Biology of the Cell. We have also introduced into transgenic flies mutant versions of DE-cadherin which should specifically block Arm or p120catenin binding. We characterized the role of TCF and Groucho in transcriptional repression of Wg-responsive genes. This work was published in Nature. We characterized the role of the C-terminus of Armadillo in transcriptional activation—this work was published in Genetics.

14. SUBJECT TERMS	15. NUMBER OF PAGES
breast cancer, cell adhesion, Wg/Wnt	45
	16. PRICE CODE

17. SECURITY CLASSIFICATION OF REPORT	18. SECURITY CLASSIFICATION OF THIS PAGE	19. SECURITY CLASSIFICATION OF ABSTRACT	20. LIMITATION OF ABSTRACT
Unclassified	Unclassified	Unclassified	Unlimited

FOREWORD

Opinions, interpretations, conclusions and recommendations are those of the author and are not necessarily endorsed by the U.S. Army.

X Where copyrighted material is quoted, permission has been obtained to use such material.

N/A Where material from documents designated for limited distribution is quoted, permission has been obtained to use the material.

N/A Citations of commercial organizations and trade names in this report do not constitute an official Department of Army endorsement or approval of the products or services of these organizations.

N/A In conducting research using animals, the investigator(s) adhered to the "Guide for the Care and Use of Laboratory Animals," prepared by the Committee on Care and use of Laboratory Animals of the Institute of Laboratory Resources, national Research Council (NIH Publication No. 86-23, Revised 1985).

X For the protection of human subjects, the investigator(s) adhered to policies of applicable Federal Law 45 CFR 46.

In conducting research utilizing recombinant DNA technology, the investigator(s) adhered to current guidelines promulgated by the National Institutes of Health.

In the conduct of research utilizing recombinant DNA, the investigator(s) adhered to the NIH Guidelines for Research Involving Recombinant DNA Molecules.

N/A In the conduct of research involving hazardous organisms, the investigator(s) adhered to the CDC-NIH Guide for Biosafety in Microbiological and Biomedical Laboratories.

Mary Q 7/22/02

PI - Signature Date

Table of Contents

(5) Introduction:

To understand abnormal cell behavior in cancer, we must first understand normal cell behavior. We focus on *Drosophila* Armadillo (Arm); Arm and its human homolog ß-catenin are critical for normal embryonic development (reviewed in Peifer, 1997). Both are key players in two separable biological processes: 1) They are components of cell-cell adhesive junctions, and 2) they act in transduction of Wingless/Wnt (Wg/Wnt) family cell-cell signals. Mutations in ß-catenin or its regulators are early steps in colon cancer and melanoma (reviewed in (Peifer and Polakis, 2000). We use the fruit fly as our model, combining classical and molecular genetics with cell biology and biochemistry. We take advantage of the speed and ease of the fly system and of its synergy with vertebrate cell biology. As one avenue to reveal Arm's roles in adherens junctions and transduction of Wg signal, we are identifying and examining the function of proteins with which Arm physically and/or functionally interacts. Our goal is to precisely define Arm/ß-catenin's dual roles, ultimately allowing the design of drugs inhibiting oncogenic ß-catenin. Our working hypotheses are: 1) Several protein partners compete to bind to the same site on Arm; the affinity of Arm for different partners is adjusted via phosphorylation of these partners, and 2) The Arm:dTCF complex activates Wg-responsive genes; dTCF represses the same genes in the absence of Arm. We will integrate approaches at all levels from combinatorial chemistry to studying gene function in intact animals, using fruit flies to carry out a functional genomics approach to understanding Arm function, and then transferring this knowledge directly to the mammalian system. Our first Aim is to understand how different partners interact with and compete with one another for binding Arm, and how phosphorylation regulates this. Our second Aim focuses on how the Arm and its partner dTCF positively and negatively regulate Wg responsive genes.

Specific Aim 1. Identify the sequence determinants mediating the binding of Armadillo/ß-catenin's protein partners to Armadillo/ß-catenin.

Specific Aim 2. Explore the mechanism of action of dTCF, a Wg/Wnt effector.

(6) Body:

This award is a combined IDEA Award and Career Development Award. The IDEA component ends this year, while the CDA continues for another year. In the three years of the IDEA Award, we made significant progress on both of our Specific Aims, which we have outlined below.

Aim 1.

Our statement of work stated:
Year 1
1. Minimize interacting regions of all three partners and begin mutagenesis.
2. Carry out two-hybrid screen for random peptides that interact with Arm.
3. Mutagenize & test in two-hybrid system potential phosphorylation sites.

Year 2
4. Complete mutational analysis of Arm targets in two hybrid system and test peptides in vivo.
5. Mutate potential phosphorylation sites in peptide models and test effects of GSK.

Year 3
6. Mutate regions required for Arm binding in the context of intact targets, reintroduce into flies and test for biological function.
7. Introduce peptides into cultured mammalian cells and test ability to bind ß-catenin and block its function.

NOTE: Much of the work described in this section was published in a paper from our lab in Molecular Biology of the Cell (Simcha et al., 2001)—below we refer to Figures in this paper, which was included in last year's Appendix.

We previously found that dAPC, DE-cadherin , and dTCF all can bind to a ~260 amino acid fragment comprising Arm's Arm repeats 3-8 (Pai et al., 1996; van de Wetering et al., 1997) McCartney et al., 1999). In the first two years of work under this grant, we minimized the region of the DE-cadherin cytoplasmic tail required for Arm binding, defined a 22 amino acid region that was sufficient, using the yeast two-hybrid system as an assay (task 1 in the statement of work; Fig. 1 of Simcha et al., (2001) in Appendix). We also defined two different 34 amino acid portions of dAPC2, containing a single 15 amino acid repeat or a single 20 amino acid repeat, as sufficient for binding Arm (McCartney et al., 1999). Because such small regions were sufficient, we have not

pursued screening for random peptides that bound Arm (task 2).

We further extended these observations by beginning to examine the sequence requirements for Arm binding, beginning our examination by focusing on the DE-cadherin target. We based these experiments on both the enrichment of acidic amino acids in all of the targets of Arm, and on a slight but intriguing sequence similarity between Arm's partners. In particular, the motif SLSSL is conserved in APC and cadherin. This is of special interest because vertebrate E-cadherin and APC are phosphorylated in this region, most likely on these serines. In APC, phosphorylation of these serines by GSK-3 enhances ß-catenin binding (Rubinfeld et al., 1996). In E-cadherin, serines in the region are phosphorylated by an unknown kinase; mutation of the serines to alanine blocks ß-catenin binding (Stappert and Kemler, 1994) . We thus made an extensive series of site-directed mutations of conserved residues (focusing in particular on acidic amino acids and on serines) within the minimal Arm binding region, including a small deletion and clustered point mutations (as outlined in tasks 1,3, and 4 of the statement of work; Fig. 5 of Simcha et al., (2001) in Appendix). These tests were initiated in year two and completed in the last year. To our surprise, many of these mutations do not block binding to Arm when tested in the context of the full length cadherin tail. This suggests that multiple points of contact may underlie binding and that changes in individual contact sites may not be sufficient to block the interaction. However, the more extensive changes do abolish binding, and some of the lesser changes reduce binding detectably, beginning to reveal key residues (Fig. 5 of Simcha et al., (2001) in Appendix).

To supplement this work using the yeast two-hybrid system, we are carrying out a collaboration with Avri Ben'Zeev of the Weizmann Institute in Israel. We provided a series of mutant cadherin constructs which they then tested in cultured mammalian cells, using a series of assays which they have developed for examining the ability of the E-cadherin cytoplasmic tail to block ß-catenin action (Sadot et al., 1998). They began this analysis in year two and have completed it in year 3. They have tested both our wild-type and mutant DE-cadherin constructs for their ability to bind to ß-catenin in mammalian cells, when expressed as GFP-fusion proteins (tasks 4,5, and 7). They examined the localization of these fusion proteins, their ability to block destruction of endogenous ß-catenin (by competing for ß-catenin binding with APC), their ability to block activation by the ß-catenin-TCF/LEF complex (by competing for ß-catenin binding with TCF/LEF), and their ability to block adherens junction formation (by competing for ß-catenin binding with-cadherin).

The results of these assays were quite revealing. First, we found that slightly longer portions of DE-cadherin are required in mammalian cells than are required in yeast, suggesting that competition with endogenous partners increases the stringency of the binding reaction Fig. 2-4 of Simcha et al., (2001) in Appendix). Second, we found that the effect of mutations was roughly parallel in yeast and in mammalian cells (with one exception), although all mutations tended to have a stronger effect in mammalian cells, likely due to competition with endogenous partners (Fig. 5-6 of Simcha et al., (2001) in Appendix). The exception was also quite revealing. While mutation of potential phosphorylation sites had little effect in yeast (Fig. 5 of Simcha et al., (2001) in Appendix), it resulted in striking reduction in binding in mammalian cells (Fig. 6 of Simcha et al., (2001) in Appendix), strongly supporting the idea that binding is normally regulated by phosphorylation (similar results were obtained by Lickert et al., (2000)). Finally, we found that different partners differ in their sensitivity to blockage by the cadherin peptide. The ß-catenin-TCF?LEF interaction is most sensitive to disruption, while the ß-catenin-E-cadherin interaction is least sensitive. The results of all of this work, both in yeast and in mammalian cells, were recently published in Molecular Biology of the Cell (Simcha et al., 2001), and the work from our lab in this paper was funded entirely by this IDEA Award. A copy is included in the Appendix, where the details of the methods used, the results, and their interpretation can be found.

While this manuscript was in preparation, a paper appeared that allowed us to carry our analysis to an even higher level. This paper reported the use of X-ray crystallography to solve the structure of a complex of *Xenopus* ß-catenin and Tcf3 (Graham et al., 2000). This thus revealed in atomic resolution how ß-catenin binds one of its partners. The authors also created a speculative model for how E-cadherin might bind ß-catenin. Using our mutagenesis data, we evaluated and extended this model, creating a detailed prediction of how E-cadherin might interact with its partner (Fig. 7 of Simcha et al., (2001) in Appendix). This model was subsequently tested by the recent publication of the structure of complex of ß-catenin and E-cadherin, also solved by X-ray crystallography (Huber and Weis, 2001). This will allow a further refinement of our understanding of how ß-catenin binds diverse partners. Together, the crystal structure, our studies, and other mutagenesis studies of ß-catenin's interaction with its partners (e.g., von Kries et al., 2000) will provide pharmaceutical companies with the insights they need to begin the rational design of inhibitors of interactions of ß-

catenin and its partners, which might have therapeutic value in cancer or other diseases.

With this information in hand, we have now turned our attention using what we learned about the interaction of Arm and DE-cadherin to blocking particular interactions of E-cadherin and its catenin partners, and examining the consequences of this in vivo. Cadherins directly interact with at least two different cytoplasmic partners, Arm and the distantly related protein p120catenin. In work funded by other sources, we have employed a similar strategy to that described above to define the p120 catenin-binding site of the DE-cadherin tail (Lu et al., 1999). We found that fly p120catenin binds to the juxta-membrane region, similar to its mammalian partners (Thoreson et al., 2000; Yap et al., 1998). We then mutagenized the DE-cadherin tail and found clustered point mutations that block p120catenin binding in yeast. We have now introduced mutations that block Arm binding, defined by our work described above, and mutations that block p120catenin binding, into the intact DE-cadherin gene (Task 6 of the Statement of Work). Three of the four mutants, along with a wild-type control, have been introduced into flies. We are now beginning to test the effects of over-expressing these constructs in a wild-type background and asking whether they can rescue animals mutant for DE-cadherin, in collaboration with Ulrich Tepass of the University of Toronto.

Aim 2. Armadillo:dTCF, a bipartite transcription factor

Year 1

1. Construct, introduce into flies and begin to test effects of *arm* mutants with C-termini replaced with known activation and repression domains.
2. Examine genetic interactions between *gro*, *wg* ,*arm* and *dTCF* mutations

Year 2

3. Complete analysis of *arm* -activation and repression domain fusions and initiate mutagenesis of Arm's C-terminus.
4. Examine physical interaction between Gro and dTCF in vitro and in vivo; Construct, introduce into flies and begin to test mutant forms of dTCF unable to bind Gro.

Year 3

5. Complete analysis of phenotypic consequences of mutations in Arm's C-terminus. Complete analyzing phenotype of mutant forms of dTCF unable to bind Gro.
6. Analyze the effects of mutant Arm constructs in cultured normal and transformed mammalian breast and colon epithelial cells.

In the three years of the IDEA Award, we made significant progress in our work on the role of Arm and dTCF in regulating Wg/Wnt responsive genes. As reported in the first annual report, in the first year, we explored in detail genetic and molecular interactions between *gro*, *wg* ,*arm* and *dTCF* (task 2 and 4 above)– this work was a collaboration with the labs of Amy Bejsovec at Northwestern and Hans Clevers at Utrecht. These data, together with a parallel analysis of the interaction between Groucho homologs and TCF/LEF proteins in mammalian cells, demonstrated that TCF proteins play a dual role in the regulation of Wg/Wnt target genes. In the absence of Wg/Wnt signaling, they act together with the co-repressor Groucho to repress Wg/Wnt responsive genes. The rise in Arm levels triggered by Wingless signaling converts this repressor into an activator, leading to the expression of Wg-target genes. This work was published in Nature (Cavallo et al., 1998); reprint included in first year).

In year two, we explored in more detail the role of Arm's C-terminus in Wg signaling (Tasks 1,3, and 5 of the Statement of Work). We found that C-terminally truncated mutant Armadillo has a deficit in Wg signaling activity, even when corrected for reduced protein levels. However, we also found that Armadillo proteins lacking all or part of the C-terminus retain some signaling ability if overexpressed, and that mutants lacking different portions of the C-terminal domain differ in their level of signaling ability. Finally, we found that the C-terminus plays a role in Armadillo protein stability in response to Wingless signal, and that the C-terminal domain can physically interact with the Arm repeat region. These data suggest that the C-terminal domain plays a complex role in Wingless signaling, and that Armadillo recruits the transcriptional machinery via multiple contact sites, which act in an additive fashion. These data were published in Genetics, with partial support from the IDEA Award (Cox et al., 1999); reprint included last year). While this work was underway, others examined the consequences of replacing the C-terminus of ß-catenin with the Engrailed repressor domain (Tasks 1 and 3 of Statement of Work), and showed that, as we had hypothesized, this repressed Wnt target genes (Montross et al., 2000). Two other groups delineated activation domains in ß-catenin and showed that a heterologous transactivator could mimic the properties of ß-catenin's C-terminus (Hsu et al., 1998; Vleminckx et al., 1999)

Career Development Award

The Career Development Award component of this grant paid a substantial portion of my salary (i.e., the PI, Mark Peifer). This substantially reduced the amount of time I had to devote to teaching and service, and thus allowed me to focus on research, both that funded by the Army and other research ongoing in my lab. I have thus acknowledged this support in additional publications produced during this period, which are listed in Section 8, and included reprints for new additions to this list (where available) in the Appendix.

(7) Key research accomplishments for the entire 3 years.

a) A 22 amino acid piece of DE-cadherin is sufficient for Armadillo binding in the yeast two-hybrid system.
b) Clusters of 3-4 point mutations in conserved sequence motifs in DE-cadherin do not block Armadillo binding in the two hybrid system, while a subset of more extensive amino acid substitutions in this region do so.
c) The minimal cadherin peptides can compete for interaction with ß-catenin in vivo, displacing its endogenous partners.
d) The effect of mutations in the core binding region parallels that assessed in yeast, with one exception.
e) In general, the requirements for interaction with ß-catenin were more stringent in mammalian cells, where endogenous partners are present, than in yeast, where they are absent, suggesting that competition between partners likely regulates complex formation in vivo.
f) Mutation of known phosphorylation sites in De-cadherin dramatically reduces binding in mammalian cells, while it had little effect on binding in yeast, suggesting that phosphorylation regulates binding in vivo.
g) Our mutagenesis studies, combined with the crystal structure of the ß-catenin:TCF complex, allowed us to make a prediction of the structure of the ß-catenin:E-cadherin complex.
h) Binding to TCF/LEF is more easily competed than that to APC/Axin, and both are more easily competed than binding to E-cadherin.
i) Groucho binds dTCF
j) Groucho acts as a dTCF co-repressor in vivo, repressing Wingless-responsive genes and thus shaping pattern of the embryonic segment.
k) Armadillo's C-terminus plays multiple roles in Armadillo function.

(8) Reportable outcomes for the entire four years.

Publications supported in part by the IDEA grant (reprints of all were submitted in previous years):

Simcha, I., Kirkpatrick, C., Sadot, E., Shtutman, M. Polevoy, G., Geiger, B., Peifer, M., and Ben-Ze'ev, A. (2001). Cadherin Sequences that Inhibit ß-catenin Signaling: a Study in Yeast and Mammalian Cells. Molecular Biology of the Cell 12: 1177-88..

Cox, R.T., Pai,L.-M., Kirkpatrick, C., Stein,J., and Peifer, M. (1999). Roles of the C-terminus of Armadillo in Wingless signaling in *Drosophila* . Genetics,153, 319-332

Cavallo, R.A., Cox, R.T., Moline, M.M., Roose, J., Polevoy, G.A., Clevers, H., Peifer, M., and Bejsovec, A. (1998). *Drosophila* TCF and Groucho interact to repress Wingless signaling activity. Nature 395, 604-608.

Additional publications acknowledging partial salary support for Mark Peifer via the CDA:

McCartney, B., Dierick, H.A., Kirkpatrick, C., Moline, M.M., Baas, A., Peifer, M., and Bejsovec, A. (1999). *Drosophila* APC2 is a cytoskeletally-associated protein that regulates Wingless signaling in the embryonic epidermis. J. Cell Biol. 146, 1303-1318 (reprint previously provided).

Tepass, U., Truong, K., Godt, D., Ikura, M., Peifer, M. (2000). Cadherins in embryonic and neural morphogenesis.. Nature Reviews: Molecular Cell Biology1: 91-100 (reprint previously provided).

McEwen, D.G., Cox, R.T., and Peifer, M. (2000). The canonical Wg and JNK signaling cascades collaborate to promote both dorsal closure and ventral patterning. Development 127, 3607-3617. (reprint previously provided).

Cox, R.T., McEwen, D.G., Myster, D.G., Duronio, R.J., Loureiro, J., and Peifer, M. (2000). A screen for mutations that suppress the phenotype of *Drosophila armadillo*, the ß-catenin homolog. Genetics 155, 1725-1740. (reprint previously provided).

McEwen, D.G., Cox, R.T., and Peifer, M. (2000). The canonical Wg and JNK signaling cascades collaborate to promote both dorsal closure and ventral patterning. Development 127, 3607-3617 (reprint previously provided).
Cox, R.T., McEwen, D.G., Myster, D.G., Duronio, R.J., Loureiro, J., and Peifer, M. (2000). A screen for mutations that suppress the phenotype of *Drosophila armadillo*, the ß-catenin homolog. Genetics 155, 1725-1740. (reprint previously provided)
Peifer, M., and Polakis, P. (2000). Wnt signaling in oncogenesis and embryogenesis: A look outside the nucleus. Science 287, 1606-1609 (reprint previously provided).
Loureiro, J.J., Akong, K., Cayirlioglu, P., Baltus, A.E., DiAntonio, A., and Peifer, M. (2001). Activated Armadillo/ß-catenin does not play a general role in cell migration and process extension in *Drosophila*. Developmental Biology 235: 33-44 (reprint included in Appendix).
McCartney, B.M., McEwen, D.G., Grevengoed,, E., Maddox, P., Bejsovec, A., Peifer, M. (2001) *Drosophila* APC2 and Armadillo participate in tethering mitotic spindles to cortical actin. Nature Cell Biology 3, 933-938 (reprint included in Appendix).
Grevengoed, E.E., Loureiro, J.J., Jesse, T.L., and Peifer, M. (2001). Abelson kinase regulates epithelial morphogene *Drosophila* . Journal of Cell Biology 155, 1185-1197 (reprint included in Appendix)..
Akong, K., McCartney, B.M., and Peifer, M. (2002). *Drosophila* APC2 and APC1 have overlapping roles in the larval brain despite their distinct intracellular localizations. Developmental Biology, in press (reprint not yet available).
Akong, K., Grevengoed, E.E., Price, M.H., McCartney, B.M., Hayden, M.A., DeNofrio, J.C., and Peifer, M. (2002). *Drosophila* APC2 and APC1 play overlapping roles in Wingless signaling in the embryo and imaginal discs. Developmental Biology, in press (reprint not yet available).

Degrees supported in part by the IDEA Award

1. Ph.D. awarded to Dr. Robert Cavallo, December 1999, entitled "New partners for Armadillo in signal transduction and cell adhesion". A portion of the work in this thesis was supported by the IDEA Award.
2. M.S. awarded to Mr. Gordon Polevoy, April 2001, entitled "Mechanisms of Armadillo's roles in signaling and adhesion." Virtually all of the work in this thesis was supported by the IDEA Award.

Presentations by Mark Peifer discussing this work.

"Cell adhesion, signal transduction and cancer: the Armadillo Connection.", Inaugural Symposium for the Developmental Genetics Programme and British Biochemical Society Annual Meeting, Krebs Institute,Sheffield, England, United Kingdom, July 1998

"Cell adhesion, signal transduction and cancer: the Armadillo Connection.", Annual Meeting, British Society of Cell Biology, Oxford, England, United Kingdom, September 1998

"Cell adhesion and signal transduction: the Armadillo Connection." ERDA Program, NIEHS, RTP NC September, 1998

"Cell adhesion and signal transduction: the Armadillo Connection." Department of Pharmocology, University of North Carolina at Chapel Hill, Chapel Hill NC October, 1998

"Cell adhesion and signal transduction: the Armadillo Connection." Department of Molecular Biosciences, University of Kansas, Lawrence KS February, 1999

"Cell adhesion and signal transduction: the Armadillo Connection." Hubrecht Laboratory of Developmental Biology, Dutch National Science Foundation, Utrecht, the Netherlands, March, 1999

"Cell adhesion and signal transduction: the Armadillo Connection." Dutch National Cancer Institute, Amsterdam, the Netherlands, March, 1999

"Cell adhesion and signal transduction: the Armadillo Connection." Department of Developmental and Cell Biology, University of California, Irvine CA, May 1999.

"Cell adhesion, signal transduction and cancer: the Armadillo Connection." Cell Contact and Adhesion Gordon Conference, Andover NH June 1999.

"Cell adhesion, signal transduction and cancer: the Armadillo Connection.", Biological Structure and Gene Expression Gordon Conference, Meriden NH August, 1999.

"Cell adhesion, signal transduction and cancer: the Armadillo Connection.", Batsheva Conference on "The dialogue between Cell Adhesion, Protein Degradation, and Transcriptional Regulation in Cancer", Weizmann Institute, Rehovot ISRAEL, November, 1999.

"Cell adhesion, signal transduction and cancer: the Armadillo Connection.", Keynote address at Keystone Conference on Intercellular Junctions, Keystone CO, February 2000.

"Cell adhesion, signal transduction and cancer: the Armadillo Connection.", at "Cell Communication", the Annual CMB Symposium, Duke University, Durham NC, March 2000.

"A Drosophila model system for examining ß-catenin function in cell adhesion and transcriptional activation.", Era of Hope, the DOD Breast Cancer Research Program Meeting, Atlanta GA June, 2000.

"Cell adhesion, signal transduction, and cancer: the Armadillo Connection." Cancer Genetics Group, Lineberger Comprehensive Cancer Center, University of North Carolina-Chapel Hill NC, July 1999.

"Cell adhesion, signal transduction, and cancer: the Armadillo Connection." Department of Genetics, Cell and Developmental Biology, University of Minnesota, Minneapolis MN, August 1999.

"Cell adhesion, signal transduction, and cancer: the Armadillo Connection." First Annual Novartis-UNC Biology Joint Retreat, University of North Carolina, Chapel Hill NC, August 1999.

"Cell adhesion, signal transduction, and cancer: the Armadillo Connection." Dept. of Biological Chemistry, Johns Hopkins University, Baltimore MD, September, 1999.

"Cell adhesion, signal transduction, and cancer: the Armadillo Connection." Dept. of Genetics, University of Georgia, Athens GA, October, 1999.

"Cell adhesion, signal transduction, and cancer: the Armadillo Connection." Institute Of Molecular Biology, University of Oregon, Eugene OR, January, 2000

"Cell adhesion, signal transduction, and cancer: the Armadillo Connection." Sphinx Pharmaceuticals/Eli Lilly, Research Triangle Park, NC, May 2000.

"Cell adhesion, signal transduction, and cancer: the Armadillo Connection." Division of Clinical Sciences Seminar Series, National Cancer Institute/NIH, Bethesda MD May 2000.

"Cell adhesion, signal transduction and cancer: the Armadillo Connection.", "Signaling by Adhesion Receptors" Gordon Conference, Newport RI July, 2000.

"Cell adhesion, signal transduction and cancer: the Armadillo Connection", The 17th Whitehead Symposium, "Molecular Machines" Whitehead Institute and MIT, Boston MA, October 2000

"Cell adhesion, signal transduction and cancer: the Armadillo Connection", The British Societies for Cell and Developmental Biology—Joint Spring meeting, "Cell and Tissue Morphogenesis" Brighton, UNITED KINGDOM, April 2001

"Cell adhesion, signal transduction and cancer: the Armadillo Connection", The 25th Annual Lineberger Comprehensive Cancer Center Symposium, "Regulatory Mechanisms in Human Cancer" Chapel Hill NC, April 2001

"Cell adhesion, signal transduction, and cancer: the Armadillo Connection". Laboratory of Molecular Carcinogenesis, NIEHS/NIH, RTP NC October, 2000

"Cell adhesion, signal transduction, and cancer: the Armadillo Connection". Memorial Sloan-Kettering Cancer Center, New York NY December, 2000

"Cell adhesion, signal transduction, and cancer: the Armadillo Connection". Department of Molecular Biology, Princeton University, Princeton NJ February 2001

"Cell adhesion, signal transduction, and cancer: the Armadillo Connection". Division of Biology, University of California at San Diego, La Jolla, CA, May 2001.

"Unexpected connections between embryogenesis and oncogenesis" Summer Undergraduate Research Program S UNC-Chapel Hill, Chapel Hill NC July, 2001

"Cell adhesion, signal transduction, and cancer: the Armadillo Connection." Department of Embryology, Carnegie Institution of Washington, Baltimore MD, September 2001

"Cell adhesion, signal transduction, and cancer: the Armadillo Connection." Department of Molecular, Cellular and Developmental Biology, University of Arizona, Tucson AZ, October 2001

"Cell adhesion, signal transduction, and cancer: the Armadillo Connection." Department of Biology, University of Carolina at Chapel Hill, Chapel Hill NC, November 2001

"Cell adhesion, signal transduction, and cancer: the Armadillo Connection." Siteman Comprehensive Cancer Cente Washington University School of Medicine, St. Louis, MO January 2002.

"Cell adhesion, signal transduction, and cancer: the Armadillo Connection." Department of Anatomy and Cell Biol East Carolina University, Greenville NC, February 2002

"A model system for the tumor suppressor APC" Keystone Meeting on "Wnt and ß-catenin signaling in Develo and Disease", Taos NM March 2002.

"Cell adhesion, signal transduction and cancer: the Armadillo Connection.", "Signaling by Adhesion Receptors" Gordon Conference, New London CT July, 2002.

List of personnel supported in part by this grant

Mark Peifer
Gordon Polevoy
Eiman Abdulrahman
Carol Ann McCormick
Shobu Odate
Kea Parker
Chad Cary
S.A. Merritt
Meredith Price
Emily Crafton
S.S. Chung
S.M. Marks
Shobu Odate
David Shuford
Fei Wang
Whitney Christian

(9) Conclusions.

We made significant progress on each of the specific aims. In carrying out Aim 1, we examined in detail the binding of DE-cadherin to Arm/ß-catenin, identifying a very small region that is sufficient for binding in the yeast two-hybrid system and identifying within that region the key amino acids required for binding. We completed an analysis of binding of wild-type and mutant peptides in mammalian cells, in collaboration with our colleagues at the Weizmann Institute. This work was published in Molecular Biology of the Cell. These data should provide a basis for understanding the interaction between the protein product of the oncogene ß-catenin and its mammalian partners in both normal development and physiology, and during oncogenesis.

In carrying out Aim 2, we found that dTCF plays a dual role in Wingless/Wnt signaling. We had previously shown that it acts together with Arm to activate Wingless target genes. In work funded in part by this grant, we found that in the absence of Arm, dTCF forms a complex with the co-repressor Groucho, and together they repress Wingless target genes. This work was published in Nature. We also examined the role of the C-terminus of Arm, which we had hypothesized acted as a transcriptional activation domain. We found that it plays a more complex role in Arm function. The

C-terminus can be divided into two regions, which contribute in an additive way to Arm's role as an activator of Wingless signaling. It also appears to regulate the stability of Arm. This work was published in Genetics. Subsequent work by others has confirmed the relevance of our results for mammalian ß-catenin. Understanding the mechanism by which Wnt target genes are repressed will provide insight into the normal and abnormal regulation of the genes responsible for oncogenesis in tumors resulting from activation of the Wnt pathway.

(10) References.

Cavallo, R. A., Cox, R. T., Moline, M. M., Roose, J., Polevoy, G. A., Clevers, H., Peifer, M. and Bejsovec, A. (1998). *Drosophila* TCF and Groucho interact to repress Wingless signaling activity. *Nature* 395, 604-608.

Cox, R. T., Pai, L.-M., Kirkpatrick, C., Stein, J. and Peifer, M. (1999). Roles of the C-terminus of Armadillo in Wingless signaling in *Drosophila. Genetics* 153, 319-332.

Graham, T. A., Weaver, C., Mao, F., Kimelman, D. and Xu, W. (2000). Crystal Structure of a beta-Catenin/Tcf Complex. *Cell* 103, 885-896.

Hsu, S. C., Galceran, J. and Grosschedl, R. (1998). Modulation of transcriptional regulation by LEF-1 in response to Wnt-1 signaling and association with ß-catenin. *Mol. Cell. Biol.* 18, 4807-4818.

Huber, A. H. and Weis, W. I. (2001). The structure of the beta-catenin/E-cadherin complex and the molecular basis of diverse ligand recognition by beta-catenin. *Cell* 105, 391-402.

Lickert, H., Bauer, A., Kemler, R. and Stappert, J. (2000). Casein kinase II phosphorylation of E-cadherin increases E-cadherin/ß-catenin interaction and strengthens cell adhesion. *J. Biol. Chem.* 275, 5090-5095.

Lu, Q., Paredes, M., Medina, M., Zhou, J., Cavallo, R., Peifer, M., Orecchio, L. and Kosik, K. (1999). δ-catenin, an adhesive junction associated protein which promotes cell scattering. *J. Cell Biol.* 144, 519-532.

McCartney, B. M., Dierick, H. A., Kirkpatrick, C., Moline, M. M., Baas, A., Peifer, M. and Bejsovec, A. (1999). *Drosophila* APC2 is a cytoskeletally-associated protein
that regulates Wingless signaling in the embryonic epidermis. *J. Cell Biol.* 146, 1303-1318.

Montross, W. T., Ji, H. and McCrea, P. D. (2000). A ß-catenin/engrailed chimera selectively suppresses Wnt signaling. *J. Cell Sci.* 113, 1759-1770.

Pai, L.-M., Kirkpatrick, C., Blanton, J., Oda, H., Takeichi, M. and Peifer, M. (1996). *Drosophila* α-catenin and E-cadherin bind to distinct regions of *Drosophila* Armadillo. *J. Biol. Chem.* 271, 32411-32420.

Peifer, M. (1997). ß-catenin as oncogene: the smoking gun. *Science* 275, 1752-1753.

Peifer, M. and Polakis, P. (2000). Wnt signaling in oncogenesis and embryogenesis-- A look outside the nucleus. *Science* 287, 1606-1609.

Rubinfeld, B., Albert, I., Porfiri, E., Fiol, C., Munemitsu, S. and Polakis, P. (1996). Binding of GSK-ß to the APC/ß-catenin complex and regulation of complex assembly. *Science* 272, 1023-1026.

Sadot, E., Simcha, I., Iwai, K., Ciechanover, A., Geiger, B. and Ben-Ze'ev, A. (2000). Differential interaction of plakoglobin and beta-catenin with the ubiquitin-proteasome system. *Oncogene* 19, 1992-2001.

Sadot, E., Simcha, I., Shtutman, M., Ben-Ze'ev, A. and Geiger, B. (1998). Inhibition of beta-catenin-mediated transactivation by cadherin derivatives. *Proc. Nat. Acad. Sci. USA* 95, 15339-44.

Simcha, I., Kirkpatrick, C., Sadot, E., Shtutman, M., Polevoy, G., Geiger, B., Peifer, M. and Ben-Ze'ev, A. (2001). Cadherin Sequences That Inhibit beta-Catenin Signaling: A Study in Yeast and Mammalian Cells. *Mol. Biol. Cell* 12, 1177-88.

Stappert, J. and Kemler, R. (1994). A short core region of E-cadherin is essential for catenin binding and is highly phosphorylated. *Cell Adhesion Commun.* 2, 319-327.

Thoreson, M. A., Anastasiadis, P. Z., Daniel, J. M., Ireton, R. C., Wheelock, M. J., Johnson, K. R., Hummingbird, D. K. and Reynolds, A. B. (2000). Selective uncoupling of p120(ctn) from E-cadherin disrupts strong adhesion. *J. Cell Biol.* 148, 189-202.

van de Wetering, M., Cavallo, R., Dooijes, D., van Beest, M., van Es, J., Loureiro, J., Ypma, A., Hursh, D., Jones, T., Bejsovec, A. et al. (1997). Armadillo co-activates transcription driven by the product of the *Drosophila* segment polarity gene *dTCF. Cell* 88, 789-799.

Vleminckx, K., Kemler, R. and Hecht, A. (1999). The C-terminal transactivation domain of ß-catenin is necessary and sufficient for signaling by the LEF-1/ßcatenin complex in *Xenopus laevis*. *Mech. Dev.* 81, 65-74.

von Kries, J. P., Winbeck, G., Asbrand, C., Schwarz-Romond, T., Sochnikova, N., Dell'Oro, A., Behrens, J. and Birchmeier, W. (2000). Hot spots in beta-catenin for interactions with LEF-1, conductin and APC. *Nat. Struct. Biol.* 7, 800-7.

Yap, A. S., Niessen, C. M. and Gumbiner, B. M. (1998). The juxtamembrane region of the cadherin cytoplasmic tail supports lateral clustering, adhesive strengthening, and interaction with p120ctn. *J. Cell Biol.* 141, 779-789.

Appendix —Reprints of publications supported in part by this grant

Loureiro, J.J., Akong, K., Cayirlioglu, P., Baltus, A.E., DiAntonio, A., and Peifer, M. (2001). Activated Armadillo/ß-catenin does not play a general role in cell migration and process extension in *Drosophila*. Developmental Biology 235: 33-44 (reprint included in Appendix).

McCartney, B.M., McEwen, D.G., Grevengoed,, E., Maddox, P., Bejsovec, A., Peifer, M. (2001) *Drosophila* APC2 and Armadillo participate in tethering mitotic spindles to cortical actin. Nature Cell Biology 3, 933-938 (reprint included in Appendix).

Grevengoed, E.E., Loureiro, J.J., Jesse, T.L., and Peifer, M. (2001). Abelson kinase regulates epithelial morphogene *Drosophila* . Journal of Cell Biology 155, 1185-1197 (reprint included in Appendix)..

Developmental Biology 235, 33–44 (2001)
doi:10.1006/dbio.2001.0292, available online at http://www.idealibrary.com on IDEAL®

Activated Armadillo/β-Catenin Does Not Play a General Role in Cell Migration and Process Extension in *Drosophila*

Joseph J. Loureiro,* Kathryn Akong,† Pelin Cayirlioglu,* Andrew E. Baltus,* Aaron DiAntonio,‡ and Mark Peifer*,†,[1]

**Department of Biology and †Curriculum in Genetics and Molecular Biology, University of North Carolina at Chapel Hill, Chapel Hill, North Carolina 27599-3280; and ‡Department of Molecular Biology and Pharmacology, Washington University School of Medicine, St. Louis, Missouri 63110*

Human β-catenin and its fly homolog Armadillo are best known for their roles in cadherin-based cell–cell adhesion and in transduction of Wingless/Wnt signals. It has been hypothesized that β-catenin may also regulate cell migration and cell shape changes, possibly by regulating the microtubule cytoskeleton via interactions with APC. This hypothesis was based on experiments in which a hyperstable mutant form of β-catenin was expressed in MDCK cells, where it altered their migratory properties and their ability to send out long cellular processes. We tested the generality of this hypothesis *in vivo* in *Drosophila*. We utilized three model systems in which cell migration and/or process extension are known to play key roles during development: the migration of the border cells during oogenesis, the extension of axons in the nervous system, and the migration and cell process extension of tracheal cells. In all cases, cells expressing activated Armadillo were able to migrate and extend cell processes essentially normally. The one alteration from normal involved an apparent cell fate change in certain tracheal cells. These results suggest that only certain cells are affected by activation of Armadillo/β-catenin, and that Armadillo/β-catenin does not play a general role in inhibiting cell migration or process extension. © 2001 Academic Press

INTRODUCTION

Cell migration and cell shape changes play key roles in morphogenesis. For example, migrating neural crest cells shape the mammalian peripheral nervous system. Likewise, dramatic cell shape changes, such as axon extension by neurons or process extension by insect tracheal cells, produce highly asymmetric cells whose asymmetry is critical to their function. Underlying both cell migration and cell shape changes are highly organized rearrangements of the actin and microtubule cytoskeletons. Recently, attention has focused on how these cytoskeletal events are regulated. Many mechanisms have been postulated and tested in cultured cells. Genetic technologies in model organisms such as *Drosophila melanogaster*, *Caenorhabditis elegans*, and the mouse now allow us to begin to test these proposed mechanisms *in vivo*. The results of *in vivo* tests sometimes differ from those in cultured cells. For example, several roles for αv-integrins postulated from *in vitro* studies were not observed in mice lacking this integrin subfamily (reviewed in Sheppard, 2000). Thus, *in vivo* tests are critical for evaluating the roles of different cytoskeletal regulators in the complex environment of the intact animal.

One potential cytoskeletal regulator during cell migration and process extension is β-catenin, a multifunctional protein adapter involved in the assembly of several multiprotein complexes with distinct biological activities. For example, β-catenin is a core component of the cadherin–catenin complex, at the heart of the cell–cell adherens junction. Transmembrane cadherins mediate intercellular adhesion, while catenin proteins bind directly or indirectly to the cadherin tail and link the adherens junction to the actin cytoskeleton. The cadherin–catenin complex plays a critical role in establishing and maintaining tissue architec-

[1] To whom correspondence should be addressed. Fax: (919) 962-1625. E-mail: peifer@unc.edu.

0012-1606/01 $35.00

ture in epithelial cells. Reduced cadherin levels have been traditionally viewed as required to allow epithelial cells to lose adhesion for neighboring cells and become migratory, both in normal situations such as neural crest migration and in pathological situations such as tumor cell metastasis. However, more recent data suggest that the picture is more complex: DE-cadherin promotes border cell migration during *Drosophila* oogenesis (Niewiadomska *et al.*, 1999), while N-cadherin promotes motile behavior in cultured mammalian tumor cells (Nieman *et al.*, 1999).

In most epithelial cells, any β-catenin that is not assembled into adherens junctions forms a complex with the tumor suppressors adenomatous polyposis coli (APC) and Axin. This interaction promotes assembly of a multiprotein complex that targets β-catenin for phosphorylation by glycogen synthase kinase-3β (GSK3β), and subsequent proteasomal destruction (reviewed in Peifer and Polakis, 2000). β-Catenin destruction can, however, be countered if the cell is exposed to Wnt family intercellular signals, which inactivate the "destruction complex," stabilize β-catenin, and allow it to enter the nucleus. There, β-catenin again acts as an adapter, in this case mediating interactions between DNA-binding proteins of the TCF/LEF family and the basal transcriptional machinery. This drives gene activation and can influence cell fate in many different ways.

A series of experiments in cultured mammalian cells suggested that β-catenin modulates cell migration and process extension (Barth *et al.*, 1997; Pollack *et al.*, 1997). Mutant forms of β-catenin that could not be targeted for proteasomal destruction, as their GSK3β phosphorylation sites had been deleted (referred to below as activated β-catenin), were expressed in cultured MDCK cells. This led to the accumulation of nonjunctional β-catenin and had dramatic effects on cell behavior. The morphology and colony-forming properties of subconfluent MDCK cells were altered, and the ability of these cells to extend cell processes or migrate in response to Hepatocyte Growth Factor (HGF)/Scatter Factor was nearly abolished. These results suggest that β-catenin can negatively regulate both cell migration and process extension in MDCK cells.

It was hypothesized that these effects of mutant β-catenin might be via its effects on APC (Barth *et al.*, 1997; Pollack *et al.*, 1997). This hypothesis was based on a variety of data suggesting that APC may be a cytoskeletal modulator, both in response to Wnt signals and possibly independent of them (reviewed in McCartney and Peifer, 2000). APC can bind and bundle microtubules *in vitro* (Munemitsu *et al.*, 1994; Smith *et al.*, 1994). Endogenous APC localizes to membrane puncta which are often associated with the ends of microtubule bundles (Näthke *et al.*, 1996), APC-GFP fusion proteins bind to and traffic along microtubules (Mimori-Kiyosue *et al.*, 2000), and *Drosophila* APC2 localizes to the cortex at the ends of the mitotic spindle of asymmetrically dividing neural stem cells (McCartney *et al.*, 1999). Further, APC binds to the protein EB1(Su *et al.*, 1995), which associates with the mitotic spindle in yeast and human cells and affects spindle function in yeast (reviewed in Bloom, 2000). Other data suggest that APC may also interact with the actin cytoskeleton. *Drosophila* APC2 colocalizes with actin in a variety of contexts (McCartney *et al.*, 1999; Yu and Bienz, 1999; Townsley and Bienz, 2000), and human APC was recently shown to associate with the Rho-GEF ASEF (Kawasaki *et al.*, 2000). When stabilized β-catenin was expressed in MDCK cells, it formed stable complexes with APC at the cell cortex (Barth *et al.*, 1997; Pollack *et al.*, 1997). These data together prompted the hypothesis that APC might promote cell migration and process extension by stabilizing microtubule bundles in cell processes, and that this role might be negatively regulated by its binding partner β-catenin. Of course, β-catenin could also affect cell migration in other ways. It might alter migration via its role as a catenin, or could indirectly affect cell behavior via effects on gene expression.

We thus set out to test the generality of the proposed role of β-catenin in cell migration and process extension in the more complex situation found in the living animal. *Drosophila* development provides a number of quite well-characterized situations in which cells migrate and/or extend processes. We chose three of the best studied as models: the migration of the border cell population of follicle cells in the ovary, the extension of axons in the central nervous system, and the combination of process extension and cell migration that occurs during the development of the tracheal system. In each case, we examined whether expression of a hyper-stable mutant form of Armadillo (Pai *et al.*, 1997; referred to below as activated Armadillo), the β-catenin homolog, perturbed any of these processes *in vivo*.

MATERIALS AND METHODS

Stocks

Canton S was used as the wild-type stock. UAS-Arm^{S10} and UAS-Arm$^{\Delta N}$ were previously described in Pai *et al.* (1997). The transgene in those stocks was expressed in specific tissues with the following GAL4 drivers: two different Elav-GAL4 drivers (Lin and Goodman, 1994; Luo *et al.*, 1994) were used for expression in embryonic postmitotic neurons, with the Elav-GAL4 line C155 of Lin and Goodman (1994) used for most experiments, C306-GAL4 and slbo-GAL4 were used for expression in oocyte follicle cells (Manseau *et al.*, 1997; Rorth *et al.*, 1998), and N722 btl-GAL4 (Shiga *et al.*, 1996) was used for expression in the embryonic tracheal system. UAS-lacZ was used to confirm expression patterns of GAL4 drivers and as a comparison with the expression of UAS-Arm^{S10}.

Antibodies and Immunodetection

Embryos were prepared for immunofluorescence as in Peifer *et al.* (1993). Samples were imaged on a Zeiss laser-scanning confocal microscope (LSM 310). Antibodies 2A12, anti-FasIII, and BP102 were purchased from the Developmental Studies Hybridoma Bank and were diluted 1:50, 1:50, and 1:100, respectively. Anti-FasII was

a gift from Corey Goodman and was used at 1:100. Preabsorbed anti-lacZ (Cappel) was used at 1:1000, and preabsorbed anti-c-myc (9E10) was used at 1:10.

Quantitation of Border Cell Migration

The extent of border cell migration was determined at stages 9, 10a, and 10b of oogenesis. The stage of each egg chamber was determined by estimating the extent of oocyte enlargement relative to the size of the entire egg chamber (20% at stage 9, 30–40% at stage 10a, and 50% at stage 10b). The extent of border cell migration was visually estimated by microscopic analysis and recorded as a fraction of the total distance from the origin of migration to the anterior end of the oocyte, and this was plotted as a function of developmental stage.

Immunoblotting

Nine- to eighteen-hour-old wild-type embryos or equivalently aged embryos carrying both a particular GAL4 driver and UAS-Arm^{S10} were collected, bleach dechorionated, and ground in an equal volume of 2× SDS–PAGE sample buffer and boiled for 5 min. Ovaries were dissected from adult females carrying both C306-GAL4 and UAS-Arm^{S10} and treated as above. Samples were analyzed by 6% SDS–PAGE and immunoblotting with preabsorbed antibody to the myc-epitope which tags Arm^{S10} (DSHB; 1:1). Equal amounts of total protein were loaded in each lane, as assessed by staining the blot with Ponceau S. HRP-conjugated secondary was used for chemiluminscent detection (Amersham). NIH Image was used for signal quantitation.

RESULTS

Activated Arm Has No Effect on Border Cell Migration

In cultured MDCK cells, expression of activated β-catenin can alter cell migration, process extension, and tubulogenesis (Barth *et al.*, 1997; Pollack *et al.*, 1997). We set out to test whether similar effects would be observed *in vivo*, using *Drosophila* as a model. To test effects on cell migration, we first examined the migration of the border cells of the fly ovary, a subset of the somatic follicle cells that surround the oocyte and nurse cells. These cells are a superb model for cell migration (reviewed in Montell, 1999). At the midpoint of oogenesis, the border cells separate from the follicular epithelium and migrate as a group between the nurse cells to the presumptive anterior end of the oocyte. The process of border cell migration is known to require DE-cadherin (Niewiadomska *et al.*, 1999). Border cells accumulate elevated levels of both Arm (Peifer *et al.*, 1993) and DE-cadherin (Niewiadomska *et al.*, 1999), consistent with them working together in adhesion in this cell type; however, if Arm function in the developing follicular epithelium is severely compromised, egg chambers degenerate prior to border cell migration (Tantenzapf *et al.*, 2000) so this cannot be tested directly. No role has been reported for Wg signaling in border cells.

To express activated Armadillo (Arm^{S10}; Pai *et al.*, 1997) specifically in the border cells, we made use of the GAL4-UAS system. We utilized two different drivers, C306-GAL4 and *slbo*-GAL4, each of which directs expression of the GAL4 transcription factor in the border cells and not in most of the other somatic cells of the ovary (Figs. 1A, 1C, and 1E). We created females carrying one of these drivers together with UAS-Arm^{S10}, in which activated Arm is driven by a promotor containing GAL4-binding sites, thus driving expression of Arm^{S10} in border cells. We confirmed Arm^{S10} expression in the border cells by staining ovaries with anti-myc antibody, which specifically recognizes the myc-epitope-tagged Arm^{S10} protein (Figs. 1B, 1D, and 1F). This also revealed that Arm^{S10} accumulated throughout the border cells, including in long cell processes. Border cell expression of activated Arm using C306-GAL4 had no significant effect on endogenous Arm, which continued to accumulate in border cells at normal levels and with unaltered subcellular localization (Figs. 2C–2G). This lack of effect of activated Arm on ubiquitous Arm accumulation seemed to be generally true, as ubiquitous expression of activated Arm in embryos using the e22c-GAL4 driver also did not significantly alter levels of endogenous wild-type Arm (Fig. 2B).

We then compared border cell migration in wild-type and activated Arm-expressing border cells. We labeled border cells with antibody to Fasciclin III (Fas III), which is specifically expressed in these cells (Brower *et al.*, 1981; Figs. 1G, 1I, and 1K) and calculated the rate at which they migrated, expressed as the ratio of border cell position from the anterior egg chamber pole to the anterior end of the oocyte, and used the retraction of the follicle cells from the

FIG. 1. Expression of activated Arm does not alter border cell migration. All panels depict egg chambers, with anterior to the left. In each set, three stages of oogenesis are displayed: (A), (B), (G), and (H) are in Stage 9. (C), (D), (I), and (J) are in Stage 10a. (E), (F), (K), and (L) are in Stage 10b. (A, C, E) Expression pattern of slbo-GAL4 revealed by crossing to UAS-lacZ and immunostaining for β-galactosidase. This driver directs expression in the border cells (indicated by arrows), the posterior polar follicle cells and some of their immediate neighbors, and in the centripetal cells which migrate between the oocyte and the nurse cells. (B, D, F) Accumulation pattern of Arm^{S10} driven by either C306-GAL4 (B, D) or slbo-GAL4 (F), and detected with antibody to the myc-epitope. Arm^{S10} accumulates throughout the migrating border cells, including in long cellular processes (arrows in B and D). (G–L) Border cell migration in wild-type (G, I, K) or Arm^{S10}-expressing (H, J, L) egg chambers, as assessed by immunofluorescence for the border cell marker anti-Fas III. Border cells are indicated by arrows. Border cell migration was qualitatively normal as assessed by this procedure.

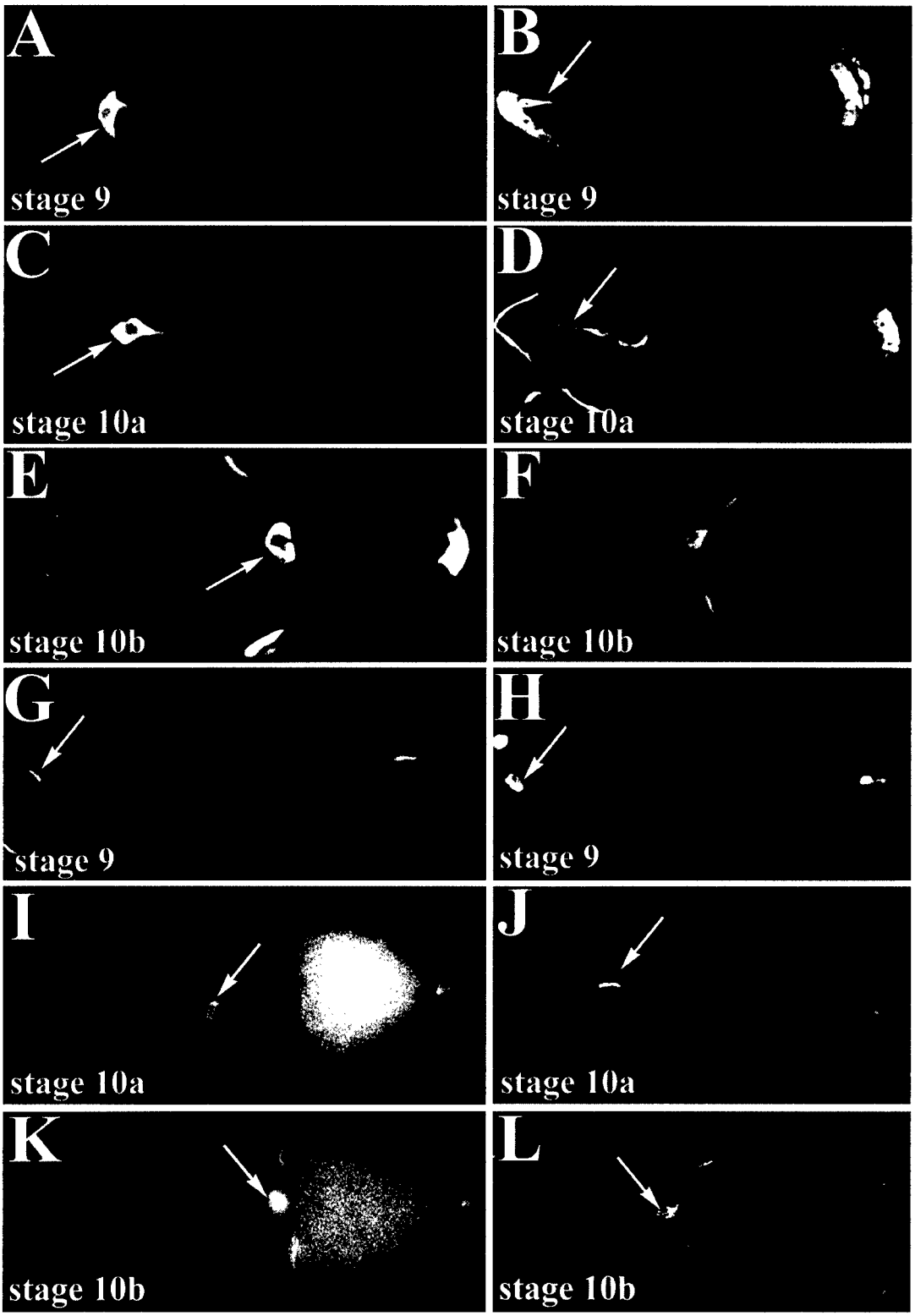

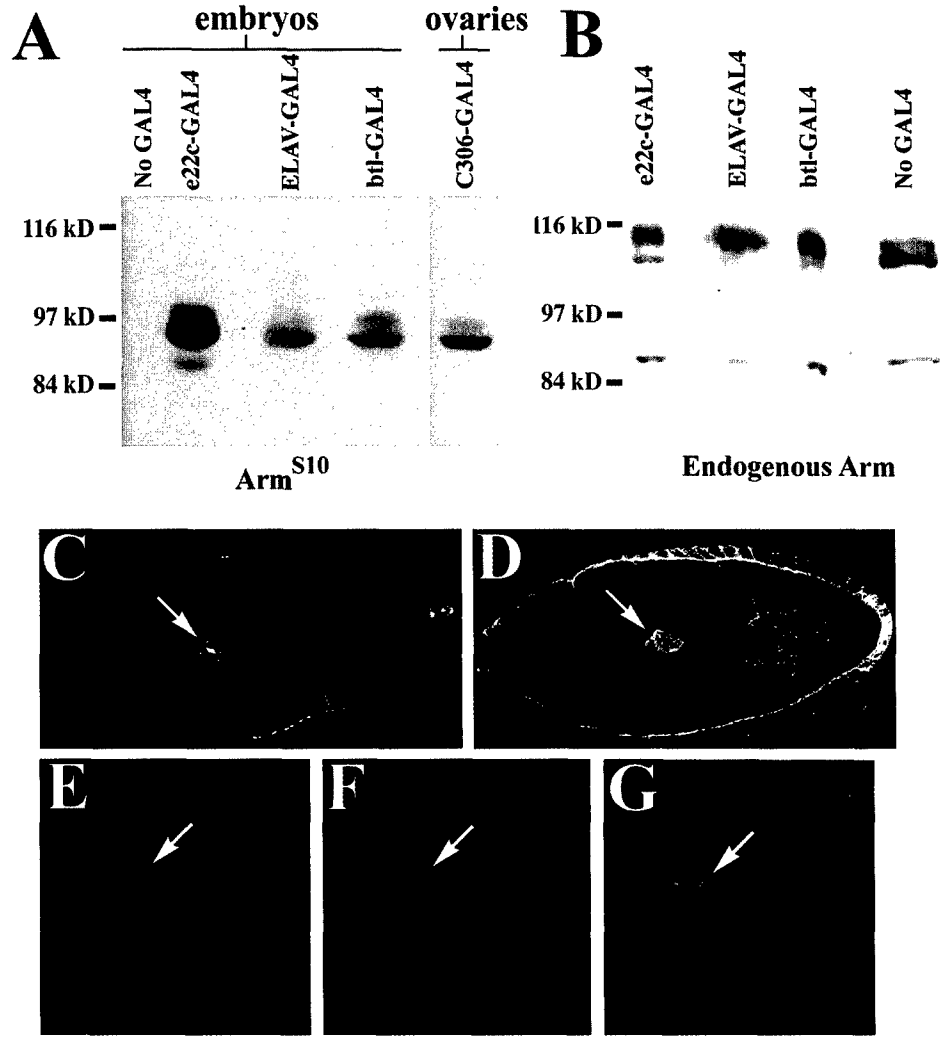

FIG. 2. Levels of expression of activated Arm driven by various GAL4 drivers, and effect of activated Arm expression on levels of endogenous Arm. (A) Equal amounts of total protein from 9 to 18-h-old wild-type embryos (leftmost lane), equivalently aged embryos carrying both the indicated GAL4 driver and UAS-Arm^{S10} (middle three lanes), or ovaries dissected from adult females carrying both C306- GAL4 and UAS-Arm^{S10} (rightmost lane) were analyzed by SDS–PAGE and immunoblotted with antibody to the myc-epitope which tags Arm^{S10}. The position of the MW markers are shown at the left and the position of Arm^{S10} is shown at the right. Note that, while e22c-GAL4 drives expression in most if not all embryonic cells, the other GAL4 drivers only drive expression in a small subset of the cells in the embryo or ovary. (B) Expression of activated Arm does not significantly reduce total levels of endogenous Arm. Equal amounts of total protein from 9 to 18-h-old wild-type embryos (rightmost lane) or equivalently aged embryos carrying both the indicated GAL4 driver and UAS-Arm^{S10} (left three lanes) were analyzed by SDS–PAGE and immunoblotted with anti-Arm monoclonal antibody 7A1, which recognizes wild-type endogenous Arm but does not recognize Arm^{S10} due to deletion of the epitope. The upper set of bands represents canonical wild-type Arm, while the lower band is the alternatively spliced neural isoform. (C–G) Expression of activated Arm in border cells using the C306-GAL4 driver does not significantly reduce levels of endogenous Arm in those cells. (C, D) Ovaries from wild-type animals (C) or from those expressing Arm^{S10} in border cells (D) were stained with anti-Arm monoclonal antibody 7A1, which recognizes wild-type endogenous Arm but does not recognize Arm^{S10}. Note that levels of endogenous Arm in border cells (arrows) remain high even after expression of activated Arm. (E–G) Endogenous wild-type Arm continues to accumulate at high levels in border cells of animals expressing activated Arm. Ovaries from animals expressing Arm^{S10} in border cells were stained with anti-Arm monoclonal antibody 7A1 (E), which recognizes wild-type endogenous Arm but does not recognize Arm^{S10}, and with anti-Arm C-terminal polyclonal antibody (F), which recognizes both endogenous Arm and activated Arm. (G) The merged images.

nurse cells and the size of the oocyte to calculate stage. Border cell migration was completely unperturbed by expression of Arm^{S10}, both in qualitative terms (Figs. 1G, 1I, and 1K vs. Figs. 1H, 1J, and 1L) and in overall rate (Figs. 3A and 3C). We also expressed in border cells a second activated form of Arm, Arm$^{\Delta N}$, which lacks both the GSK3β

phosphorylation sites and also the α-catenin-binding site (Pai *et al.*, 1996, 1997). Arm$^{\Delta N}$ expression also had no discernable effect on border cell migration (Fig. 3B). Consistent with this, females expressing C306-GAL4 and UAS-Arm^{S10} are fertile at 25°C (data not shown).

These results are unlikely to be due to low levels of transgene expression. We examined the level of expression of activated Arm driven by the C306-GAL4 driver by immunoblotting (Fig. 2), comparing expression driven by this GAL4 driver to that of the e22c-GAL4 driver in embryos, which we previously characterized. e22c-GAL4 drives ubiquitous expression of Arm at levels comparable to those of endogenous wild-type Arm (Cox *et al.*, 1999; Pai *et al.*, 1997). In comparison, when normalized to equivalent amounts of total protein analyzed, C306-GAL4 drove expression of activated Arm to levels about fivefold less than those driven by e22c-GAL4. However, on a cell-by-cell basis, expression driven by C306-GAL4 is likely considerably higher, as e22c-GAL4 drives ubiquitous expression, while, in ovaries carrying the C306-GAL4 driver and UAS-Arm^{S10}, only a small fraction of the cells (the border cells) express activated Arm. We thus expect we are driving expression to levels similar to or exceeding those of endogenous Arm. This is similar to the relative levels of activated and endogenous β-catenin seen in the previous experiments in MDCK cells where alterations in cell migration and process extension were noted (Barth *et al.*, 1997; Pollack *et al.*, 1997).

Activated Arm Does Not Significantly Alter Axon Outgrowth

To examine cell process extension, we turned to a second cell type in which process extension plays an critical role. Cells of the central nervous system (CNS) send out long processes, forming the axonal scaffold of the CNS and extending axons into the periphery. Axon outgrowth depends on a variety of different cues. Among these is information from the cadherin/catenin complex—embryos lacking cadherin or catenin function have defects in the outgrowth of certain axon tracts (Iwai *et al.*, 1997; Loureiro and Peifer, 1998). Consistent with this role, Arm accumulates heavily in the axons of the developing CNS (Loureiro and Peifer, 1998). Arm also plays a role in CNS development via its role in Wg signaling—this role is early in the process, in assigning neuroblasts specific identities (Chu-Lagraff and Doe, 1993; Loureiro and Peifer, 1998; Richter *et al.*, 1998). There is no known role for Wg signaling in axon outgrowth in the embryonic CNS, though it does play a role in axon outgrowth in the visual centers of the larval brain (Kaphingst and Kunes, 1994).

Mammalian APC localizes to the termini of neurites (Näthke *et al.*, 1996), and overexpression of activated β-catenin blocked HGF-stimulated process extension by MDCK cells (Pollack *et al.*, 1997). We thus tested whether expression of activated Arm affected axon outgrowth in *Drosophila*. We once again used the GAL4-UAS system, making

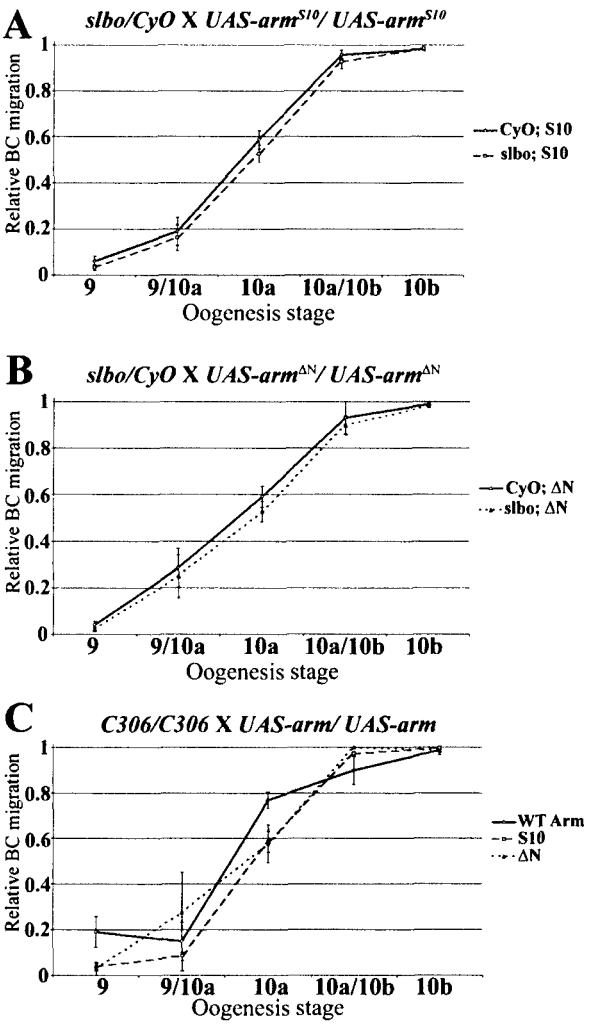

FIG. 3. The rate of migration of border cells expressing various forms of activated Armadillo. (A, B) Ovaries dissected from slbo-GAL4; UAS-Arm^{S10} or slbo-GAL4; UAS-Arm$^{\Delta N}$ females were compared to females from the same crosses that did not express activated Armadillo. (A) Egg chambers accumulating Arm^{S10} (slbo; S10; n = 367) have a comparable border cell migration pattern as egg chambers that do not express Arm^{S10} (CyO; S10; n = 277). (B) Border cell migration in egg chambers accumulating Arm$^{\Delta N}$ (slbo; ΔN; n = 258) was indistinguishable from that in control egg chambers that do not express Arm$^{\Delta N}$ (CyO; ΔN; n = 126). (C) Similar results were seen using the GAL4 driver C306. Overexpression of wild-type Arm^{S2} (WT Arm; n = 149), Arm^{S10} (S10; n = 194), or Arm$^{\Delta N}$ (ΔN; n = 61) in egg chambers did not grossly alter the progression of border cells through the nurse cells. In all graphs, standard error bars are shown for each time point.

use of Elav-GAL4, which specifically drives expression in the postmitotic CNS and PNS (Lin and Goodman, 1994; Luo *et al.*, 1994; Fig. 4A). We targeted expression to postmitotic cells both because this is when axons are extended, and because earlier work revealed that Wg signaling acts through Arm to pattern neural precursors (Chu-Lagraff and Doe, 1993;

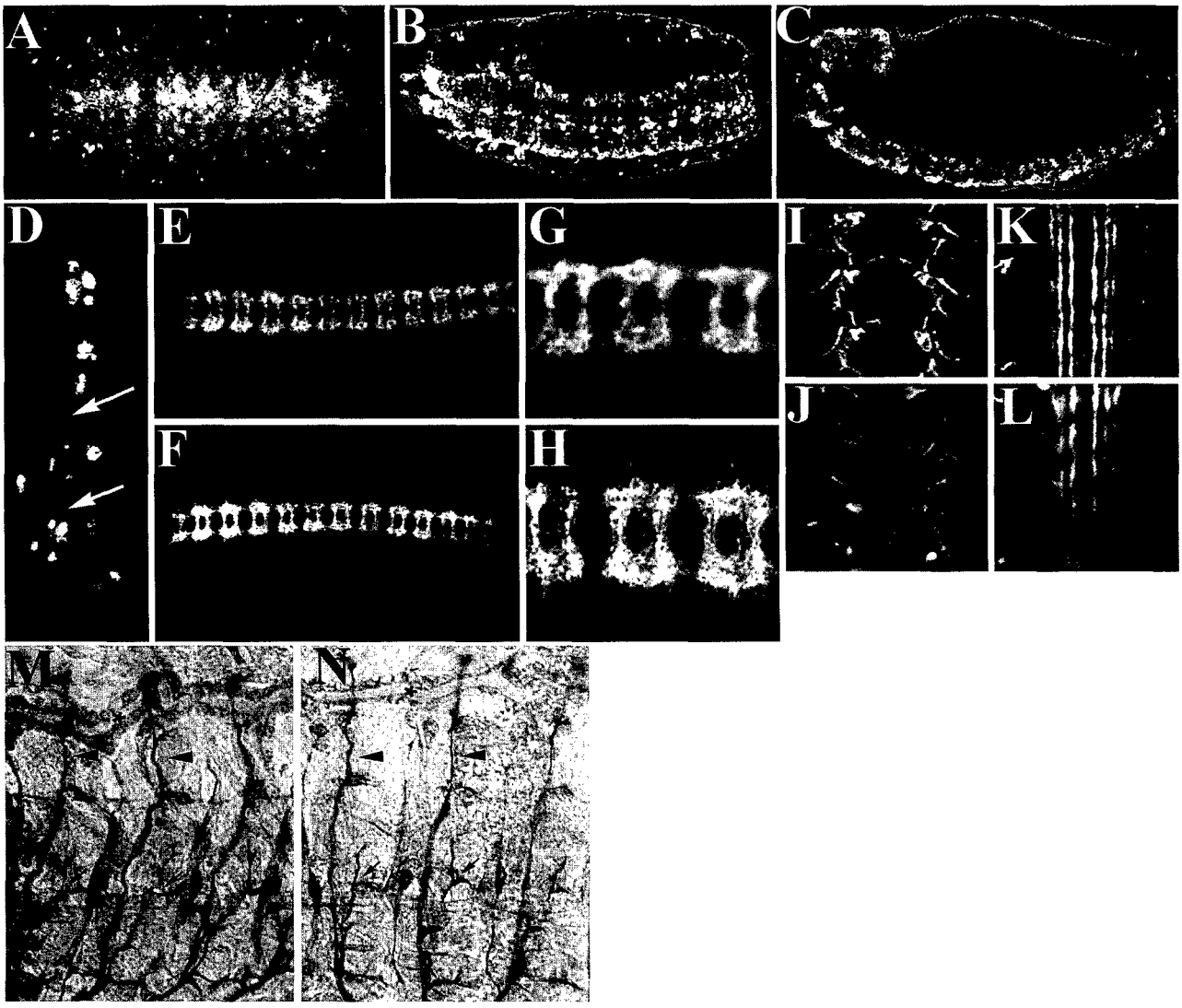

FIG. 4. Expression of activated Arm does not block axon outgrowth during development of the embryonic nervous system. (A) Ventral view of a stage 16 embryo, showing the expression pattern of Elav-GAL4 as revealed by crossing to UAS-lacZ and immunostaining for β-galactosidase. (B–D) Accumulation pattern of UAS-Arm^{S10} driven by Elav-GAL4, in the CNS (B; ventral view; C, lateral cross-section) and PNS (D, lateral view) of stage 16 embryos, as detected with antibody to the myc-epitope. Arm^{S10} protein appears to accumulate primarily in neuronal nuclei and cell bodies, though some axonal accumulation can be seen in the CNS (data not shown) and the PNS (arrows) (D). (E–H) The development of the CNS appeared normal as assessed by staining with the pan-axonal marker BP102. We should note that we cannot rule out subtle changes in the trajectory of individual axons in this analysis. (E–H) Ventral views of stage 16 embryos; (G) and (H) are close-ups. (E, G) Wild-type embryos. (F, H) Embryos expressing UAS-Arm^{S10}. (I–L) The pattern of axons positive for Fas II also appears normal both early (I, J) and later (K, L) in development, as assessed by immunofluorescence with anti-Fas II. (I–L) Close-ups of ventral views of stage 16 embryos. (I, K) Wild-type; (J, L) Embryos expressing UAS-Arm^{S10}. (M, N) Photomicrographs of stage 17 wild-type embryos (M) and embryos expressing Arm^{S10} in all neurons (N) stained with mAb 1D4 (anti-Fas II). Axons from the segmental nerve extend and branch at the appropriate choice point (arrows). Axons from the intersegmental nerve (marked with arrowheads) extend past the trachea (*) to their dorsal muscle targets.

Loureiro and Peifer, 1998), and we wanted to avoid indirect effects via mispatterning. Elav-GAL4 drove strong and specific expression of Arm^{S10} protein in the cells of the CNS and PNS (Figs. 4B–4D). Interestingly, unlike wild-type Arm, which accumulates predominantly in axons (Loureiro and Peifer, 1998), Arm^{S10} accumulated predominantly in cell bodies, in a punctate pattern which may represent nuclear accumulation (Figs. 4B and 4C). Arm^{S10} could also be observed at lower levels in the axons of the PNS (Fig. 4D). We examined levels of expression of activated Arm by immunoblotting, using the

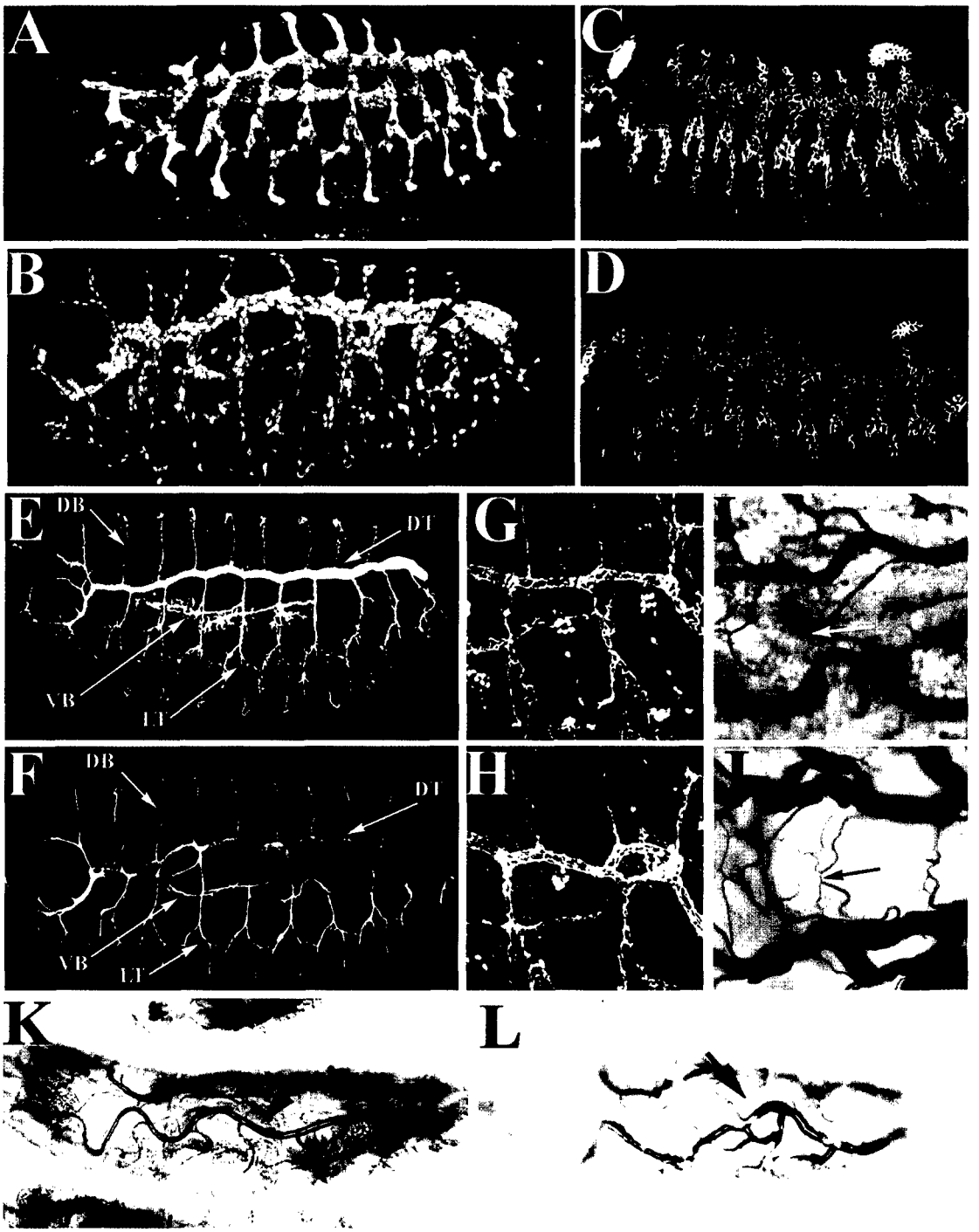

FIG. 5. Expression of activated Armadillo does not prevent tracheal cell migration or process extension, but does alter tracheal cell fates. In all pictures anterior is to the left, and all are lateral views, except (I) and (J) which are viewed from the dorsal side. (A) The expression pattern of btl-GAL4 in a stage 15 wild-type embryo as assessed using UAS-lacZ and immunofluorescence with anti-β-galactosidase antibodies. The dorsal trunk and visceral branches are indicated with green and red arrows, respectively. (B) The accumulation pattern of Arm^{S10} driven by btl-GAL4 in a stage 15 embryo, detected by immunofluorescence with antibodies directed against the myc-epitope. Note that Arm^{S10} protein accumulates throughout tracheal cells, but is concentrated in nuclei. At this stage, the dorsal trunk is enlarged and has abnormal ventrally directed loops or outgrowths (green arrows), while the visceral branches are sometimes reduced (red arrows). (C, D) Fas II expression in the developing trachea of stage 13 wild-type (C) or Arm^{S10}-expressing embryos (D). The Fas II expression pattern is quite normal at this stage. (E, F) The tracheal system of stage 15 wild-type (E) and Arm^{S10}-expressing embryos (F) revealed with antibodies against

ubiquitously expressed e22c-GAL4 as a positive control. Levels of Arm^{S10} driven by Elav-GAL4 are within three- to fivefold of those driven by e22c-GAL4 (Fig. 2). Taking into account the fraction of cells which make up the CNS, we thus estimate that Elav-GAL4 drives Arm^{S10} expression at or near the level of endogenous wild-type Arm within the cells of the CNS. Expression of activated Arm in the CNS did not substantially reduce levels of either the canonical Arm isoforms or the alternately spliced neural isoform (Fig. 2B).

We then examined the effect of Arm^{S10} expression on the development of the axon pattern. We utilized antibodies to both a general neuronal marker, BP102 (Figs. 4E and 4G), and to a marker of a subset of axons, the cell adhesion molecule Fasciclin II (Fas II; Figs. 4I and 4K). We chose this latter marker as the Fas II-positive neurons are among those whose axon pattern requires the function of the N-cadherin/catenin system (Iwai *et al.*, 1997; Loureiro and Peifer, 1998). The CNS of an embryo expressing Arm^{S10} under Elav-GAL4 control appeared wild-type in its axon patterns, as visualized both using BP102 (Figs. 4E and 4G vs. Figs. 4F and 4H) or anti-Fas II (Figs. 4I and 4K vs. Figs. 4J and 4L). We also used anti-FasII to examine the outgrowth of peripheral motoneuron axons. We found that axons of the segmental and intersegmental nerves appeared essentially normal when expressing Arm^{S10} (Fig. 4M vs. 4N). It should be noted that we cannot, of course, assess every axon and thus cannot rule out subtle differences. Consistent with a normal axon pattern, most if not all animals expressing Arm^{S10} under Elav-GAL4 control lived to adulthood (data not shown; Ahmed *et al.*, 1998).

Activated Arm Does Not Prevent Tracheal Cell Migration or Cell Rearrangements but Does Alter Tracheal Cell Fates

The third cell type we utilized were the tracheal cells, which undergo a dramatic, postmitotic program of cell migrations, cell rearrangements, and process extension to produce the larval tracheal system (reviewed in Manning and Krasnow, 1993). Several of these morphogenetic events closely parallel the events observed in the migration of MDCK cells stimulated by HGF (Barth *et al.*, 1997; Pollack *et al.*, 1997). For example, in forming the tracheal vessels, tracheal cells migrate out as a line of cells, some of which later rearrange to form multicellular tubes with a lumen. Tracheal cells also extend terminal branches that resemble the cell extensions produced by the MDCK cells. Arm and DE-cadherin are expressed at high levels in the developing tracheae, and tracheal development is known to require cadherin–catenin function (Uemura *et al.*, 1996).

We tested a number of GAL4 drivers for expression of Arm^{S10} in the tracheal system. Several drivers (e.g., E132 or P127) activated Wg signaling in the epidermis, as assessed by the production of excess naked cuticle (data not shown). We thus did not examine these further, as the interpretation of the results would thus have been complicated by alterations in the landscape across which tracheal cells were migrating. We instead focused on a tracheal driver that did not affect epidermal cell fate choices (data not shown), btl-GAL4. This driver directs expression throughout the tracheal system from the time at which tracheal cells invaginate (Fig. 5A).

btl-GAL4 drove strong expression of Arm^{S10} throughout the tracheal system (Fig. 5B), as assessed using an antibody directed against the myc-epitope. Arm^{S10} protein accumulated throughout tracheal cells, including in cell processes, although it was enriched in tracheal nuclei (Fig. 5B). The level of activated Arm expression, as measured by immunoblotting, was higher than those driven by Elav-GAL4 (Fig. 2). By comparison with e22c-GAL4 (Cox *et al.*, 1999) and taking into account the relatively small proportion of the embryo which gives rise to the trachea, it appears that levels of Arm^{S10} accumulation driven by btl-GAL4 likely approximate or exceed the levels of endogenous Arm.

Many aspects of tracheal development appeared unperturbed by Arm^{S10} expression driven by btl-GAL4. The proper pattern and approximately correct number of tracheal cells were present soon after invagination, as revealed by Fas II staining (Fig. 5C vs. 5D). These cells were able to migrate to distant locations, as do wild-type tracheal cells, and to form many normal tracheal structures. For example, tracheal cells organized dorsal and lateral longitudinal trunks, as well as dorsal tracheal branches, transverse connectives, and visceral tracheal branches (Fig. 5E vs. 5F). In fact, many segments of individual embryos looked nearly normal. Normal-looking terminal branches were also observed (Fig. 5I vs. 5J). One striking and consistent defect was noted, however. In many segments, we noted a pronounced hypertrophy of the presumptive dorsal longitudinal trunk, often associated with a corresponding reduction in the

---

the tracheal lumenal marker 2A12. The dorsal branches (DB) and lateral trunk (LT) appear quite normal. Ectopic loops and ventral outgrowths of the dorsal trunk (DT) are observed in the embryo expressing Arm^{S10} (red arrows). The segment with a loop lacks a normal visceral branch (VB). (G, J) Close-ups showing the cellular morphology of the normal dorsal trunk (G) and of an ectopic loop in an embryo expressing Arm^{S10} (H), revealed by antibodies to DE-cadherin. The loop has a cellular morphology similar to that of the normal dorsal trunk. (I–L) Transmitted light micrographs of first instar larvae. (I, J) Dorsal view of wild-type (I) or Arm^{S10}-expressing (J) first instar larva, showing that fine tracheal branches (arrows) can be formed even in segments with large loops in the dorsal trunk. (K, L) Lateral view of wild-type (K) or Arm^{S10}-expressing (L) first instar larva. The arrow indicates the dorsal trunk, which in the wild-type larva has filled with air, as indicated by the clear outline of the tracheal lumen. In the mutant larva, normal gas-filling has not occurred (note gaps in outline of tracheal lumen).

presumptive visceral branch (Fig. 5B). The resulting dorsal trunk was misshapen, often forming loops ventral to and reconnecting with the dorsal longitudinal trunk, or ventral outgrowths (Figs. 5B, 5F, 5H, 5J, and 5L). These loops had lumens of a diameter more similar to that of the dorsal longitudinal trunk than of the transverse connective (Fig. 5H). These defects were associated with gas-filling problems in larvae after hatching, as assessed by Nomarski optics (Fig. 5L). None of these defects was ever observed in wild-type controls.

This phenotype resembled that caused by the overexpression of the zinc-finger transcription factor Spalt (Kuhnlein and Schuh, 1996). At this point in our analysis, we learned that two other groups were independently investigating the role of the Wingless signaling pathway during tracheal development (Chihara and Hayashi, 2000; Llimargas, 2000). These groups observed similar tracheal defects resulting from activation of the Wg pathway by several means, including misexpression of Wg itself and of activated Arm. They further found that this phenotype resulted from inappropriate transcriptional activation of the *spalt* gene. This suggests that the phenotype we and they observed was not due to a direct effect of activated Arm on the cytoskeleton, but rather was mediated via its role as a transcriptional coactivator.

DISCUSSION

A novel role of β-catenin has been suggested by mammalian tissue culture studies. Activated β-catenin has an inhibitory role in HGF-induced process outgrowth and cell migration of MDCK epithelial cells (Barth *et al.*, 1997; Pollack *et al.*, 1997). Expression of activated β-catenin dramatically modulated cell behavior: the ability of cells to form colonies was altered, and their ability to send out cell processes, migrate, and form tubular processes in response to HGF was substantially reduced. Interestingly, activated forms of β-catenin had the same effects regardless of whether they were able to bind α-catenin. Although both forms of activated β-catenin bind E-cadherin, neither appeared to disrupt the function of endogenous wild-type β-catenin at the adherens junction. This suggests that activated β-catenin may disrupt other processes. The authors thus hypothesized that β-catenin acts as a negative regulator of cell migration, perhaps via its interaction with APC. This hypothesis was supported by experiments in the murine colon epithelium (Wong *et al.*, 1998). Here, epithelial migration along the crypt-villus axis was slowed by expression of activated β-catenin; here, however, the orderliness of migration was not affected, and the morphology of the epithelial cells was normal.

We tested the generality of this hypothesis by examining the effect of expressing activated Arm in several cell types in *Drosophila*, selected because cell migration and process extension are part of their normal developmental or physiological program. The experiments above led to the hypothesis that Arm/β-catenin might inhibit cell migration via effects on APC. Previous work also revealed that activated Arm is a powerful modulator of cell fate in certain tissues, via its transcriptional role. For example, it mimics activation of Wg signaling and thus shapes cell fate in the embryonic epidermis, the wing, or the eye (Pai *et al.*, 1997; Zecca *et al.*, 1996; Ahmed *et al.*, 1998). Given Arm's ability to modulate morphogenesis via transcriptional and potentially nontranscriptional effects, we anticipated that misexpression of activated Arm would have drastic consequences in the three model tissues selected.

To our surprise, the effects of activated Arm were quite modest. We first tested the effects on border cell migration or axon outgrowth. Both processes seemed good candidates to be affected, as both involve cell migration or process extension over a cellular substrate and both require cadherin–catenin function (Iwai *et al.*, 1997; Loureiro and Peifer, 1998; Niewiadomska *et al.*, 1999). However, in both cases, no significant defects were observed. We also tested whether activated Arm would alter the cell migratory events and cell shape changes that occur during morphogenesis of the tracheal system. Tracheal cells resemble the MDCK cells whose migration is affected by activated β-catenin in several ways—the two divergent cell types share the ability to migrate in columns from an epithelial progenitor, to form multicellular tubes, and also to send out long cell processes. We thus were surprised at how little perturbation of tracheal development was caused by expression of activated Arm. The cell biological abilities of tracheal cells were essentially unimpaired—cells retained the ability to migrate in columns, form tubes, and extend processes. The one striking effect that was observed appeared to be a misallocation of cells into different cell types, with more cells choosing the dorsal tube fate and fewer cells choosing the visceral branch fate. This change did result in a dramatic change in the morphogenesis of a subset of the tracheal system, as these two cell types differ significantly in their cellular behaviors.

From these data, we can draw two general conclusions. First, these data point out very clearly that the response of a cell to activated Arm/β-catenin varies substantially between different tissues. While some cells, such as the epithelial cells of the embryonic epidermis or the imaginal discs, respond to activated Arm with dramatic shifts in cell fate, other cell types, such as the border cells or postmitotic neurons, seem to be refractory to its effects. This was particularly striking as activated Arm was observed to accumulate in or even become concentrated in the nuclei of the cells in which it was expressed. This conclusion is further substantiated by a study by Schüpbach and Wieschaus (1998) in which they found that expression of activated Arm in various follicle cell subsets had little or no effect on eggshell morphology or fertility. Several possible explanations may explain this differential sensitivity. First, cells may vary in their expression of Arm's transcriptional partner dTCF—we view this as less likely, as dTCF is expressed at apparently uniform levels in different cells in

the embryo (van de Wetering *et al.*, 1997). Second, the Arm/dTCF complex may require other cofactors to regulate gene expression, which are not uniformly expressed. We feel the most likely explanation, however, is that most Wingless-target genes may only be activated by the combinatorial action of different transcription factors which deliver inputs from a variety of different signal transduction pathways (e.g., Halfon *et al.*, 2000). This allows activation of different subsets of target genes in different tissues, and also ensures that inappropriate activation of a given pathway will often not have serious consequences, unless the tissue is already programmed to respond to that pathway. Thus, for example, in the tracheae, the only cells affected by expression of activated Arm are those which normally are programmed to respond to Wg signal (Chihara and Hayashi, 2000; Llimargas, 2000; our data).

Our second conclusion is that expression of activated Arm/β-catenin does not have a general inhibitory effect on cell migration or process extension. These processes were unaffected by expression of activated Arm in the border cells or neurons, and were only affected in a small proportion of cells in the developing trachea. These observations provide a striking contrast to the dramatic effects of activated β-catenin expression in MDCK cells (Barth *et al.*, 1997; Pollack *et al.*, 1997) and the significant, though less dramatic, effects seen in the colon epithelium of mice (Wong *et al.*, 1998). It is possible that these differences could be due to differences in level of expression of activated Arm/β-catenin. However, we think this is less likely, as in our experiments (Fig. 2) and those of Barth *et al.* (1997) and Pollack *et al.* (1997), the level of expression of activated Arm/β-catenin was approximately equal to that of endogenous Arm/β-catenin, while in the experiments of Wong *et al.* (1998), the activated β-catenin accumulated to levels only three- to fivefold higher than that of the endogenous protein. There are several alternate explanations for the differences between our results and those in MDCK cells. First, as discussed above with respect to Arm/β-catenin's transcriptional effects, there may be differences in expression of partners or cofactors required for effects of β-catenin on migration—e.g., APC family members. Second, it may be that the effects observed in the MDCK and colon cells were mediated by the transcriptional role of β-catenin—in the colon, at least, it is already clear that these cells respond to activation of the Wnt pathway by altering their transcriptional profile. We and others have found that expression of activated Arm in the dorsal trunk cells of the trachea leads to dramatic alterations in the morphogenesis of this cell type; this effect is clearly due to effects on the Wg/Wnt regulated transcriptional program, with the downstream transcription factor Spalt a key target (Chihara and Hayashi, 2000; Llimargas, 2000). Thus β-catenin's role in cell migration may be primarily indirect, via alterations in cell fate mediated by its role in regulating gene expression. This can now be tested directly in mammalian cells by examining whether downstream gene expression via the TCF/LEF pathway is essential for β-catenin's effects.

ACKNOWLEDGMENTS

We thank Greg Beitel for answering many questions about tracheal development and for pointing out the work on *spalt* and Wingless signaling. We are also very grateful to Greg Beitel, Mark Krasnow, Denise Montell, and the Bloomington *Drosophila* Stock Center for fly stocks, to Mark Krasnow, Corey Goodman, and Greg Beitel for providing antibodies, to Susan Whitfield for assistance with the Figures, and to Vicki Bautch and Bob Duronio for helpful discussions. This work was supported by a grant from the National Institutes of Health to M.P. (GM47857). K.A. was supported by the UNC M.D.-Ph.D. Program, A.B. was supported by National Science Foundation Award DBI-9605149, "Research Experiences for Undergraduates," A.D. was supported by a Burroughs–Wellcome Career Award, and M.P. was supported in part by a Career Development Award from the U.S. Army Breast Cancer Research Program.

REFERENCES

Ahmed, Y., Hayashi, S., Levine, A., and Wieschaus, E. (1998). Regulation of Armadillo by a *Drosophila* APC inhibits neuronal apoptosis during retinal development. *Cell* **93,** 1171–1182.

Barth, A. I. M., Pollack, A. L., Altschuler, Y., Mostov, K. E., and Nelson, W. J. (1997). Amino-terminal deletion of β-catenin results in stable co-localization of mutant β-catenin with APC protein and altered MDCK cell adhesion. *J. Cell Biol.* **136,** 693–706.

Bloom, K. (2000). It's a kar9ochore to capture microtubules. *Nat. Cell Biol.* **2,** E96–E98.

Brower, D. L., Smith, R. J., and Wilcox, M. (1981). Differentiation within the gonads of *Drosophila* revealed by immunofluorescence. *J. Embryol. Exp. Morphol.* **63,** 233–242.

Chihara, T., and Hayashi, S. (2000). Control of tracheal tubulogenesis by Wingless signaling. *Development* **127,** 4433–4442.

Chu-Lagraff, Q., and Doe, C. (1993). Neuroblast specification and formation regulated by *wingless* in the *Drosophila* CNS. *Science* **261,** 1594–1597.

Cox, R. T., Pai, L.-M., Miller, J. M., Orsulic, S., Stein, J., McCormick, C. A., Audeh, Y., Wang, W., Moon, R. T., and Peifer, M. (1999). Membrane-tethered *Drosophila* Armadillo cannot transduce Wingless signal on its own. *Development* **126,** 1327–1335.

Halfon, M. S., Carmena, A., Gisselbrecht, S., Sackerson, C. M., Jimenez, F., Baylies, M. K., and Michelson, A. M. (2000). Ras pathway specificity is determined by the integration of multiple signal-activated and tissue-restricted transcription factors. *Cell* **103,** 63–74.

Iwai, Y., Usui, T., Hirano, S., Steward, R., Takeichi, M., and Uemura, T. (1997). Axon patterning requires DN-Cadherin, a novel neuronal adhesion receptor, in the Drosophila embryonic CNS. *Neuron* **19,** 77–89.

Kaphingst, K., and Kunes, S. (1994). Pattern formation in the visual centers of the Drosophila brain: *wingless* acts via *decapentaplegic* to specify the dorsoventral axis. *Cell* **78,** 437–448.

Kawasaki, Y., Senda, T., Ishidate, T., Koyama, R., Morishita, T., Iwayama, Y., Higuchi, O., and Akiyama, T. (2000). Asef, a link between the tumor suppressor APC and G-protein signaling. *Science* **289,** 1194–1197.

Kuhnlein, R. P., and Schuh, R. (1996). Dual function of the region-specific homeotic gene spalt during Drosophila tracheal system development. *Development* **122,** 2215–2223.

Lin, D. M., and Goodman, C. S. (1994). Ectopic and increased expression of Fasciclin II alters motoneuron growth cone guidance. *Neuron* **13,** 507–523.

Llimargas, M. (2000). wingless and its signalling pathway have common and separable functions during tracheal development. *Development* **127,** 4407–4417.

Loureiro, J., and Peifer, M. (1998). Roles of Armadillo, a *Drosophila* catenin, during central nervous system development. *Curr. Biol.* **8,** 622–632.

Luo, L., Liao, Y. J., Jan, L. Y., and Jan, Y. N. (1994). Distinct morphogenetic functions of similar small GTPases: Drosophila Drac1 is involved in axonal outgrowth and myoblast fusion. *Genes Dev.* **8,** 1787–1802.

Manning, G., and Krasnow, M. A. (1993). Development of the *Drosophila* tracheal system. In "The Development of *Drosophila melanogaster* " (M. Bate and A. Martinez-Arias, Eds.), Vol. 1, pp. 609–685. Cold Spring Harbor Laboratory Press, Cold Spring Harbor, NY.

Manseau, L., Baradaran, A., Brower, D., Budhu, A., Elefant, F., Phan, H., Philip, A. V., Yang, M., Glover, D., Kaiser, K., Palter, K., and Selleck, S. (1997). GAL4 enhancer traps expressed in the embryo, larval brain, imaginal discs, and ovary of Drosophila. *Dev. Dyn.* **209,** 310–322.

McCartney, B. M., Dierick, H. A., Kirkpatrick, C., Moline, M. M., Baas, A., Peifer, M., and Bejsovec, A. (1999). *Drosophila* APC2 is a cytoskeletally-associated protein that regulates Wingless signaling in the embryonic epidermis. *J. Cell Biol.* **146,** 1303–1318.

McCartney, B. M., and Peifer, M. (2000). Teaching tumor suppressors new tricks. *Nat. Cell Biol.* **2,** E58–E60.

Mimori-Kiyosue, Y., Shiina, N., and Tsukita, S. (2000). Adenomatous polyposis coli (APC) protein moves along microtubules and concentrates at their growing ends in epithelial cells. *J. Cell Biol.* **148,** 505–518.

Montell, D. J. (1999). The genetics of cell migration in *Drosophila melanogaster* and *Caenorhabditis elegans* development. *Development* **126,** 3035–3046.

Munemitsu, S., Souza, B., Müller, O., Albert, I., Rubinfeld, B., and Polakis, P. (1994). The APC gene product associates with microtubules *in vivo* and promotes their assembly *in vitro*. *Cancer Res.* **54,** 3676–3681.

Näthke, I. S., Adams, C. L., Polakis, P., Sellin, J. H., and Nelson, W. J. (1996). The Adenomatous Polyposis Coli (APC) tumor suppressor protein localizes to plasma membrane sites involved in active cell migration. *J. Cell Biol.* **134,** 165–180.

Nieman, M. T., Prudoff, R. S., Johnson, K. R., and Wheelock, M. J. (1999). N-cadherin promotes motility in human breast cancer cells regardless of their E-cadherin expression. *J. Cell Biol.* **147,** 631–644.

Niewiadomska, P., Godt, D., and Tepass, U. (1999). DE-Cadherin is required for intercellular motility during Drosophila oogenesis. *J. Cell Biol.* **144,** 533–547.

Pai, L.-M., Kirkpatrick, C., Blanton, J., Oda, H., Takeichi, M., and Peifer, M. (1996). *Drosophila* α-catenin and E-cadherin bind to distinct regions of *Drosophila* Armadillo. *J. Biol. Chem.* **271,** 32411–32420.

Pai, L.-M., Orsulic, S., Bejsovec, A., and Peifer, M. (1997). Negative regulation of Armadillo, a Wingless effector in *Drosophila*. *Development* **124,** 2255–2266.

Peifer, M., Orsulic, S., Sweeton, D., and Wieschaus, E. (1993). A role for the *Drosophila* segment polarity gene *armadillo* in cell adhesion and cytoskeletal integrity during oogenesis. *Development* **118,** 1191–1207.

Peifer, M., and Polakis, P. (2000). Wnt signaling in oncogenesis and embryogenesis: A look outside the nucleus. *Science* **287,** 1606–1609.

Pollack, A. L., Barth, A.I.M., Altschuler, Y., Nelson, W. J., and Mostov, K. E. (1997). Dynamics of β-catenin interactions with APC protein regulate epithelial tubulogenesis. *J. Cell Biol.* **137,** 1651–1662.

Richter, S., Hartmann, B., and Reichert, H. (1998). The wingless gene is required for embryonic brain development in Drosophila. *Dev. Genes Evol.* **208,** 37–45.

Rorth, P., Szabo, K., Bailey, A., Laverty, T., Rehm, J., Rubin, G. M., Weigmann, K., Milan, M., Benes, V., Ansorge, W., and Cohen, S. M. (1998). Systematic gain-of-function genetics in Drosophila. *Development* **125,** 1049–1057.

Schüpbach, T., and Wieschaus, E. (1998). Probing for gene specificity in epithelial development. *Int. J. Dev. Biol.* **42,** 249–255.

Sheppard, D. (2000). In vivo functions of integrins: Lessons from null mutations in mice. *Matrix Biol.* **19,** 203–209.

Shiga, Y., Tanaka-Matakatsu, M., and Hayashi, S. (1996). A nuclear GFP/β-galactosidase fusion protein as a marker for morphogenesis in living Drosophila. *Dev. Growth Differ.* **38,** 99–106.

Smith, K. J., Levy, D. B., Maupin, P., Pollard, T. D., Vogelstein, B., and Kinzler, K. W. (1994). Wild-type but not mutant APC associates with the microtubule cytoskeleton. *Cancer Res.* **54,** 3672–3675.

Su, L. K., Burrell, M., Hill, D. E., Gyuris, J., Brent, R., Wiltshire, R., Trent, J., Vogelstein, B., and Kinzler, K. W. (1995). APC binds to the novel protein EB1. *Cancer Res.* **55,** 2972–2977.

Tanentzapf, G., Smith, C., McGlade, J., and Tepass, U. (2000). Apical, lateral, and basal polarization cues contribute to the development of the follicular epithelium during Drosophila oogenesis. *J. Cell Biol.* **151,** 891–904.

Townsley, F. M., and Bienz, M. (2000). Actin-dependent membrane association of a Drosophila epithelial APC protein and its effect on junctional armadillo. *Curr. Biol.* **10,** 1339–1348.

van de Wetering, M., Cavallo, R., Dooijes, D., van Beest, M., van Es, J., Loureiro, J., Ypma, A., Hursh, D., Jones, T., Bejsovec, A., Peifer, M., Mortin, M., and Clevers, H. (1997). Armadillo coactivates transcription driven by the product of the *Drosophila* segment polarity gene *dTCF*. *Cell* **88,** 789–799.

Wong, M. H., Rubinfeld, B., and Gordon, J. I. (1998). Effects of forced expression of an NH2-terminal truncated β-catenin on mouse intestinal epithelial homeostasis. *J. Cell Biol.* **141,** 765–777.

Yu, X., and Bienz, M. (1999). Ubiquitous expression of a Drosophila adenomatous polyposis coli homolog and its localization in cortical actin caps. *Mech. Dev.* **84,** 69–73.

Zecca, M., Basler, K., and Struhl, G. (1996). Direct and long-range action of a wingless morphogen gradient. *Cell* **87,** 833–844.

Received for publication January 18, 2001
Revised March 15, 2001
Accepted April 5, 2001
Published online May 30, 2001

Article

Abelson kinase regulates epithelial morphogenesis in *Drosophila*

Elizabeth E. Grevengoed,[1] Joseph J. Loureiro,[2] Traci L. Jesse,[3] and Mark Peifer[1,2,3]

[1]Curriculum in Genetics and Molecular Biology, [2]Department of Biology, and [3]Lineberger Comprehensive Cancer Center, University of North Carolina at Chapel Hill, Chapel Hill, NC 27599

Activation of the nonreceptor tyrosine kinase Abelson (Abl) contributes to the development of leukemia, but the complex roles of Abl in normal development are not fully understood. *Drosophila* Abl links neural axon guidance receptors to the cytoskeleton. Here we report a novel role for *Drosophila* Abl in epithelial cells, where it is critical for morphogenesis. Embryos completely lacking both maternal and zygotic Abl die with defects in several morphogenetic processes requiring cell shape changes and cell migration. We describe the cellular defects that underlie these problems, focusing on dorsal closure as an example. Further, we show that the Abl target Enabled (Ena), a modulator of actin dynamics, is involved with Abl in morphogenesis. We find that Ena localizes to adherens junctions of most epithelial cells, and that it genetically interacts with the adherens junction protein Armadillo (Arm) during morphogenesis. The defects of *abl* mutants are strongly enhanced by heterozygosity for *shotgun*, which encodes DE-cadherin. Finally, loss of Abl reduces Arm and α-catenin accumulation in adherens junctions, while having little or no effect on other components of the cytoskeleton or cell polarity machinery. We discuss possible models for Abl function during epithelial morphogenesis in light of these data.

Introduction

The nonreceptor tyrosine-kinase Abl is the cellular homologue of *v-abl*, the transforming gene of Abelson (Abl)* murine leukemia virus (for review see Zou and Calame, 1999; Mauro and Druker, 2001). Bcr-Abl, an activated, chimeric form of Abl resulting from a chromosomal translocation, plays a causative role in human chronic myelogenous and acute lymphocytic leukemia. Bcr-Abl has deregulated tyrosine kinase activity, and an inhibitor of this kinase has shown promise in treating leukemia. Multiple substrates for oncogenic Abl kinase in diverse signaling pathways have been identified, revealing complex effects of Abl misregulation.

Abl's normal role has remained more elusive. Abl homologues are found in all animals. All share conserved NH_2-terminal SH3, SH2, and tyrosine kinase domains, as well as distinct COOH-terminal F- and G-actin binding domains (for review see Lanier and Gertler, 2000). Mammalian Abl, unlike its fly homologue, also contains nuclear import and export signals and a COOH-terminal DNA binding domain, and thus it localizes to both nuclei and the cytoplasm. In nuclei, it is thought to regulate the cell cycle and the response to DNA damage (for review see Van Etten, 1999). Cytoplasmic Abl predominantly associates with the actin cytoskeleton (e.g., van Etten et al., 1994) and can be found at cell–matrix junctions in cultured cells (Lewis et al., 1996). The different subcellular pools of Abl may perform distinct functions, though Abl can translocate to nuclei in response to cytoplasmic cues (Lewis et al., 1996). Bcr-Abl exclusively localizes to the cytoplasm, suggesting that its role in oncogenesis involves cytoplasmic targets.

In *Drosophila*, Abl localizes to the axons of the central nervous system (CNS) (Bennett and Hoffmann, 1992). In epithelial cells, Abl's localization varies with stage of development and tissue, but it is often concentrated near the apical cortex. Abl localizes to apical cell junctions soon after cells form and to the apical cytoplasm during gastrulation and in imaginal discs. In contrast, it is diffusely cytoplasmic in extended germband embryos.

Genetic analyses in mice and flies have begun to shed light on Abl's biological function. *abl* mutant mice are embryonic-viable but runted and exhibit defects in develop-

The online version of this paper contains supplemental material.

Address correspondence to Mark Peifer, CB#3280, Department of Biology, Coker Hall, University of North Carolina at Chapel Hill, Chapel Hill, NC 27599-3280. Tel.: (919) 962-2271. Fax: (919) 962-1625. E-mail:peifer@unc.edu

Elizabeth E. Grevengoed and Joseph J. Loureiro contributed equally to this paper.

*Abbreviations used in this paper: Abl, Abelson; abl^{MZ}, *abl* maternal/zygotic; Arm, Armadillo; CNS, central nervous system; dab, disabled; Ena, Enabled; GFP, green fluorescent protein; scb, scab; shg, shotgun.

Key words: Abelson kinase; Armadillo; adherens junctions; enabled; *Drosophila*

ment of the bones, immune system, and sperm. A null mutation and a COOH-terminal truncation removing the actin binding domains have similar phenotypes, suggesting that the interaction with actin is functionally important (for review see Van Etten, 1999). Analysis of Abl function in mice is complicated by the presence of the related kinase Arg; mice lacking both *abl* and *arg* die as embryos with defects in neurulation that may reflect problems in actin organization (Koleske et al., 1998).

In *Drosophila*, analysis of the single Abl homologue primarily revealed roles in neural development. *abl* mutants are pupal lethal with defects in retinal development (Henkemeyer et al., 1987); they also have subtle CNS defects in which certain axons stop short of innervating their target muscles (Wills et al., 1999b). Much more severe CNS defects are seen in *abl* mutants that are also heterozygous or homozygous for the neural cell adhesion molecule *fasciclin*, the receptor tyrosine phosphatase *dLAR*, the axon guidance receptor *robo*, the adaptor *disabled (dab)*, the Rho-family GEF *trio*, or the actin regulator *profilin* (for review see Lanier and Gertler, 2000). These data led to a model in which Abl transduces signals from neural cell surface receptors, influencing actin dynamics in growth cones.

In doing so, Abl is thought to act via one of its substrates, Enabled (Ena; Comer et al., 1998). Originally identified as a suppressor of *abl; dab/+* mutants (Gertler et al., 1990), Ena is a member of the Ena/VASP family (for review see Lanier and Gertler, 2000), which modulate actin dynamics (Gertler et al., 1996). *Drosophila ena* mutants are embryonic lethal with defects in the CNS and its peripheral projections (Gertler et al., 1990; Wills et al., 1999a). The effects of *ena* mutations are opposite to those of *abl;* axons go past their muscle targets rather than stopping short, consistent with the idea that Abl negatively regulates Ena. Like Abl, Ena is thought to act downstream of the axon guidance receptors Robo (Bashaw et al., 2000) and dLAR (Wills et al., 1999a), mediating cytoskeletal events.

Our interest in *abl* emerged from its genetic interactions with the adherens junction protein Armadillo (Arm; Loureiro and Peifer, 1998). We investigate morphogenesis, the process by which animals create their complex body plans by organized cell shape changes and rearrangements. Epithelial cells must remain in intimate contact throughout morphogenesis, and in order to change shape or move must coordinate their actin cytoskeletons. Cells accomplish these tasks via cell–cell adherens junctions, which form a continuous adhesive belt around the apex of each cell that anchors a contractile ring of actin filaments (for review see Tepass et al., 2000). Junctions are organized around transmembrane cadherins. Human E-cadherin mediates cell–cell adhesion and organizes a multiprotein complex of catenins bound to its cytoplasmic tail, binding directly to β-catenin, which in turn anchors actin via interactions with α-catenin. *Drosophila* E-cadherin, Arm (the β-catenin homologue), and α-catenin function similarly.

Cadherin-catenin–mediated adhesion must be dynamic, allowing cell movement during morphogenesis (for review see Tepass et al., 2000). We used a genetic approach in *Drosophila* to identify regulators of epithelial morphogenesis. *abl* mutations substantially enhance the CNS defects of *arm* mutants. Further, *abl* genetically interacts with *arm* in the epidermis (Loureiro and Peifer, 1998). This suggested that Abl acts in epidermal cells during morphogenesis. Thus, we investigated whether Abl regulates epithelial development in *Drosophila*. Previous studies of Abl function relied on zygotic mutations, and thus the maternal contribution of Abl may have masked roles in other developmental processes. We removed this maternal contribution, analyzing *abl* maternal/zygotic mutants. This revealed a requirement for Abl in epithelial morphogenesis. Here we report the characterization of this role.

Results

Abelson is essential for embryonic morphogenesis

Previous studies identified a role for Abl in the CNS. Zygotic *abl* mutants have subtle CNS defects, that are enhanced in double mutant combinations (for review see Lanier and Gertler, 2000). We found previously that *abl* interacts with *arm* in its role as a catenin during CNS development (Loureiro and Peifer, 1998), where Arm works with N-cadherin (Iwai et al., 1997). We also observed genetic interactions between *abl* and *arm* in the epidermis. Thus, we hypothesized that Abl might also act in epithelial cells, and that this role might be masked by maternally contributed Abl. To test this, we removed maternal and zygotic Abl using the FLP dominant female sterile technique (Chou and Perrimon, 1996) to generate *abl* heterozygous females whose germ lines are homozygous *abl* mutant. These females contribute no wild-type Abl to their progeny. When crossed to

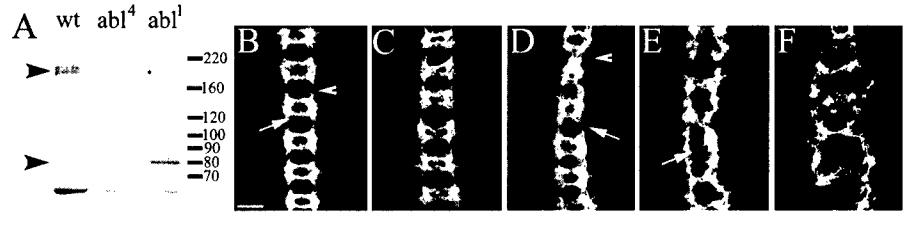

Figure 1. **Complete loss of Abl disrupts CNS development.** (A) Cell extracts from 3-h-old wild-type embryos or embryonic progeny of females with *abl* mutant germlines, immunoblotted with anti-Abl antibody. Wild-type Abl is ~180 kD (top arrow). abl^4 does not produce a protein recognized by this antibody. abl^1 produces a truncated protein product of ~80 kD (bottom arrow). (B–F) Embryos (anterior up) labeled with mAb BP102, which labels all axons. (B) Wild-type CNS, with a scaffold of longitudinal (arrowhead) and commissural (arrow) axons. (C and D) Maternally *abl* mutant but zygotically-rescued embryos have relatively wild-type CNS development, with occasional collapsed longitudinal axons (D, arrowhead) and gaps in axon bundles (D, arrow). (E and F) abl^{MZ} mutants exhibit severe disruptions in CNS development. Most exhibit loss of commissural axons (arrow, E) and some have defects in both longitudinal and commissural axons (F). Bar, 25 μm.

Table I. **Embryonic viability of *abl* maternal and zygotic mutants**

Genotype	Percentage hatched	*n*
abl^1 glc x +/+	92.9	878
abl^4 glc x +/+	89	365
abl^4 glc x shg^2/+	39.5	283[a]
abl^1 glc x shg^2/+	71.1	669[a]
abl^4 glc x shg^{R69}/+	70.4	409[a]
abl^1 glc x scb^2/+	92.3	339[a]
abl^1 glc x abl^1/+	41.0	751[b]
abl^4 glc x abl^4/+	35.6	1149[b]
abl^4 glc; TnAblWT or + x abl^4/+	76	290[c]
abl^4 glc; TnAblK-N or + x abl^4/+	40	299[c]
abl^4 glc; *ena* or +/+ x abl^4/+	61	142[c]
abl^4 glc x shg^2/+; abl^4/+	35.4	398
abl^4 glc x shg^{R69}/+; abl^4/+	38	522

glc, germline clone; TnAblWT, wild-type Abl transgene; TnAblK-N, a kinase-dead Abl trangene (Henkemeyer et al., 1990).
[a]These *shg* or *scb* mutants were balanced with *CyO*.
[b]These *abl* mutants were balanced with TM3.
[c]Only half of the mothers carried the indicated Abl transgene or were heterozygous for *ena*.

abl heterozygous males, half the progeny are maternally and zygotically *abl* mutant, while the other half receive a wild-type copy of *abl* paternally. We used two *abl* alleles: abl^1 produces a truncated protein, and abl^4 is a protein null (Bennett and Hoffmann, 1992; Fig. 1 A). The results were essentially identical with both alleles, and, where tested, were identical when embryos were transheterozygotes.

Embryos lacking both maternal and zygotic Abl (below referred to as abl^{MZ}) die at the end of embryogenesis, while those that receive wild-type paternal Abl survive and go on to adulthood (Table I and unpublished data). Since Abl's role was first defined in the CNS, we examined axon outgrowth using the antibody BP102, which labels all axons of the ventral nerve cord. Zygotic *abl* mutant embryos have subtle defects in CNS development (Wills et al., 1999b). We found that in *abl* maternal mutants that are paternally rescued (identified using a green fluorescent protein [GFP]-marked chromosome), the CNS is normal or has subtle defects (Fig. 1, C and D) which resemble those of *abl dab/abl+* embryos (Gertler et al., 1989). In contrast, maternal/zygotic *abl* mutants have severe defects in CNS development (Fig. 1, E and F). One common feature was a reduction in the commissures which cross the midline. This phenotype resembles that of *abl dab* double mutants (Gertler et al., 1989) and is consistent with previous analysis of the effects of Abl overexpression, which had the opposite effect: enhanced midline crossing (Bashaw et al., 2000). Thus, maternal Abl obscures a role for Abl in CNS axon outgrowth.

We then examined whether Abl plays a role in epithelial development that is obscured by maternally contributed Abl. We first looked at the cuticle, secreted by the epidermal epithelium. abl^{MZ} mutants exhibit defects in three morphogenetic processes, all of which require orchestrated cell shape changes and cell migration: germband retraction, head involution, and dorsal closure (Table II). Approximately 7% of abl^{MZ} mutants completely fail to germband retract or complete head involution (Fig. 2 B), whereas ~14% exhibit partial germband retraction and dorsal closure defects (Fig. 2 C). Approximately 67% of abl^{MZ} mutants have more subtle defects in dorsal closure (Fig. 2, D and F), whereas ~12% are wild-type in appearance or have minor head involution defects. In contrast, *abl* maternal mutants that inherit a paternal wild-type *abl* gene are rescued to normal embryogenesis and adulthood; most hatching larvae are wild-type whereas 5% have slight defects in germband retraction and dorsal patterning. Previous work revealed that certain Abl functions require kinase activity, whereas others do not (Henkemeyer et al., 1990). We found that maternal Abl's role in morphogenesis requires kinase activity, as both the embryonic phenotype and adult viability are rescued by a kinase-active Abl transgene but not by a kinase-dead version (Table I; unpublished data).

One important clue to Abl's function may come from its intracellular localization. Previous work (Bennett and Hoffmann, 1992) documented that *Drosophila* Abl is found in axons of the CNS. Abl is also expressed in epithelial cells, with enrichment in the apical cortical cytoplasm during cellularization, early gastrulation, and in the epithelial cells of the imaginal discs. In later embryos, it is diffuse in the cytoplasm. The original Abl antibody from the Hoffmann lab is no longer available. We attempted to extend this work by generating an anti-Abl polyclonal antibody. This works well on

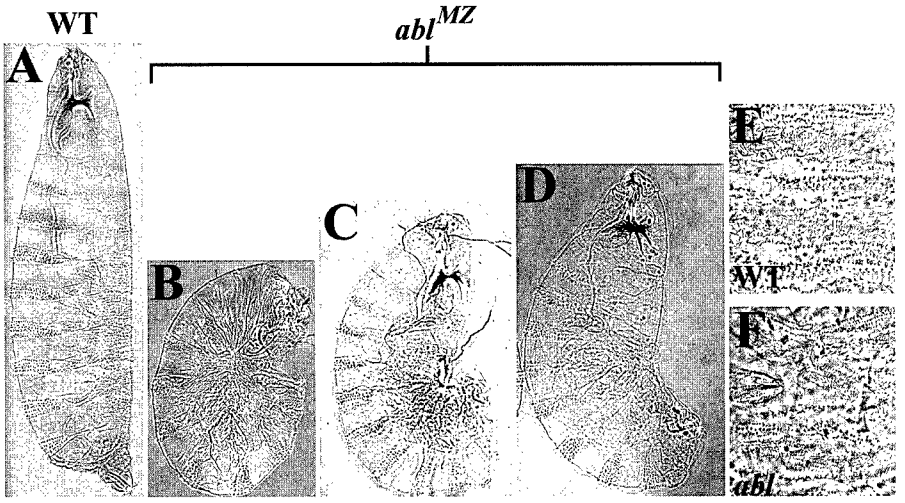

Figure 2. **abl^{MZ} mutants have defects in epithelial morphogenesis.** Cuticle preparations, anterior up. In A–D, dorsal is to the right. (A) Wild-type. (B–D) The range of phenotypes in abl^4 maternal/zygotic mutants, a similar range is observed in abl^1 . (B) Approximately 7% of abl^{MZ} mutants have head involution defects and completely fail to germband retract. (C) ~14% of abl^{MZ} mutants partially fail to germband retract and have variable dorsal closure defects. Note the dorsal hole (arrow). (D) Approximately 67% of abl^{MZ} mutants have dorsal closure defects. (E) Wild-type dorsal hair pattern. (F) Misaligned dorsal hairs in abl^{MZ} mutant.

Table II. **Percentage of dead embryos which have the following defects**

Genotype	U-shaped[a]	Tail-up[b]	Dorsal defects[c]	Wild-type	Dorsal and head defects[d]	*n*
	%	%	%	%	%	
abl^4 glc x +/+			Not applicable as almost all hatch			
abl^4 glc x shg^2/+	7	2	45	6	40	298
abl^4 glc x shg^{R69}/+	10	2	54	2	32	121
abl^4 glc x abl^4/+	7	14	67	6	6	388
abl^4 glc x shg^2/+; abl^4/+	2	5	13	10	70	141
abl^4 glc x shg^{R69}/+; abl^4/+	3	1	60	4	38	307
abl^1 glc x abl^1/+	1	13	67	17	1	91
abl^1 glc x scb^2/+; abl^1/+	3	8	75	10	5	63

[a]Embryos in this class exhibited a complete failure in germband retraction.
[b]Embryos in this class exhibited strong defects in germband retraction and also often had defects in dorsal closure.
[c]Embryos in this class exhibited defects in dorsal closure ranging from dorsal holes to defects in the dorsal pattern.
[d]Embryos in this class exhibited severe defect in head involution; most also showed defects in dorsal closure and/or germband retraction.

immunoblots (Fig. 1 A), but does not show specific staining in situ, as assessed using embryos maternally and zygotically mutant for the protein-null abl^4 (unpublished data).

Loss of Abl disrupts cell migration and cell shape changes during dorsal closure

Previous studies supported a role for Abl in signaling from cell surface receptors to the actin cytoskeleton during axon outgrowth (Wills et al., 1999a; Bashaw et al., 2000). Having identified a role for Abl in epithelial tissues, we hypothesized that Abl might act there by a similar mechanism. One place to address this is during dorsal closure, when lateral epidermal epithelial sheets migrate toward the dorsal midline, enclosing the embryo in epidermis. Dorsal closure involves dynamic actin reorganization to form an acto-myosin purse string in cells at the leading edge of the sheet (Young et al., 1993), as well as orchestrated cell shape changes and cell migration (Kiehart et al., 2000). Since Abl plays a role in dorsal closure, we wondered whether Abl modulates these cellular events.

To compare cell shape changes and cell migration in wild-type and abl^{MZ} mutants, we examined embryos during dorsal closure, using antiphosphotyrosine to label both adherens junctions and the leading edge actin cable. As wild-type dorsal closure initiates, leading edge cells elongate uniformly along the dorsal-ventral axis, perpendicular to the leading edge (Fig. 3 A, arrow). As closure proceeds, successive rows of cells lateral to the leading edge also uniformly elongate (Fig. 3, B and C, arrow). The lateral epithelial sheets eventually meet at the dorsal midline, and cells intercalate with one another, making the dorsal surface a continuous epithelial sheet with little midline discontinuity (Figs. 3, D and E, arrow).

abl^{MZ} mutants have striking defects in the cellular events of dorsal closure. Cells fail to change shape in a coordinated fashion (Fig. 3, F–J). As leading edge cells begin to elongate, cells do not elongate uniformly in comparison to their neighbors (Fig. 3, F and G, arrows), and groups of cells have overly broad or narrowed leading edges (arrowheads). As cell shape is likely maintained against tension along the leading edge from the actin cable, altered cell shapes may result from alterations in the polymerization or anchoring of actin (see below). We also observed groups of cells that completely fail to change shape (Fig. 3, G–I, asterisks). As closure proceeds, the cell shape defects persist as cells behind the leading edge begin to elongate (Fig. 3, G–I). Not all abl^{MZ} mutants close dorsally, but those that do show a variety of defects at the cellular level. Some embryos maintain groups of cells that have never elongated (Fig. 3 I, asterisks). Other embryos fail to properly align the opposing epithelial sheets at the midline upon completion of closure (Fig. 3 J, arrow), likely contributing to the altered dorsal hair patterning evident in the cuticles (Fig. 2 F). A subset of the abl^{MZ} mutants fail to complete germband retraction (Figs. 2 C and 3, K and L). In these embryos, cells along the leading edge exhibit the same cell shape abnormalities during dorsal closure as mutants that complete germband retraction (Fig. 3 L, arrows). A fraction of the cells in abl^{MZ} mutants become multinucleate due to defects in cellularization (unpublished data). We verified that cell shape and migration defects during dorsal closure are independent of cell shape disruption due to polyploidy (Fig. 3 O).

The failure to initiate uniform cell shape changes in abl^{MZ} mutants is similar to the phenotype we observed in *arm* zygotic mutants (McEwen et al., 2000). These embryos have only maternal Arm, and thus their levels of wild-type Arm are substantially reduced. While *arm* mutants are more severely compromised in their ability to complete dorsal closure than are abl^{MZ} mutants, leading edge cells of both *arm* (Fig. 3, M and N) and abl^{MZ} mutants fail to elongate uniformly as closure is initiated.

The defects in cell morphology during dorsal closure in abl^{MZ} mutants led us to examine localization of actin and of the Abl target Ena, an actin regulator during this process. In the initial stages of dorsal closure, as cells along the leading edge begin to elongate, Ena surrounds the cell membrane but is enriched at vertices of cell–cell contact and at adherens junctions of leading edge cells (Fig. 4 A, left, red). Actin localizes around the entire cell and begins to accumulate at the leading edge at this stage (Fig. 4 A, middle, green; Young et al., 1993). As closure proceeds, Ena accumulates at uniformly high levels in adherens junctions of leading edge cells (Fig. 4 C, left, red), while actin forms a uniform and tightly localized band along the leading edge (Fig. 4 D middle, green).

The localization of both Ena and actin is altered during dorsal closure in abl^{MZ} mutants, and these changes parallel the changes in cell shape. As closure initiates, Ena is enriched at adherens junctions, but the level of Ena is not

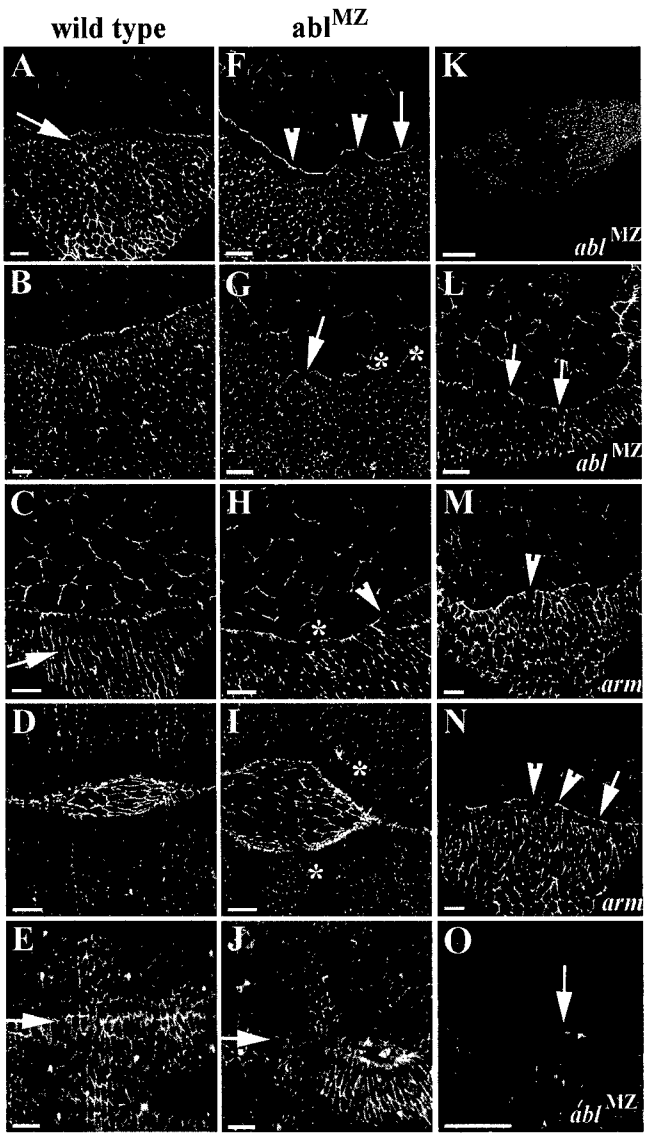

Figure 3. ***abl*^{MZ} mutants fail to undergo coordinated changes in cell shape during dorsal closure.** Embryos labeled with antiphosphotyrosine. Anterior is to the left. (A–E) Wild-type at progressively later stages of dorsal closure. (A–C) Lateral views. (D and E) Dorsal views. (A) Leading edge cells have begun to uniformly elongate (arrow). (B and C) Successive lateral cell rows uniformly elongate (arrow). (D) Lateral epithelial sheets zip together. (E) Closure is complete, with lateral epithelial cells evenly matched at the midline (arrow). (F–J) *abl*^{MZ} mutants at progressively later stages of dorsal closure. (F–H) Lateral and (I–J) dorsal views. (F) Leading edge cells do not elongate uniformly (arrow). Some cells have broadened or constricted leading edges (arrowheads). (G and H) Lateral cells have begun to elongate, but do so nonuniformly (arrow). Some cells have broadened or narrowed leading edges (arrowheads). Other groups of cells completely fail to elongate (asterisks). (I) *abl*^{MZ} mutants that proceeded through dorsal closure. Small groups of cells have still completely failed to change shape (asterisks). (J) *abl*^{MZ} mutant that completed closure. Epithelial sheets often fail to align properly at the midline (arrow). (K and L) Some *abl*^{MZ} mutants initiate dorsal closure even though they have not completed germband retraction. Cell shape defects are also seen in these embryos (arrows). (M and N) *arm*^{XP33} mutants have cell shape defects similar to *abl*^{MZ} mutants. Cells fail to elongate uniformly (arrow) and have broadened or narrowed leading edges (arrowheads). (O) Cell shape defects in *abl*^{MZ} mutants are not caused by multinucleate cells. *abl*^{MZ}, double-labeled with antiphosphotyrosine and with propidium iodide, labeling nuclei. Mononucleate cells have defects in shape (arrow). Bars: (A–J and L–O) 10 μm; (K) 50 μm.

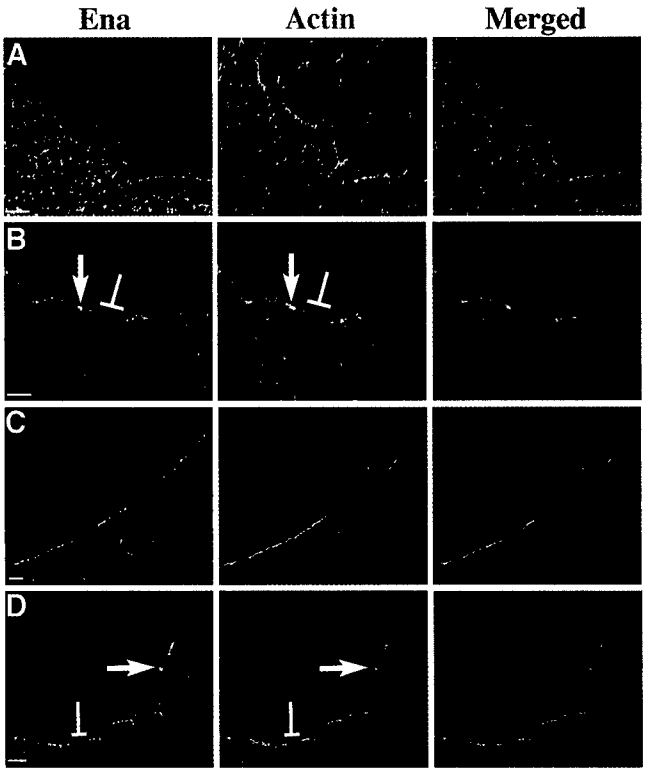

Figure 4. **Complete loss of Abl alters Ena and actin localization during dorsal closure.** Lateral view. Embryos double-labeled with anti-Ena (red) and phalloidin (green), labeling F-actin. (A) Stage 13 wild-type embryo with leading edge cells initiating elongation. Ena (left, red) is enriched at vertices of cell–cell contact. Actin (middle, green) outlines all cell membranes and is beginning to accumulate at the leading edge. Actin and Ena colocalize at cell junctions. (B) Stage 13 *abl*^{MZ} mutant. Ena (left, red) and Actin (middle, green) enrichment is not uniform at the leading edge. Both are enriched in some cells (arrows) and depleted in others (brackets). (C) Stage 14 wild-type embryo. More lateral cells have undergone uniform elongation. Ena is uniformly enriched at adherens junctions of leading edge cells (left, red). Actin forms a tight cable along the leading edge (middle, green). Ena and actin colocalize at adherens junctions as actin expands along the entire leading edge. (D) Stage 14 *abl*^{MZ} mutant. Nonuniform localization of Ena and Actin persists. Cells with excess Ena (left, arrow) often accumulate excess Actin (middle, arrow), whereas cells with diminished Ena levels (left, bracket) have diminished levels of Actin (middle, bracket) Bars, 10 μm.

uniform in different cells (Fig. 4 B, arrow vs. bracket). The actin cable is also not uniform; levels of actin often change in parallel to Ena (Fig. 4 B). This uneven distribution of Ena and actin persists throughout dorsal closure (Fig. 4 D). Changes in Ena and actin levels often correlate with defects in cell shape. Cells with constricted leading edges tend to accumulate abnormally high levels of both proteins, whereas cells with broadened leading edges tend to have lower levels of Ena in junctions and lower levels of leading edge actin. This correlation may be explained by the fact that the leading edge is under tension, presumably due to the contractile actin cable (Kiehart et al., 2000). Defects in actin cable assembly or anchoring within individual cells could lead those cells to splay open at the leading edge; adjacent cells might then hypercontract due to the release of the tension normally exerted by their neighbors.

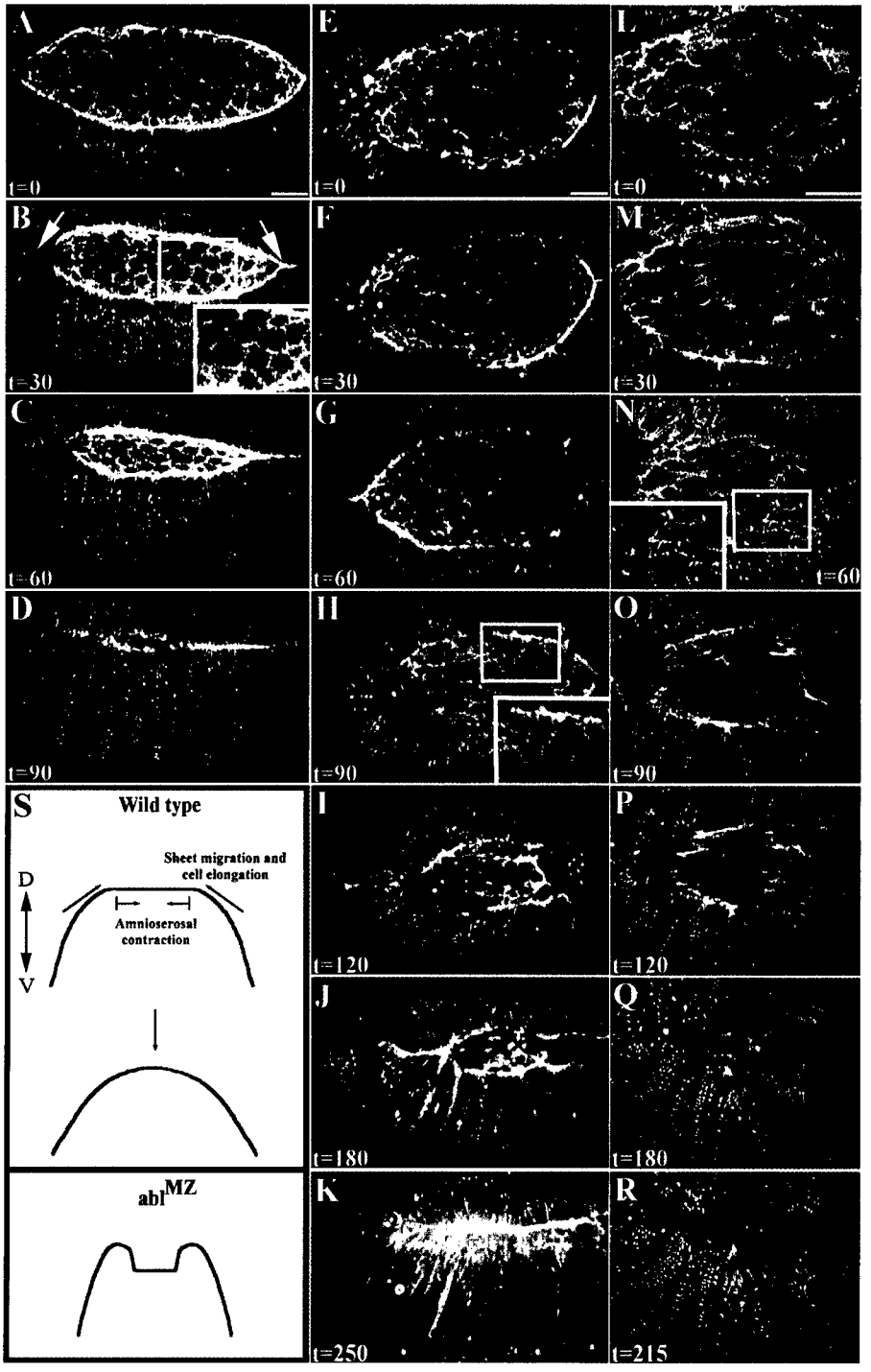

Figure 5. **Dorsal closure is substantially slowed in *abl*^{MZ} mutants.** Dorsal view of embryos expressing moesin-GFP, anterior to the right. Time is in minutes. Insets in (B, H, and N) display actin-rich filopodia extending from amnioserosa or leading edge cells. (A–D) Wild-type embryo at 30 min intervals during dorsal closure. (A) The leading edge of the dorsal closure front is uniformly enriched in actin. Lateral epithelial sheets elongate uniformly. (B) 30 min. Amnioserosa cells are undergoing apical constriction and the embryo is zipping together at the anterior and posterior ends (arrows). (C) 60 min. Amnioserosa cells have constricted apically and remain in the same plane of focus as the lateral epithelial sheets. (D) 90 min. Dorsal closure is complete. (E–K) *abl*^{MZ} mutant. The amnioserosa cells in E are comparable in surface area to the wild-type in A. (F–H) As closure progresses, amnioserosa cells constrict and lateral epithelial cells elongate, but dorsal closure is delayed relative to wild-type (compare D and H). If one matches embryos based on the length of the leading edge (compare A and G), closure is still delayed. This embryo took >4 h to complete closure (K). (L–R) A different *abl*^{MZ} mutant at higher magnification, illustrating the folding-under of the leading edge and failure to complete closure. (S) Cross-section diagram depicting one interpretation of the defects of *abl*^{MZ} mutants. In wild-type embryos, the rate at which lateral cells elongate, the sheets migrate, and amnioserosa cells constrict are tightly coordinated. In *abl*^{MZ} mutants, the leading edge folds under the more lateral epidermis, perhaps because leading edge cells migrate too slowly or amnioserosa cell constriction is slowed (these events are likely coupled), forcing the sheet to fold under. Time-lapse videos supplementing this figure are available at http://www.jcb.org/cgi/content/full/jcb.200105102/DC1. Bars, 25 μm.

Dorsal closure is slowed in *abl* mutants

Multiple forces drive dorsal closure, including forces generated by cell shape changes, contraction of the leading edge actin-myosin cable, and pulling forces exerted by amnioserosa cells. These forces act combinatorially, so disruption of one force slows but does not prevent closure (Kiehart et al., 2000). *abl*^{MZ} mutants display defects in both cell shape and in the actin cable, yet many embryos complete closure, albeit imperfectly. To analyze how *abl*^{MZ} mutants compensate for disruptions in cell shape and the actin cable, we performed time-lapse confocal microscopy on embryos undergoing closure (see videos available at http://www.jcb.org/cgi/content/full/jcb.200105102/DC1). We analyzed transgenic flies expressing the actin binding domain of Moesin fused to GFP (Kiehart et al., 2000), allowing us to visualize actin dynamics in real time.

During dorsal closure in living wild-type embryos, the leading edge becomes uniformly enriched in actin as leading edge cells elongate (Fig. 5 A). Amnioserosa cells, the large squamous cells exposed on the dorsal surface of the embryo, undergo apical constriction (Kiehart et al., 2000), decreasing in surface area throughout closure (Fig. 5, A–D). Finally, as the lateral epithelial sheets migrate toward one another, closure is initiated at the anterior and posterior ends of the opening (Fig. 5 B, arrows) and the sheets zip together from the ends (Fig. 5, A–D) (Jacinto et al., 2000). Once the cells

initiate elongation and the front is enriched in actin, dorsal closure is completed in a little over 1.5 h.

Dorsal closure is substantially slowed in abl^{MZ} mutants. It is not simple to define an equivalent starting point for abl^{MZ} and wild-type embryos, as the dorsal/ventral extent of the amnioserosa is larger in abl^{MZ} mutants, both in cell number and distance (compare Fig. 5 A to E). This may be due to defects in cell rearrangements during germband retraction. However, regardless of whether we compared embryos with equivalent amnioserosa surface areas (Fig. 5 A vs. E) or with roughly equivalent length leading edges (Fig. 5 A vs. G), closure is substantially delayed in abl^{MZ} mutants, taking two to three times longer than normal. At the cellular level, lateral cells elongate on schedule in the mutants (despite defects in cell shape) and amnioserosa cells apically constrict, though more slowly than in wild-type.

Time-lapse imaging also revealed defects that were not apparent in our fixed images. As closure proceeds, the leading edge of the lateral epidermis folds under the more lateral cells that follow it (Fig. 5, J, Q, and R). This suggests that while lateral epithelial cells continue to elongate and migrate, driving sheet extension, leading edge cells do not migrate toward one another at an appropriate rate (diagram in Fig. 5 S). Our movies also suggest that filopodial extensions from the leading edge might aid in the eventual closure, as they do in wild-type (Jacinto et al., 2000), actively zipping the epidermal sheets together. Filopodial extensions from epidermal and amnioserosa cells are present in both wild-type and abl^{MZ} mutants, and even appear more fre-

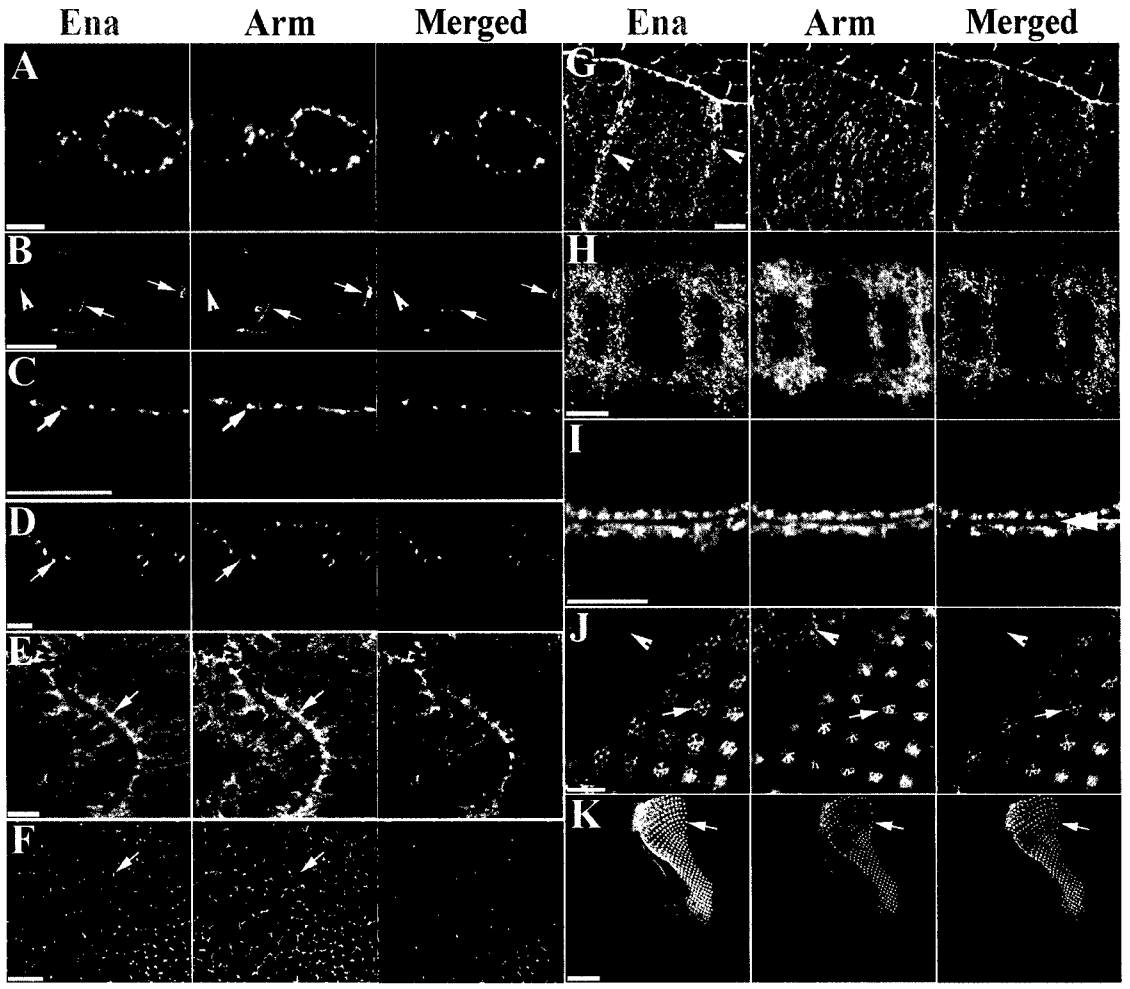

Figure 6. **Ena and Arm colocalize at adherens junctions throughout development.** All images (except I) are anterior to the right. Ena is green and Arm is red in merged images. (A) Stage 3 egg chamber. Ena and Arm are enriched in apical adherens junctions of follicle cells. (B and C) Stage 10 egg chamber. Levels of Ena and Arm drop, but both remain at adherens junctions. Anterior (border cells) and posterior polar follicle cells are enriched in both Ena and Arm (B, arrows). Ena and Arm also colocalize to nurse cell membranes (B, arrowhead). (D–G) During embryogenesis Ena and Arm colocalize to adherens junctions of epithelial tissues. (D) Cross-section, stage 9 embryo. Ectodermal adherens junctions (arrow). (E) Adherens junctions of polarized cells of the invaginating hindgut (arrow). (F) Apical view, stage 9 embryo. Ena is enriched at vertices of cell–cell contact (arrow), whereas Arm is more uniform. (G) During dorsal closure Ena is enriched at adherens junctions of leading edge cells, but it is also found in the cytoplasm of cells at the segment boundary (arrowheads). (H) Ena and Arm both localize to axons. (I–K) Imaginal discs. (I) Apical surfaces of two epithelial sheets opposed to one another in the wing imaginal disc (arrow). Ena and Arm colocalize to apical adherens junctions, and are also found at the apical surface. (J and K) In eye imaginal discs cell differentiation occurs after the morphogenetic furrow passes. In undifferentiated cells, Ena and Arm colocalize to cell boundaries (J, arrowhead). As groups of cells begin differentiating as photoreceptors (J, arrow), Ena localizes uniformly to all cells of the precluster. Arm, in contrast, accumulates at high levels in a subset of these cells. Later, Ena and Arm colocalize in photoreceptor rhabdomeres (K, arrow). Bars: (A–J) 10 μm; (K) 50 μm.

quent in late-stage mutants (Fig. 5, B, H, and N, insets). We suspect epithelial sheet migration is compromised in *abl* mutants due to the discontinuity of the leading edge actin cable and the cell shape defects. In this situation, filopodia may be needed to locate the opposing epidermis and eventually zip up the embryo.

ena suppresses the *abl* phenotype and localizes to adherens junctions

The best characterized substrate of *Drosophila* Abl is Ena. Mutations in *ena* suppress the effects of *abl dab* mutations (Gertler et al., 1995). We thus examined whether *ena* might act with Abl in epithelial morphogenesis. Data from the Hoffmann lab supported this possibility: they found that females homozygous for *abl* mutations, which are normally sterile, become fertile when they are also heterozygous for *ena* (Bennett and Hoffmann, 1992). We thus generated homozygous *abl* germline clones in females that were heterozygous for *ena* (for experimental reasons only 50% of the females generated in the experiment are *ena* heterozygotes) and crossed them to *abl* heterozygous males. *ena* heterozygosity significantly rescued the abl^{MZ} embryonic lethality (Table I).

These data suggest that Ena misregulation contributes to the defects in morphogenesis we observed in abl^{MZ} mutants. We thus examined Ena localization in epithelial tissues, as this might reveal, at least in part, where Abl is acting. We used two different anti-Ena antibodies (Gertler et al., 1995; Bashaw et al., 2000) with similar results. We found that Ena colocalizes with Arm at adherens junctions throughout most stages of development. During early oogenesis, Ena and Arm are strongly enriched at adherens junctions of follicle cells surrounding the germline (Fig. 6 A; Baum and Perrimon, 2001) and remain enriched at junctions, though at lower levels as oogenesis proceeds (Figs. 6, B and C). During embryogenesis, Ena begins to accumulate in adherens junctions at the onset of gastrulation (unpublished data) and colocalizes with Arm at adherens junctions in germband-extended embryos (Fig. 6 D, arrow) and in fully polarized cells, such as the invaginating hindgut (Fig. 6 E, arrow). Arm localizes uniformly around cells (Fig. 6 F), whereas Ena, though present all around the plasma membrane, is enriched at vertices of cell–cell contact (Fig. 6 F, arrow). Ena is strongly enriched in adherens junctions of leading edge cells during dorsal closure (Figs. 4 C and 6 G), and also localizes to the cytoplasm in a stripe of epidermal cells at the segmental boundary (Fig. 6 G, arrowheads). Ena and Arm also localize to CNS axons (Gertler et al., 1990; Fig. 6 H). During larval development, Ena and Arm are strongly enriched at adherens junctions of the highly polarized imaginal disc epithelia, precursors of the adult epidermis (Figs. 6 I, arrow), as well as in the specialized junctions of the photoreceptor rhabdomeres (Fig. 6, J and K). Thus, Arm and Ena colocalize in adherens junctions in most epithelial cells.

ena and *arm* genetically interact during dorsal closure

Our genetic experiments suggest that Ena misregulation plays a role in the defects in morphogenesis of abl^{MZ} mutants (Table I). As Ena localizes to adherens junctions, we wondered whether it might work with adherens junction components during morphogenesis. We thus looked for genetic interactions between *ena* and *arm*. We crossed females heterozygous for mutations in both *arm* and *ena* to males heterozygous for *ena*. Both *arm* and *ena* are embryonic lethal; as *arm* is on the X-chromosome, we expect 43% of the dead progeny to be *arm* mutant, 43% to be *ena* mutant, and 14% to be *arm; ena* double mutants. Null alleles of Arm have dorsal closure defects, due to a combination of affects on cell adhesion and Wg signaling (McEwen et al., 2000), whereas weaker *arm* alleles do not have dorsal closure defects. We first tested the weakest allele of *arm*, $arm^{H8.6}$, in which dorsal closure is normal, although segment polarity is affected (Fig. 7 B). Although *ena* homozygotes are embryonic lethal, most of the dead embryos only have mild defects in head involution (Gertler et al., 1990; Fig. 7 C). A small fraction (~5%) have dorsal pattern defects indicative of mild problems in dorsal closure. When we generated $arm^{H8.6}$; ena^{GC1} double mutants, we found strong synergistic defects in both head involution and dorsal closure (Fig. 7 D; Table III). Mutations in *ena* also enhance the dorsal closure defects of the stronger *arm* mutants arm^{XM19}, arm^{XP33} (unpublished data), and arm^{YD35} (Fig. 7, E and F; Table III), though it is difficult to rule out the possibility that these interactions are simply additive.

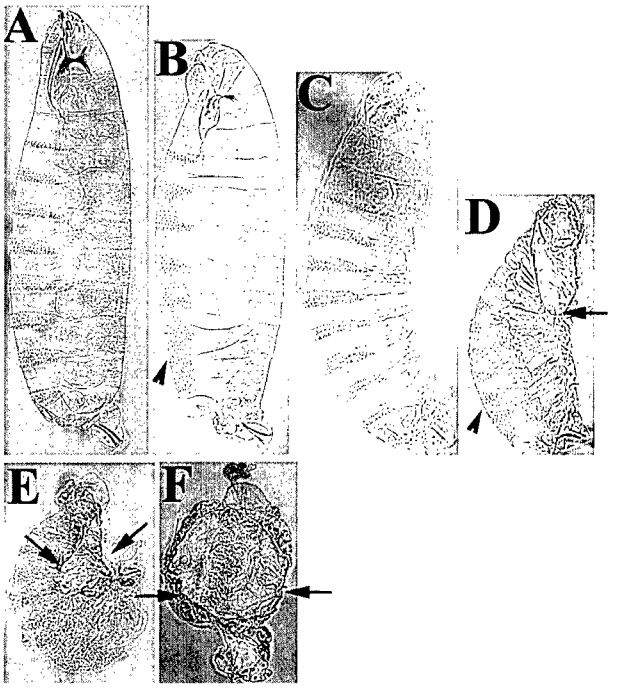

Figure 7. **Mutations in *ena* enhance *arm*'s dorsal closure defects.** Cuticle preparations, anterior up. (A) Wild-type. (B) $arm^{H8.6}$ mutants have segment polarity defects due to defects in Wingless signaling (arrowhead), but head involution and dorsal closure are normal. (C) ena^{210}/ena^{GC1}. (D) $arm^{H8.6}$/Y; ena^{GC1}/ena^{GC1}. Note strong defects in dorsal closure and head involution (arrow), with no change in the segment polarity phenotype (arrowhead). (E) arm^{YD35} mutants have a dorsal hole (arrows), as well strong segment polarity defects. (F) The dorsal side of arm^{YD35}; ena^{210}/ena^{210} embryos is completely open (arrows).

Table III. ***arm* and *ena* genetically interact**

Cross	Percentage of dead embryos with: *arm* ø-type	*ena* ø-type	*arm; ena*	*n*
$arm^{H8.6}$/+; ena^{GC1}/+ × +/Y; ena^{GC1}/+	34	53	13	218
arm^{YD35}/+; ena^{GC1}/+ × +/Y; ena^{GC1}/+	51	35	14	635
Predicted by Mendelian ratios	43	43	14	

Mutations in DE-cadherin enhance the *abl* phenotype

The genetic interactions between *arm* and *abl* in the CNS and epidermis (Loureiro and Peifer, 1998) and the localization of Ena to adherens junctions suggest that Abl might act in part at adherens junctions. In cultured mammalian cells Abl localizes to cell–matrix junctions (Lewis et al., 1996). As one test of the possible sites of Abl action during morphogenesis, we looked for dose-sensitive genetic interactions between *abl* and genes encoding proteins involved in epithelial adhesion: DE-cadherin (encoded by *shotgun* (*shg*); Tepass et al., 1996; Uemura et al., 1996), which mediates cell–cell adhesion, and *scab* (*scb*), an integrin α-chain which mediates cell-matrix adhesion during dorsal closure (Stark et al., 1997).

We saw strong genetic interactions of *abl* with the cadherin *shg*, but not with the integrin *scb*. We crossed females with *abl* mutant germlines to males heterozygous for *shg* or *scb*. All progeny lack maternal Abl and are zygotically *abl* heterozygous, receiving a wild-type copy paternally. Zygotic wild-type Abl normally rescues all of these embryos to viability (Table I). However, shg^2 heterozygosity led to lethality of *abl*/+ embryos (Table I). Only 40% of the progeny hatch, and the dead embryos have dorsal closure and germband retraction defects similar to abl^{MZ} mutants. Many also have severe defects in head involution (Fig. 8 B, arrow). Similar, though somewhat less penetrant, results were seen with the *shg* null allele, shg^{R69} (Table I). In contrast, we saw no effects on the survival of *abl*/+ embryos of removing one copy of *scb* (Table I). To increase the sensitivity of this genetic interaction assay, we crossed females with *abl* mutant germ lines to *abl*/+; *shg*/+ or *abl*/+; *scb*/+ males. Half of the progeny lack both maternal and zygotic Abl, and half of those are also heterozygous for either *shg* or *scb*. Heterozygosity for shg^2 substantially enhanced the abl^{MZ} phenotype (Fig. 8 D; Table II). Approximately half of the dead embryos (presumably those that were *abl/abl;* shg^2/+) had a prominent dorsal anterior hole not seen in abl^{MZ} mutants (Fig. 8 D); these embryos also had the typical spectrum of dorsal closure and germband retraction defects. We saw similar phenotypic enhancement in abl^{MZ} embryos heterozygous for the *shg* null allele, shg^{R69}. (Fig. 8 E; Table II). In contrast, this sensitized assay did not uncover a significant genetic interaction between *abl* and *scb* (Table II).

Loss of Abl decreases the amount of junctional arm and α-catenin

The genetic interactions between *abl* and *shg* suggested that some of the morphogenesis defects observed could result from effects of Abl at adherens junctions. Alternately, they might result from more nonspecific effects on cell polarity or the cytoskeleton. We thus examined the subcellular localization of adherens junction proteins and other markers of cell polarity in abl^{MZ} mutants. To control for variability between experiments, we analyzed mixed populations of wild-type and mutant embryos that had undergone simultaneous fixation, staining, and microscopy. We used a wild-type strain carrying a GFP transgene, allowing us to unambiguously discriminate between wild-type and mutant embryos. The mutant embryos had fathers which were heterozygous for *abl* and a different GFP-transgene, to differentiate abl^{MZ} from paternally rescued embryos.

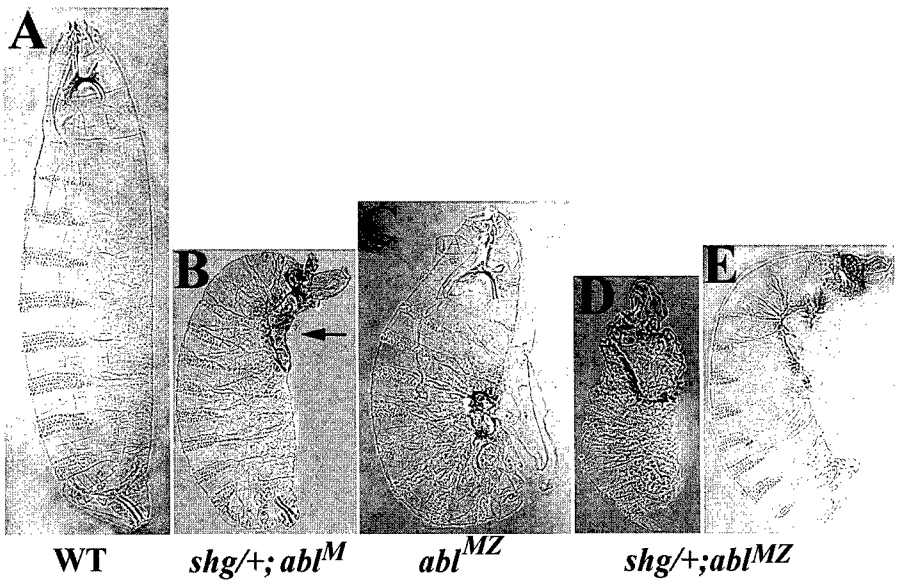

Figure 8. **DE-cadherin (*shg*) genetically interacts with Abl.** Cuticle preparations, anterior up. (A) Wild-type. (B) abl^4/abl^4 × shg^2/*CyO*. abl^4 maternal mutants are zygotically rescued, with all hatching as larvae and most appearing wild-type. *shg* heterozygosity prevents zygotic rescue of *abl* maternal mutants and leads to morphogenesis defects. Note defects in dorsal closure and head involution (arrow). (C) abl^{MZ} mutants die during embryogenesis with defects in epithelial morphogenesis. (D and E) *shg* heterozygosity enhances the abl^{MZ} phenotype. (D) 70% of lethal progeny of abl^4/abl^4 × shg^2/+; abl^4/+ have cuticles that are reduced in size with a large dorsal-anterior hole. (E) 30% of the lethal progeny of abl^4/abl^4 × shg^{R69}/+; abl^4/+ have a prominent dorsal-anterior hole.

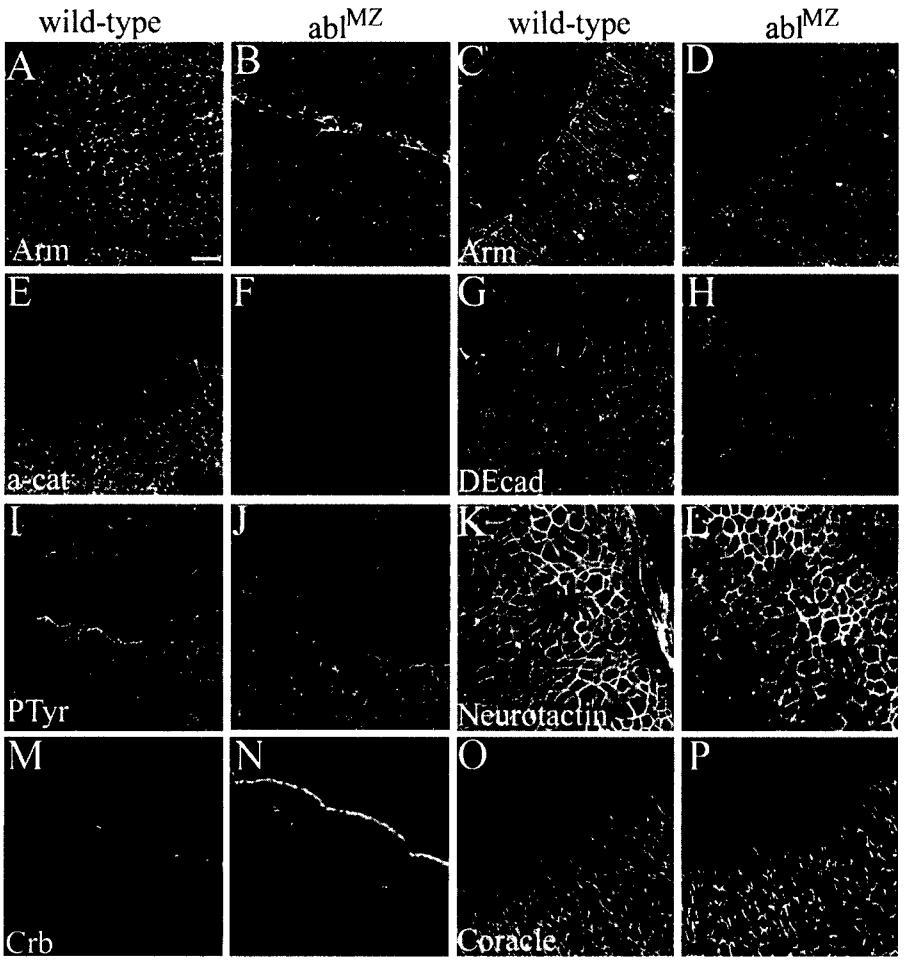

Figure 9. **Levels of junctional Arm and α-catenin are reduced in *abl*^{MZ} mutants.** Embryos labeled with anti-Arm (A–D), anti–α-catenin (E and F), anti–DE-cadherin (G and H), antiphosphotyrosine (I and J), anti-Neurotactin (K and L), anti-Crumbs (M and N), and anti-Coracle (O-P). (A and B) Stage 8. (C and D) Stage 14. (A and C) Wild-type. Arm localizes to adherens junctions. (B and D) *abl*^{MZ} mutants. Arm accumulates at reduced levels in adherens junctions. (E and F) Stage 13. (E) Wild-type. α-catenin localizes to adherens junctions. (F) *abl*^{MZ} mutant. α-catenin accumulates at reduced levels in adherens junctions. (G–J) Stage 13. DE-cadherin localizes to adherens junctions, without striking differences in localization or levels between wild-type (G) and *abl*^{MZ} mutants (H). Phosphotyrosine localizes to adherens junctions, without noticeable differences between wild-type (I) and *abl*^{MZ} mutants (J). (K and L) Stage 11. Neurotactin localizes to the baso-lateral membrane without noticeable differences between wild-type (K) and *abl*^{MZ} mutants (L). (M and N) Cross-sectional views, Stage 11. Crumbs localizes to the apical membrane of epithelial cells without striking differences between wild-type (M) and *abl*^{MZ} mutants (N). (O and P) Stage 13. Coracle localizes to septate junctions with no striking difference in levels between wild-type (O) and *abl*^{MZ} mutants (P). Bar, 10 μm.

abl^{MZ} mutants had reduced levels of Arm in adherens junctions. This was first noticeable in germband-extended embryos (Fig. 9, A and B) and became more pronounced during dorsal closure in wild-type (Fig. 9, C and D). Cross-sectional views suggest that the decrease in Arm at adherens junctions is not due to mislocalization of Arm to a different place in the cell (unpublished data), and we also think it is unlikely to be solely due to the alterations in cell shape in the mutant. Given these effects on Arm, we analyzed other adherens junction components. α-catenin, a protein that links Arm to the actin cytoskeleton, also showed reduced accumulation in adherens junctions (Fig. 9, E and F). The localization of both Arm and α-catenin was more variable in paternally rescued embryos, with reduction in some individuals but not others (unpublished data). The accumulation of DE-cadherin at junctions also may be slightly reduced in *abl*^{MZ} mutants (Figs. 9, G and H), but this effect was less pronounced than that on Arm or α-catenin. We also examined several other cortical or membrane markers. The accumulation of phosphotyrosine in adherens junctions (Fig. 9, I and J), Coracle at septate junctions (Fig. 9, O and P), Neurotactin at the basolateral membrane (Fig. 9, K and L), and Crumbs at the apical membrane (Fig. 9, M and N) were only slightly reduced or unaffected. In doing these experiments, we also observed that the defects in cell shape in *abl*^{MZ} mutants are not restricted to dorsal closure. We observed defects in the uniform apical constrictions that occur in cells along the ventral midline (Fig. 9, A and B). Defects in cell shape changes and cell migration could also explain the observed defects in germband retraction.

To complement these immunofluorescence assays, we examined total protein levels of Arm and other proteins in the progeny of *abl*^{1} germline mutant females crossed to *abl* heterozygous males. Half of these embryos are *abl*^{MZ} and the other half are zygotically rescued. To ensure that embryos were similarly aged and to remove unfertilized eggs from the samples, we selected living embryos at the cellular blastoderm stage and then let them develop for given amounts of time. Total levels of Arm protein are significantly reduced throughout development compared with wild-type (Fig. 10, A–C). Similar reductions in Arm protein were observed in *abl*^{1} (unpublished data). In contrast to Arm, the levels of two unrelated control proteins, Pnut and BicD, were unaffected by loss of Abl function (Fig. 10, A–C). We next examined the levels of other adherens junction proteins. Reduction in Abl function also led to reduction in α-catenin protein levels (Fig. 10 A). In contrast, levels of DE-cadherin are not altered in *abl* mutants (Fig. 10, A–C). We then assessed whether these effects were specific for adherens junction proteins, by examining the levels of other markers of cell polarity or the cytoskeleton. We saw either subtle reduction or no effect of *abl* mutations on the levels of actin, the septate junction protein Coracle, and the apical marker Crumbs (Fig. 10, B and C).

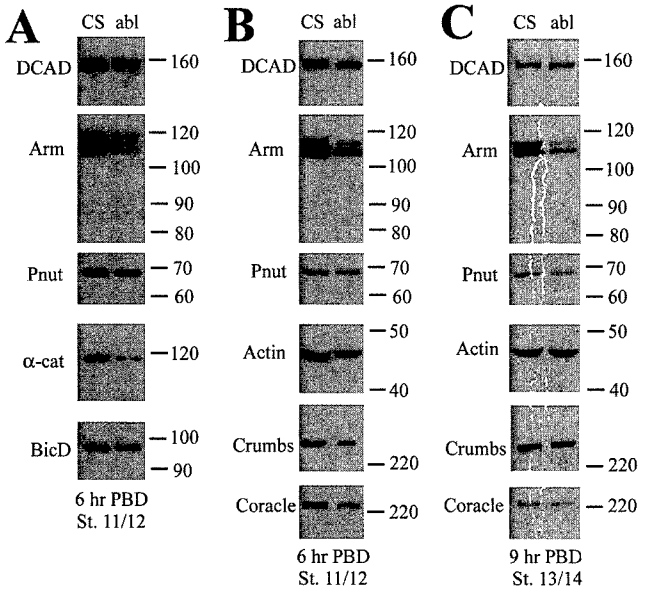

Figure 10. **Total levels of Arm and α-catenin are reduced in *abl* mutants.** *abl* germline mutant females were mated to *abl* heterozygous males and progeny were picked at the cellular blastoderm stage and aged for the indicated time postblastoderm (PBD). Wild-type embryos (Canton S [CS]) served as a control. Cell extracts were fractionated by SDS-PAGE and immunoblotted with the indicated antibodies. Molecular weight markers are to the right. Bicaudal D (BicD) or Peanut (Pnut) are loading controls. Each vertical set of samples represents sequential reprobing of the same blot. (A and B) Stage 11/12 embryos (6 h postblastoderm). (C) Stage 13/14 embryos (9 h postblastoderm).

Discussion

Activation of Abl tyrosine kinase plays a key role in the development of certain human leukemias (for review see Zou and Calame, 1999). Despite the attention paid to its role in oncogenesis, the complex roles Abl plays in normal cells are not as well understood. Here we report a novel role for Abl in epithelial cells, in which it regulates cell shape changes and cell migration during epithelial morphogenesis in vivo. These data may have broader implications, providing insights into the possible underlying cause of some of the defects seen in the mouse *abl* mutants and *abl; arg* double mutants, and may also provide insight into the role Bcr-Abl plays in leukemic cells. Further, these data provide in vivo evidence for a role for a tyrosine kinase in epithelial morphogenesis. This has been suspected from the actions of activated kinases in cultured cells (for review see Daniel and Reynolds, 1997), but our experiments test this in the intact animal.

It is useful to compare what we observed in the epidermis with Abl's role in axon outgrowth, where it is thought to modulate communication between at least two transmembrane axon guidance receptors, Robo and dLAR, and the actin cytoskeleton (for review see Lanier and Gertler, 2000). Abl is thought to antagonize Ena in this process. The *ena* and *abl* phenotypes were surprising in one respect. Ena/VASP proteins had been thought to enhance actin polymerization based on promotion of intracellular motility of the bacteria *Listeria*. However, while promoting actin polymerization might be expected to drive growth cone extension and axon outgrowth, Ena promotes growth cone repulsion and axon stalling (Bashaw et al., 2000; Wills et al., 1999a,b), whereas Abl has opposite effects. Work in cultured fibroblasts led to similar conclusions: Ena/VASP proteins inhibit cell migration (Bear et al., 2000).

Building on this model, Abl and Ena might play analogous roles in epithelial cells, translating extracellular signals into changes in the actin cytoskeleton. This sort of cytoskeletal modulation plays a key role in cell migration and cell shape changes during epithelial morphogenesis. One model consistent with our data is that Abl acts at adherens junctions during morphogenesis. Cadherins and catenins play important roles in morphogenesis in all animals. Severe reduction in *Drosophila* Arm (Cox et al., 1996) or DE-cadherin (Tepass et al., 1996) function leads to early loss of epithelial integrity. Less severe reduction in cadherin/catenin function affects head involution, dorsal closure, and other morphogenetic processes (Tepass et al., 1996; Uemura et al., 1996; McEwen et al., 2000). In fact, many epithelial defects of *DE-cadherin* mutants are blocked by blocking morphogenetic movements (Tepass et al., 1996), suggesting that modulating adhesion is critical to morphogenesis.

Several lines of evidence support the possibility that the morphogenetic defects of abl^{MZ} mutants result, at least in part, from Abl action at adherens junctions. First, the effects on dorsal closure, germband retraction, and head involution are strongly enhanced by reducing the dose of DE-cadherin. Second, the defects in cell shape during dorsal closure resemble, in part, those of *arm* mutants. Third, the defects in morphogenesis are suppressed by mutations in *ena*, which is primarily found at adherens junctions. Finally, we observed a reduction in junctional Arm and α-catenin in abl^{MZ} mutants. It is important to note, however, that any role for Abl at adherens junctions would be a modulatory one. It is not absolutely essential for adherens junction assembly or function. Of course, it remains possible that other tyrosine kinases may act redundantly with Abl. The relationship between the cadherin-catenin system, Abl, and Ena that may occur in epithelial cells could also exist in the CNS. Arm and DN-cadherin play roles in axon outgrowth in *Drosophila*, and in this role *arm* interacts genetically with *abl* (Iwai et al., 1997; Loureiro and Peifer, 1998).

One target of Abl might be Ena, which could regulate actin dynamics in the actin belt underlying the adherens junction. Just as local modulation of actin dynamics likely regulates growth cone extension or stalling, the cell shape changes and cell migration characteristic of morphogenesis will require modulation of actin dynamics and junctional linkage. The idea that Ena may regulate cell–cell adhesion recently received strong support from work in cultured mammalian keratinocytes, where inhibiting Ena/VASP function prevented actin rearrangement upon cell–cell adhesion (Vasioukhin et al., 2000). This model was further supported by work published while our paper was under review, which demonstrated that both Abl and Ena regulate actin polymerization at the adherens junctions of ovarian follicle cells in *Drosophila* (Baum and Perrimon, 2001).

Other models are also consistent with our data. Abl may act directly on the actin cytoskeleton, with its effects on

junctions a more indirect consequence. Junctional linkage to actin is critical for effective cell adhesion (Hirano et al., 1992) and alterations in actin polymerization could affect the ability to assemble stable cadherin–catenin complexes, as was observed in cultured mammalian cells (Quinlan and Hyatt, 1999), resulting in the observed loss of Arm from junctions. Abl could also play a more general role in the establishment and maintenance of cell polarity. Finally, studies of cultured mammalian cells also suggest that Abl acts at cell-matrix junctions to modulate responses to integrin-mediated adhesion by associating with and phosphorylating focal adhesion proteins like paxillin and Crkl (for review see Van Etten, 1999). In doing so, it may influence both tethering to actin and signal transduction. *Drosophila* integrins play important roles in morphogenetic processes such as dorsal closure and germband retraction (for review see Brown et al., 2000). We did not detect genetic interactions between *abl* and *scab*, the integrin α-chain that plays a role in dorsal closure (Stark et al., 1997). However, this does not rule out interplay between integrins and Abl in morphogenesis. It is now important to test these different models by investigating the mechanism by which Abl and Ena act during morphogenesis.

Materials and methods

Fly stocks and phenotypic analysis

All mutations are described in Flybase (http://flybase.bio.indiana.edu/). abl^1 and abl^4 germ line clones were generated by the FLP dominant female sterile technique (Chou and Perrimon, 1996). 48–72-h-old *hsflp:abl FRT 79D-F/ovo*^{D1} *FRT 79D-F* larvae were heat shocked for 3 h at 37°C. Only homozygous *abl* mutant germ cells develop in these females. Stocks to generate *abl* germ line clones, *hsflp;Dr*^{MIO}*/TM3*, *FRT3L79D-F/TM3*, and *ovo*^{D1} *FRT3L79D-F/TM3*, were from the Bloomington *Drosophila* Stock Center. *abl* and *ena* alleles were from M. Hoffmann (University of Wisconsin, Madison, WI). The wild-type was Canton-S. Transgenic lines expressing *histone-GFP*, the actin binding domain of Moesin fused to GFP (Kiehart et al., 2000), or *UAS-GFP* under the control of *sim-GAL4* were provided by R. Saint (University of Adelaide, South Australia, Australia), D. Kiehart (Duke University, Durham, NC), and S. Crews (University of North Carolina, Chapel Hill, NC), respectively. Cuticle preparations were as in Wieschaus and Nüsslein-Volhard (1986).

Immunolocalization and immunoblotting

Embryos were bleach dechorionated and fixed for 20 min in 1:1 4% formaldehyde/0.1 M Pipes/2 mM $MgSO_4$/1 mM EGTA/0.1% NP-40:heptane. For DE-cadherin localization, embryos were fixed for 1 h in the same fix with 0.3% Triton X-100 added. Vitelline membranes were removed with methanol. For actin visualization, embryos were fixed for 5 min in 1:1 37% formaldehyde:heptane and their vitelline membranes were removed manually. Larval tissues were dissected in insect media and fixed in 4% paraformaldehyde in PBS for 20 min. Ovaries were dissected and fixed as in Peifer et al. (1993). All tissues were blocked and stained in PBS/1% goat serum/0.1% TritonX-100 (PBS/2% BSA/0.3% Triton X-100 was used for DE-cadherin staining). Antibodies used were mouse monoclonals antiphosphotyrosine (Upstate Biotechnology; 1:1,000), anti-Arm N27A1 (DSHB, 1:200), anti-Ena (1:500; Bashaw et al., 2000), BP102 (DSHB, 1:200), anti-Crumbs (DSHB; 1:2), anti-Coracle (9C and 16B, R. Fehon; 1:500 each), and anti-Neurotactin (DSHB; 1:5); rabbit polyclonals anti-Arm N2 (1:200) and anti-Ena (1:500) (Gertler et al., 1995); and rat monoclonals anti–α-catenin (1:250) (Oda et al., 1993) and anti–DE-cadherin (1:250) (Oda et al., 1994). Actin was visualized using Alexa 488 phalloidin (Molecular Probes). For DNA visualization, embryos were treated with 300 μg/ml RNase for 30 min at room temperature and stained for 20 min with 10 μg/ml propidium iodide. A ZEISS 410 laser scanning confocal microscope was used. For biochemical experiments, embryos were placed in halocarbon oil to allow staging under the dissecting microscope, picked at the cellular blastoderm stage, and aged defined periods of time. Extract preparation and cell fractionation were as in Peifer et al. (1993). Samples were analyzed by 6% SDS-PAGE, transferred to nitrocellulose and immunoblotted with mouse anti-Arm N27A1 (1:500), anti-Bicaudal D (B. Suter, McGill University, Montreal, Canada; 1:500), anti-pnut at (DSHB;1:30), antiactin (Chemicon; 1:250), rat anti–DE-cadherin1 (1:100), anti–α-catenin, anticoracle (both 1:500), and anticrumbs (1:50).

Time lapse microscopy

Wild-type embryos imaged were homozygous for Moesin-GFP (Kiehart et al., 2000), whereas *abl* mutant embryos imaged were derived from abl^1 germ line clone females crossed to abl^1, *FRT 79D-F*, moesin-GFP/*TM3* males; thus, the only GFP fluorescent embryos in this collection are those that are *abl* maternal/zygotic mutants. Embryos were bleach dechorionated and mounted in halocarbon oil (series 700; Halocarbon Products Corporation) between a coverslip and a gas permeable membrane (Petriperm; Sartorius Corporation). Images were captured every 30 s using a PerkinElmer Wallac Ultraview Confocal Imaging System, and image analysis was performed using NIH Image 1.62.

Online supplemental material

Time-lapse videos are available to supplement Fig. 5. Images were captured every 25 s and the videos are played at a rate of 10 frames/s. Videos are available at http://www.jcb.org/cgi/content/full/jcb.200105102/DC1.

We are grateful to E. Crafton and Z. Ozsoy for help with genetic interaction assays; to M. Hoffmann, G. Bashaw, R. Fehon, F. Fogerty, D. Kiehart, R. Saint, T. Uemura, U. Tepass, N. Brown, B. Suter, S. Crews, the Bloomington *Drosophila* Stock Center, and the Developmental Studies Hybridoma Bank for stocks or antibodies; to S. Whitfield for assistance with the figures; and to B. Duronio, B. McCartney, and the reviewers for helpful comments.

This work was supported by National Institutes of Health (NIH) grant R01 GM47857 to M. Peifer. E.E. Grevengoed was supported by NIH 5T32GM07092 and 1T32CA72319. T.L. Jesse was supported by NIH 5T3CA09156 and 1F32GM20797. M. Peifer was supported in part by the U.S. Army Breast Cancer Research Program.

Submitted: 22 May 2001
Revised: 5 November 2001
Accepted: 6 November 2001

References

Bashaw, G.J., T. Kidd, D. Murray, T. Pawson, and C.S. Goodman. 2000. Repulsive axon guidance: Abelson and Enabled play opposing roles downstream of the roundabout receptor. *Cell.* 101:703–715.

Baum, B., and N. Perrimon. 2001. Spatial control of the actin cytoskeleton in *Drosophila* epithelial cells. *Nat. Cell Biol.* 3:883–890.

Bear, J.E., J.J. Loureiro, I. Libova, R. Fassler, J. Wehland, and F.B. Gertler. 2000. Negative regulation of fibroblast motility by Ena/VASP proteins. *Cell.* 101: 717–728.

Bennett, R.L., and F.M. Hoffmann. 1992. Increased levels of the *Drosophila* Abelson tyrosine kinase in nerves and muscles: Subcellular localization and mutant phenotypes imply a role in cell-cell interactions. *Development.* 116:953–966.

Brown, N.H., S.L. Gregory, and M.D. Martin-Bermudo. 2000. Integrins as mediators of morphogenesis in *Drosophila*. *Dev. Biol.* 223:1–16.

Chou, T.B., and N. Perrimon. 1996. The autosomal FLP-DFS technique for generating germline mosaics in *Drosophila* melanogaster. *Genetics.* 144:1673–1679.

Comer, A.R., S.M. Ahern-Djamali, J.-L. Juang, P.D. Jackson, and F.M. Hoffmann. 1998. Phosphorylation of Enabled by the *Drosophila* Abelson tyrosine kinase regulates the in vivo function and protein-protein interactions of Enabled. *Mol. Cell. Biol.* 18:152–160.

Cox, R.T., C. Kirkpatrick, and M. Peifer. 1996. Armadillo is required for adherens junction assembly, cell polarity, and morphogenesis during *Drosophila* embryogenesis. *J. Cell Biol.* 134:133–148.

Daniel, J.M., and A.B. Reynolds. 1997. Tyrosine phosphorylation and cadherin/catenin function. *Bioessays.* 19:883–891.

Gertler, F., R. Bennett, M. Clark, and F. Hoffmann. 1989. *Drosophila* abl tyrosine kinase in embryonic CNS axons: a role in axonogenesis is revealed through dosage-sensitive interactions with disabled. *Cell.* 58:103–113.

Gertler, F., J. Doctor, and F. Hoffman. 1990. Genetic suppression of mutations in the *Drosophila abl* proto-oncogene homolog. *Science.* 248:857–860.

Gertler, F.B., A.R. Comer, J. Juang, S.M. Ahern, M.J. Clark, E.C. Liebl, and F.M.

Hoffmann. 1995. *enabled*, a dosage-sensitive suppressor of mutations in the *Drosophila* Abl tyrosine kinase, encodes an Abl substrate with SH3 domain-binding properties. *Genes Dev.* 9:521–533.

Gertler, F.B., K. Niebuhr, M. Reinhard, J. Wehland, and P. Soriano. 1996. Mena, a relative of VASP and *Drosophila* Enabled, is implicated in the control of microfilament dynamics. *Cell.* 87:227–239.

Henkemeyer, M., F. Gertler, W. Goodman, and F. Hoffmann. 1987. The *Drosophila* Abelson proto-oncogene homolog: identification of mutant alleles that have pleiotropic effects late in development. *Cell.* 51:821–828.

Henkemeyer, M., S. West, F. Gertler, and F. Hoffmann. 1990. A novel tyrosine kinase-independent function of *Drosophila* abl correlates with proper subcellular localization. *Cell.* 63:949–960.

Hirano, S., N. Kimoto, Y. Shimoyama, S. Hirohashi, and M. Takeichi. 1992. Identification of a neural α-catenin as a key regulator of cadherin function and multicellular organization. *Cell.* 70:293–301.

Iwai, Y., T. Usui, S. Hirano, R. Steward, M. Takeichi, and T. Uemura. 1997. Axon patterning requires DN-Cadherin, a novel neuronal adhesion receptor, in the *Drosophila* embryonic CNS. *Neuron.* 19:77–89.

Jacinto, A., W. Wood, T. Balayo, M. Turmaine, A. Martinez-Arias, and P. Martin. 2000. Dynamic actin-based epithelial adhesion and cell matching during *Drosophila* dorsal closure. *Curr. Biol.* 10:1420–1426.

Kiehart, D.P., C.G. Galbraith, K.A. Edwards, W.L. Rickoll, and R.A. Montague. 2000. Multiple forces contribute to cell sheet morphogenesis for dorsal closure in *Drosophila*. *J. Cell Biol.* 149:471–490.

Koleske, A.J., A.M. Gifford, M.L. Scott, M. Nee, R.T. Bronson, K.A. Miczek, and D. Baltimore. 1998. Essential roles for the Abl and Arg tyrosine kinases in neurulation. *Neuron.* 21:1259–1272.

Lanier, L.M., and F.B. Gertler. 2000. From Abl to actin: Abl tyrosine kinase and associated proteins in growth cone motility. *Curr. Opin. Neurobiol.* 10:80–87.

Lewis, J.M., R. Baskaran, S. Taagepera, M.A. Schwartz, and J.Y. Wang. 1996. Integrin regulation of c-Abl tyrosine kinase activity and cytoplasmic-nuclear transport. *Proc. Nat. Acad. Sci. USA.* 93:15174–15179.

Loureiro, J., and M. Peifer. 1998. Roles of Armadillo, a *Drosophila* catenin, during central nervous system development. *Curr. Biol.* 8:622–632.

Mauro, M.J., and B.J. Druker. 2001. Chronic myelogenous leukemia. *Curr. Opin. Oncol.* 13:3–7.

McEwen, D.G., R.T. Cox, and M. Peifer. 2000. The canonical Wg and JNK signaling cascades collaborate to promote both dorsal closure and ventral patterning. *Development.* 127:3607–3617.

Oda, H., T. Uemura, Y. Harada, Y. Iwai, and M. Takeichi. 1994. A *Drosophila* homolog of cadherin associated with Armadillo and essential for embryonic cell-cell adhesion. *Dev. Biol.* 165:716–726.

Oda, H., T. Uemura, K. Shiomi, A. Nagafuchi, S. Tsukita, and M. Takeichi. 1993. Identification of a *Drosophila* homologue of α-catenin and its association with *armadillo* protein. *J. Cell Biol.* 121:1133–1140.

Peifer, M., S. Orsulic, D. Sweeton, and E. Wieschaus. 1993. A role for the *Drosophila* segment polarity gene *armadillo* in cell adhesion and cytoskeletal integrity during oogenesis. *Development.* 118:1191–1207.

Quinlan, M.P., and J.L. Hyatt. 1999. Establishment of the circumferential actin filament network is a prerequisite for localization of the cadherin-catenin complex in epithelial cells. *Cell Growth Differ.* 10:839–854.

Stark, K.A., G.H. Yee, C.E. Roote, E.L. Williams, S. Zusman, and R.O. Hynes. 1997. A novel alpha integrin subunit associates with betaPS and functions in tissue morphogenesis and movement during *Drosophila* development. *Development.* 124:4583–4594.

Tepass, U., E. Gruszynski-DeFeo, T.A. Haag, L. Omatyar, T. Török, and V. Hartenstein. 1996. *shotgun* encodes *Drosophila* E-cadherin and is preferentially required during cell rearrangement in the neurectoderm and other morphogenetically active epithelia. *Genes Dev.* 10:672–685.

Tepass, U., K. Truong, D. Godt, M. Ikura, and M. Peifer. 2000. Cadherins in embryonic and neural morphogenesis. *Nat. Rev. Mol. Cell. Biol.* 1:91–100.

Uemura, T., H. Oda, R. Kraut, S. Hayashi, Y. Kotaoka, and M. Takeichi. 1996. Zygotic *Drosophila* E-cadherin expression is required for processes of dynamic epithelial cell rearrangement in the *Drosophila* embryo. *Genes Dev.* 10:659–671.

Van Etten, R.A. 1999. Cycling, stressed-out and nervous: cellular functions of c-Abl. *Trends Cell Biol.* 9:179–186.

van Etten, R.A., P.K. Jackson, D. Baltimore, M.C. Sanders, P.T. Matsudeira, and P. Janmey. 1994. The COOH terminus of the c-Abl tyrosine kinase contains distinct F- and G-actin binding domains with bundling activity. *J. Cell Biol.* 124:325–340.

Vasioukhin, V., C. Bauer, M. Yin, and E. Fuchs. 2000. Directed actin polymerization is the driving force for epithelial cell-cell adhesion. *Cell.* 100:209–219.

Wieschaus, E., and C. Nüsslein-Volhard. 1986. Looking at embryos. *In Drosophila*, A Practical Approach. D.B. Roberts, editor. IRL Press, Oxford, England. 199–228.

Wills, Z., J. Bateman, C.A. Korey, A. Comer, and D. Van Vactor. 1999a. The tyrosine kinase Abl and its substrate enabled collaborate with the receptor phosphatase Dlar to control motor axon guidance. *Neuron.* 22:301–312.

Wills, Z., L. Marr, K. Zinn, C.S. Goodman, and D. Van Vactor. 1999b. Profilin and the Abl tyrosine kinase are required for motor axon outgrowth in the *Drosophila* embryo. *Neuron.* 22:291–299.

Young, P.E., A.M. Richman, A.S. Ketchum, and D.P. Kiehart. 1993. Morphogenesis in *Drosophila* requires nonmuscle myosin heavy chain function. *Genes Dev.* 7:29–41.

Zou, X., and K. Calame. 1999. Signaling pathways activated by oncogenic forms of Abl tyrosine kinase. *J. Biol. Chem.* 274:18141–18144.

Drosophila APC2 and Armadillo participate in tethering mitotic spindles to cortical actin

Brooke M. McCartney*†, Donald G. McEwen*†, Elizabeth Grevengoed‡, Paul Maddox*, Amy Bejsovec§ and Mark Peifer*†‡¶

*Department of Biology, University of North Carolina at Chapel Hill, Chapel Hill, North Carolina 27599-3280, USA
†Lineberger Comprehensive Cancer Center, University of North Carolina at Chapel Hill, Chapel Hill, North Carolina 27599-3280, USA
‡Curriculum in Genetics and Molecular Biology, University of North Carolina at Chapel Hill, Chapel Hill, North Carolina 27599-3280, USA
§Department of Biology, Duke University, Durham, North Carolina 27708-1000, USA
¶e-mail: peifer@unc.edu

Proper positioning of mitotic spindles ensures equal allocation of chromosomes to daughter cells. This often involves interactions between spindle and astral microtubules and cortical actin[1]. In yeast and *Caenorhabditis elegans*, some of the protein machinery that connects spindles and cortex has been identified but, in most animal cells, this process remains mysterious. Here, we report that the tumour suppresser homologue APC2 and its binding partner Armadillo both play roles in spindle anchoring during the syncytial mitoses of early *Drosophila* embryos. Armadillo, α-catenin and APC2 all localize to sites of cortical spindle attachment. APC2–Armadillo complexes often localize with interphase microtubules. Zeste-white 3 kinase, which can phosphorylate Armadillo and APC, is also crucial for spindle positioning and regulates the localization of APC2–Armadillo complexes. Together, these data suggest that APC2, Armadillo and α-catenin provide an important link between spindles and cortical actin, and that this link is regulated by Zeste-white 3 kinase.

One system for investigating spindle anchoring is the syncytial blastoderm of the *Drosophila* embryo. A series of nuclear divisions occur without cytokinesis, regulated by complex interactions between actin, microtubules and centrosomes (reviewed in ref. 2). During nuclear cycle 10, nuclei migrate to the periphery, where they divide parallel to the cortex. Adjacent spindles are separated by pseudocleavage furrows, membrane invaginations lined with cortical actin. Defects in pseudocleavage furrow formation result in nuclear collisions and subsequent nucleus loss. Inhibitor studies suggest that spindles are anchored to the cortex via cortical actin: if this link is broken, spindles detach, lose their orientation parallel to the cortex and are removed into the embryo interior. Mutations in several genes result in nucleus loss[3–6]. These genes regulate mitotic fidelity, checkpoint control or pseudocleavage furrow assembly, thus acting either upstream or independent of the machinery tethering spindles to the cortex.

Here, we report that adenomatous polyposis coli proteins (APCs) might help to bridge the gap between spindles and cortex. Human APC is a tumour suppresser that negatively regulates Wnt/Wingless signalling by facilitating phosphorylation of the key Wnt/Wingless effector β-catenin (*Drosophila* Armadillo (Arm)) by glycogen synthase kinase 3β (*Drosophila* Zeste-white 3 (Zw3); reviewed in ref. 7). This targets β-catenin for proteolytic destruction.

APCs might also regulate cytoskeletal function, as they interact or localize with microtubules and actin (reviewed in ref. 8). Mammalian APC localizes to cortical puncta where microtubule bundles terminate, suggesting that APCs might tether microtubules to the cortex[9]. APCs associate with microtubules in several different ways. A carboxy-terminal microtubule-binding site present in human APC is absent in some family members, including APC2 (reviewed in ref. 8). However, a second microtubule-binding site lies in a region conserved in all APC family members[10]. Human APC also interacts indirectly with microtubules via the microtubule-binding protein EB1 (a homologue of yeast Bim1 (reviewed in ref. 8)); it is not clear whether other APC family members bind EB1. Finally, the amino-terminal two-thirds of APC, which is well conserved in all APC family members, moves along microtubules toward their plus ends, presumably via association with a motor protein[11]. APC proteins also localize with actin in many contexts[12–15].

To address whether APC family proteins regulate cytoskeletal function, we examined *Drosophila* APC2 function during syncytial development. APC2 has a dynamic localization pattern that largely parallels that of actin[12,13] (Fig. 1). During interphase, APC2 localizes with actin in the caps above each nucleus (Fig. 1a). As chromosomes condense, APC2 accumulates in pseudocleavage furrows (Fig. 1b,c), where it remains through anaphase. APC2 becomes enriched near the spindle poles during anaphase (Fig. 1d) and, in telophase, re-enters the forming actin caps. Thus, APC2 is present at the cortex where astral microtubules are thought to contact actin, anchoring the spindle. To examine APC2 function during syncytial stages, we compared wild-type embryos with maternal and zygotic *APC2* mutants (henceforth *APC2* mutants). We used two *APC2* alleles: a mutation in the Arm repeats ($APC2^{\Delta 5}$) and a truncation similar to those found in human tumours ($APC2^{d40}$). Both alleles are embryonic lethal owing to constitutive Wingless signalling[12] (data not shown).

APC2 mutants have obvious defects in syncytial development (Figs 2,3). In wild-type embryos, nuclei divide parallel to the cortex (Fig. 2a,d). In *APC2* mutants, however, nuclei migrate to the cortex normally but then many nuclei are lost from the cortex into the internal cytoplasm (Fig. 2b,e, arrows). Nuclear loss is observed in the wild type at a much lower frequency (<5% of nuclei) as a consequence of abnormal mitoses (reviewed in ref. 2). When spindles and chromosomes are removed from the surface in *APC2* mutants, centrosomes remain behind (data not shown), continuing to organize pseudocleavage furrows (Fig. 3d) and actin caps (Fig. 3h) of reduced size. Cortical retention of centrosomes also occurs in other 'nuclear fall-out' mutants[3], suggesting that centrosomes have additional mechanisms of cortical attachment or that they are not subject to the machinery that transports spindles to the interior.

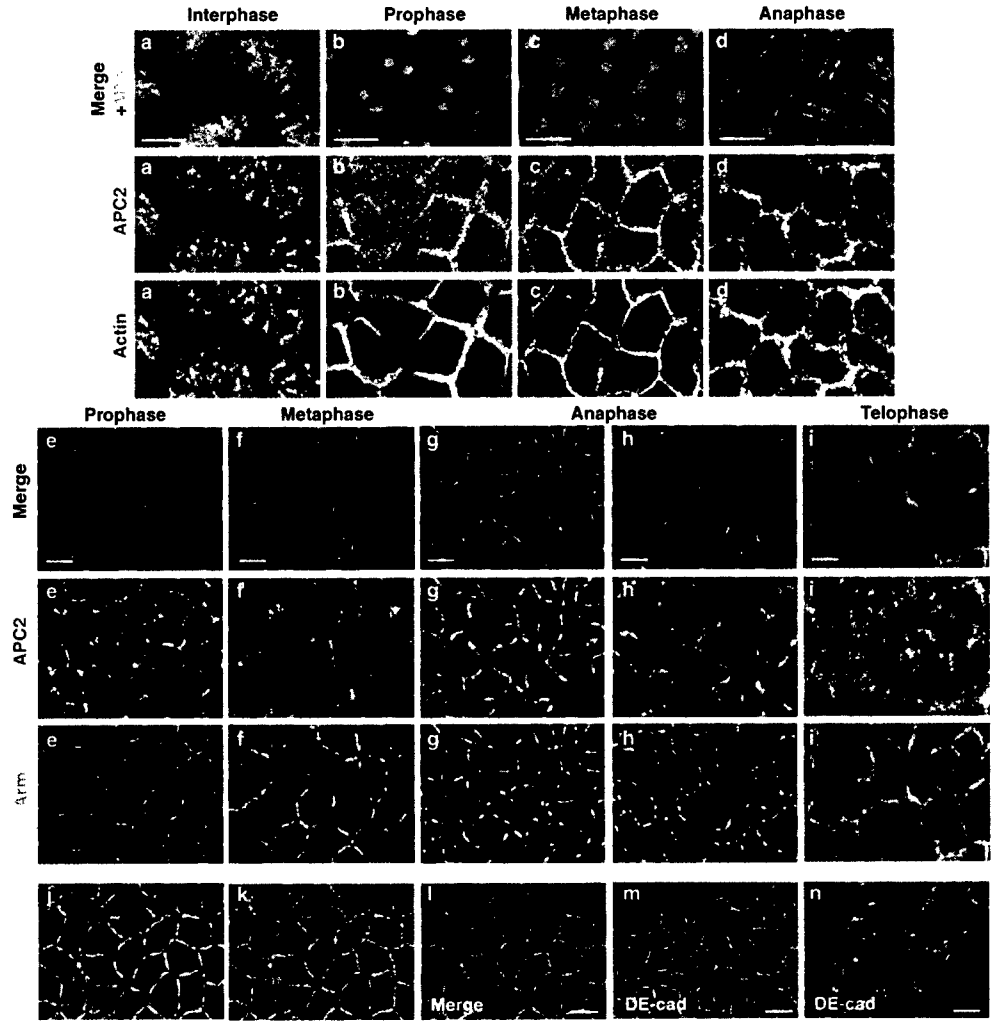

Figure 1 **APC2, Arm, α-catenin (α-cat) and DE-cadherin (DE-cad) localize to pseudocleavage furrows during wild-type syncytial development. a–d,** Formaldehyde-fixed wild-type embryos stained with anti-APC2 antibody (blue), phalloidin to reveal F-actin (red) and anti-tubulin antibody (green). **a,** During interphase, APC2 and actin localize to microvilli in the actin caps, which lie over baskets of microtubules (MTs). **b,** During prophase, actin and APC2 begin to accumulate in the forming pseudocleavage furrows. **c,** During metaphase, APC2 and actin localize to pseudocleavage furrows. **d,** During late anaphase, actin and APC2 begin to relocalize to caps; they remain in pseudocleavage furrows longest at the 'cell' ends, where spindles are attached to the cortex. **e–i,** Heat–methanol-fixed wild-type embryos stained with anti-APC2 (red) and anti-Arm (green) antibodies. **e,** During prophase, Arm begins to be recruited to forming pseudocleavage furrows. APC2 localizes to punctate structures at the cortex. **f,g,** During metaphase (**f**) and early anaphase (**g**), Arm and APC2 both accumulate in pseudocleavage furrows, where they overlap but do not precisely co-localize. **h,** During late anaphase, APC2 begins to disappear from pseudocleavage furrows, with the remaining protein concentrated at the ends of 'cells'. Arm remains in pseudocleavage furrows and also accumulates at higher levels at 'cell' ends. **i,** During telophase, APC2 relocalizes to forming actin caps. Arm disappears from pseudocleavage furrows, with the only remaining cortical Arm at 'cell' ends. **j–l,** Heat–methanol-fixed metaphase wild-type embryo stained with anti-Arm (**j, l**; green) and anti-α-cat (**k, l**; red) antibodies. Arm and α-cat localize precisely at pseudocleavage furrows. **m,n,** Wild-type embryos during metaphase (**m**) or anaphase (**n**) stained with anti-DE-cadherin, which localizes to pseudocleavage furrows. Cortical localization is strongest when pseudocleavage furrows were deepest (data not shown). Scale bar, 10 μm.

We considered two mechanisms for nucleus loss in *APC2* mutants: (1) abnormal mitoses owing to pseudocleavage furrow disruption or spindle defects, triggering a checkpoint response; and (2) disrupted cortical tethering of nuclei, leading more directly to nucleus loss. If nucleus loss was due to abnormal mitoses, we should see nuclear collisions resulting from the disruption of pseudocleavage furrows or defects in spindle function, as observed in other nucleus-loss mutations[3–6]. However, overall nuclear (Fig. 3d and data not shown) and actin organization seem to be normal in *APC2* mutants, and neither pseudocleavage furrows (Fig. 3d,l,m) nor actin caps (Fig. 3h) are disrupted.

We next examined spindle morphology during early peripheral divisions, when astral microtubules are prominent during late mitosis (Fig. 3i,j). Overall spindle morphology and astral microtubules appear normal in *APC2* mutants (Fig. 3j). However, during later peripheral divisions, spindles adjacent to regions of nuclear loss exhibited a spectrum of defects ranging from spindles attached by only one pole (Fig. 3l, arrowheads) to partially 'collapsed' spindles (Fig. 3m, arrows). We suspect that these spindles are in the process of detaching before transportation to the interior.

The absence of broad cytoskeletal defects in *APC2* mutants is unusual among nucleus-loss mutants and suggests that APC2 does not regulate global actin organization or play an essential role in spindle assembly. Instead, it might help to tether spindles to the

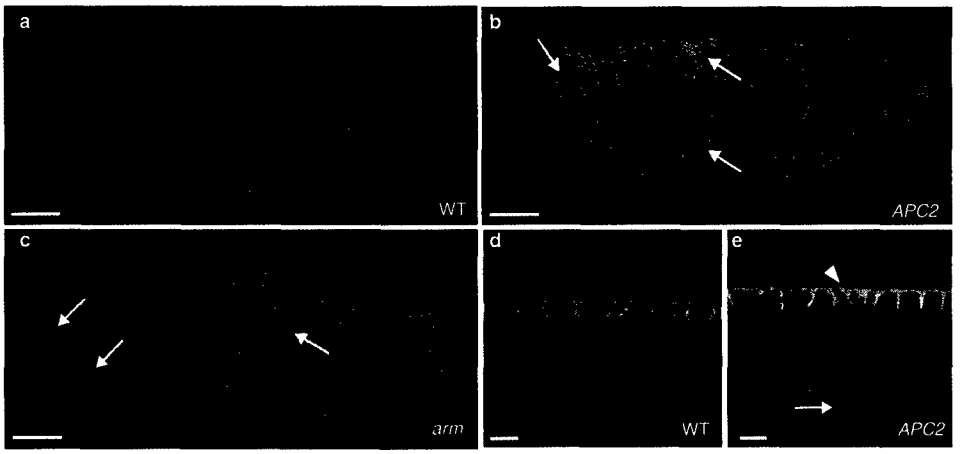

Figure 2 **Mutation of *APC2* or *arm* results in the loss of nuclei from the cortex in syncytial *Drosophila* embryos. a–c**, Surface views of embryos stained to visualize pseudocleavage furrows (anti-phosphotyrosine; green) and chromosomes (anti-phosphohistone; blue). **a**, Wild-type (WT) embryo illustrating the network of pseudocleavage furrows that surround dividing nuclei during late syncytial mitoses. **b**, $APC2^{\Delta S}$ embryo. Arrows indicate regions where nuclei have detached from the cortex, leaving smaller 'cells' that do not contain chromosomes. **c**, arm^{XP33} embryo. Arrows indicate similar regions of nucleus loss. **d,e**, Cross-sectional views of syncytial embryos during mitosis stained to reveal spindles (anti-tubulin; red) and the actin cytoskeleton (phalloidin; green). **d**, In a wild-type embryo, spindles are oriented parallel to the cortex and are enclosed by actin-based pseudocleavage furrows. **e**, In $APC2^{\Delta S}$ embryos, spindles that have detached from the cortex are found in the interior cytoplasm (arrow), leaving behind small pseudocleavage furrows (arrowhead). Scale bars, 40 μm (**a–c**), 10 μm (**d,e**)

cortex. This hypothesis is consistent with APC2's localization with actin to pseudocleavage furrows[12,13] (Fig. 1a–d) and its localization to cortical sites near spindle poles in asymmetrically dividing larval neuroblasts[12]. It is also consistent with the localization of human APC to membrane puncta in which microtubule bundles terminate[9].

In later development, APC2 binds Arm, helping to target it for phosphorylation by Zw3 kinase. We thus examined whether these partners might work with APC2 in syncytial embryos. Arm localizes throughout the cytoplasm and at the cortex during syncytial development. Heat–methanol fixation, which has been used before to visualize actin-associated proteins, allows one selectively to visualize cortical Arm by removing the cytoplasmic Arm that otherwise obscures it[16]. Using this fixation method, we found that a significant amount of Arm localizes to pseudocleavage furrows (Fig. 1e–i), with strong enrichment there during metaphase and anaphase. Much of the APC2 remains cortically associated in heat–methanol-fixed embryos (Fig. 1e–i), perhaps because it is tightly bound to the cytoskeleton. Like Arm, APC2's localization to pseudocleavage furrows is most pronounced during metaphase and anaphase (Fig. 1f,g). APC2 leaves pseudocleavage furrows before Arm and relocalizes to forming actin caps (Fig. 1i).

We next asked whether Arm and Zw3 play a role in syncytial development, examining embryos maternally and zygotically mutant for the strong *arm* allele arm^{XP33} or for either of two *zw3* alleles, $zw3^{M1\text{-}1}$ and $zw3^{D127}$. Like *APC2*, *zw3* mutants are embryonic lethal owing to constitutive Wingless signalling[12,17,18]. Embryos with the arm^{XP33} mutation have severe defects in epithelial organization after cellularization[19], but we had not previously examined syncytial development. Both *zw3* (Fig. 3b,o) and *arm* (Figs 2c, 3f) mutants have syncytial defects essentially identical to those in *APC2* mutants, consistent with APC2, Arm and Zw3 acting together to regulate nuclear tethering.

Studies of spindle attachment in yeast suggest a mechanism by which these proteins might function. Yeast Kar9 mediates interactions between the spindle and cortex by joining the microtubule-binding protein Bim1 to the actin-binding proteins Bud6 and Bni1 (reviewed in ref. 20). Kar9 thus provides a model for how APC2 might function; like Kar9, APC2 might interact with actin indirectly. Human APC forms a complex with both β-catenin (an Arm homologue) and the actin-binding protein α-catenin[21] (α-cat). Arm could tether APC2 to cortical actin through Arm's interaction with α-cat, analogous to Arm's role in adherens junctions, where it links α-cat (and thus actin) to DE-cadherin.

To test this, we compared α-cat localization during wild-type syncytial development to that of Arm. Arm and α-cat localize strongly together in pseudocleavage furrows (Fig. 1j–l), putting them in the right place to mediate interactions between cortical actin and APC2. We also examined the catenins' junctional partner DE-cadherin. As cadherins are generally restricted to cell–cell contacts, we had not anticipated that they would be found in syncytial embryos. However, DE-cadherin also localizes to pseudocleavage furrows (Fig. 1m,n). Perhaps cadherin–catenin complexes play an adhesive role there, linking adjacent membranes in furrows and anchoring cortical actin. As APC and E-cadherin bind Arm mutually exclusively[22], it is unlikely that DE-cadherin plays a direct role in anchoring microtubules to the cortex.

To test further the hypothesis that Arm and α-cat link APC2 to the cortex, we examined the effect of *APC2* and *arm* mutations on APC2, Arm and α-cat localization. We hypothesize that spindle tethering to cortical actin is disrupted in *APC2* mutants. Consistent with this, both mutant *APC2* proteins no longer associate with the cortex (Fig. 4b; data not shown). The $APC2^{d40}$ truncation removes much of the Arm-binding region, so APC2's ability to bind Arm might be required for cortical localization. APC2's Arm repeats are also required, because $APC2^{\Delta S}$ is mislocalized. Arm and α-cat localization are unaltered in $APC2^{\Delta S}$ mutants (Fig. 4a,h). By contrast, APC2 cortical localization is significantly reduced in arm^{XP33} mutants (Fig. 4q,r,t,u).

These data are consistent with a model in which a complex of α-cat, Arm and APC2 helps to link cortical actin with astral microtubules (see Fig. 5i). Because not all nuclei detach from the cortex in *APC2* mutants, other mechanisms must compensate; multiple partially redundant mechanisms might tether spindles to the cortex, as in yeast (reviewed in ref. 20). In the absence of one tethering system, the others might be partially sufficient. In addition, neither *APC2* allele nor arm^{XP33} are protein null alleles, so residual APC2 or Arm function may explain the partial phenotype. Finally, the second fly APC (ref. 23) could be partially redundant.

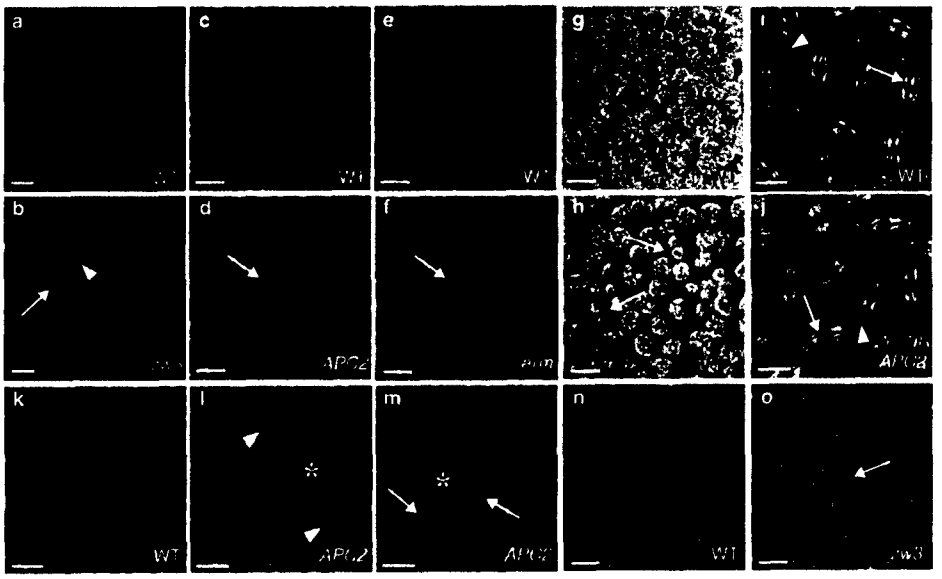

Figure 3 **Mutation of *zw3*, *APC2* or *arm* results in the loss of nuclei from the cortex in syncytial *Drosophila* embryos. a,b**, Cross-sectional views of syncytial embryos during mitosis stained to reveal nuclei (anti-phosphohistone; blue) and the cortex (anti-phosphotyrosine; green). **a**, In wild-type (WT) embryos, nuclei divide at and parallel to the cortex. Because nuclei divide at random angles to one another within the plane of the membrane, some nuclei divide perpendicular to the plane of section. **b**, In $zw3^{M1\text{-}1}$ mutants, nuclei detach (arrowhead) from the cortex and are observed in the interior cytoplasm (arrow). **c–f**, Surface views of syncytial embryos stained to reveal chromosomes (anti-phosphohistone; blue) and the cortex (anti-phosphotyrosine; green). **c,e**, Wild-type embryos (**c**, anaphase; **e**, prophase) in which pseudocleavage furrows separate dividing nuclei. **d,f**, Embryos carrying $APC2^{\Delta S}$ (**d**) or arm^{XP33} (**f**). Nuclear loss is revealed by small pseudocleavage furrows that do not contain nuclei (arrows). **g,h**, Embryos in interphase stained with phalloidin to visualize F-actin. **g**, In wild-type embryos, cortical actin rearranges into caps above each nucleus. **h**, In $APC2^{\Delta 40}$ embryos, actin caps appear generally normal, although they are reduced in size (arrows) where nuclei have been lost. **i,j**, Embryos in anaphase/telophase stained with anti-tubulin. The wild type (**i**) and $APC2^{\Delta S}$ mutants (**j**) have similar spindles (arrows) and astral microtubules (arrowheads). **k–m**, Embryos in metaphase stained to reveal spindles (anti-tubulin; red) and the actin cytoskeleton (phalloidin; green). **k**, Wild-type embryo. **l,m**, $APC2^{\Delta S}$ embryos. In regions of nuclear loss (asterisks), one sees spindles that are attached to the cortex at only one pole (arrowheads) or that are 'collapsed' in appearance (arrows). These might represent spindles in the process of detaching. Consistent with this, 'pseudo-cells' containing defective spindles are nearly normal in size. **n,o**, Metaphase embryos stained to reveal spindles (anti-tubulin; red) and centrosomes (anti-centrosomin; green). **n**, Wild-type embryos with centrosomes at the poles of each spindle. **o**, Embryo carrying $zw3^{M1\text{-}1}$. In areas of nuclear loss, free centrosomes remain at the cortex. Scale bars, 10 μm.

To examine the role of Zw3 kinase in this process, we examined APC2 and Arm localization in *zw3* mutants. We observed striking changes in both Arm and APC2 localization, suggesting that Zw3 regulates the association of APC2–Arm complexes with the cortex, microtubules or both. Whereas Arm continues to localize to pseudocleavage furrows, cortical APC2 is substantially reduced (Fig. 4d–f). Instead, APC2 and Arm both accumulate in membrane-associated and cytoplasmic puncta (Fig. 4d–f, arrows). Similar puncta are also seen in later *zw3* embryos (Fig. 5f). By contrast, α-cat remains cortical in *zw3* mutants and does not accumulate in APC2–Arm puncta (Fig. 4j–l).

The APC2–Arm puncta are reminiscent of puncta formed by APC in mammalian and *Xenopus* cells[9,11], which localize to microtubule plus ends. We thus examined whether APC2–Arm puncta associate with microtubules, focusing on polarized ectodermal epithelial cells after gastrulation, for ease of visualization. Most APC2 in both the wild type and *zw3* mutants is found in the apical 1 μm of the cell. In these epithelial cells, apical microtubules form a dense unoriented web (Fig. 5a,b, middle), as observed in other polarized epithelia[24]. In single confocal sections, most microtubules appear as dots in cross section or as short segments (Fig. 5b, middle, arrowheads).

In wild-type embryos, APC2 localizes to bright cortical puncta at the apical surface, in the region of the adherens junction and in the cytoplasm (Fig. 5a, red). Cortical APC2 puncta often localize with microtubule ends, as do cytoplasmic puncta (Fig. 5b, arrowheads). In *zw3* mutants, some APC2 puncta are found at the cortex, but cytoplasmic puncta are much more numerous than in the wild type (Fig. 5c, red). As in the wild type, many puncta localize with microtubules; most appear to localize to microtubule ends (Fig. 5d,e, arrowheads). Arm also localized to microtubule-associated puncta (data not shown). The mechanism by which APC2–Arm complexes associate with microtubules and the identities of hypothetical linker proteins that mediate this association (see Fig. 5i) remain to be elucidated.

We used an Arm–green-fluorescent-protein (Arm–GFP) fusion to examine the dynamic behaviour of puncta in *zw3* mutants. In wild-type embryos, Arm–GFP accumulates at pseudocleavage furrows and, in later stages, localizes to adherens junctions, as does endogenous Arm (not shown). In *zw3* mutants, Arm–GFP accumulates at adherens junctions and in puncta (Fig. 5g,h), like endogenous Arm (Fig. 5f). We examined Arm–GFP puncta in living *zw3* mutants during and after cellularization. Arm puncta are dynamic (Fig. 5h; see Supplementary Information). Some are tethered to the cortex, others move short distances in the cytoplasm and a subset move across the cell (Fig. 5h, arrowheads). Puncta colliding with the cortex are often captured by it.

These data suggest that Zw3 kinase regulates the localization of APC2–Arm complexes. Zw3 kinase phosphorylates both Arm and APC (reviewed in ref. 7). Zw3 could influence APC2–Arm localization by phosphorylating APC2; phosphorylation of human APC by Zw3's homologue, GSK-3β, reduces APC's ability to bind

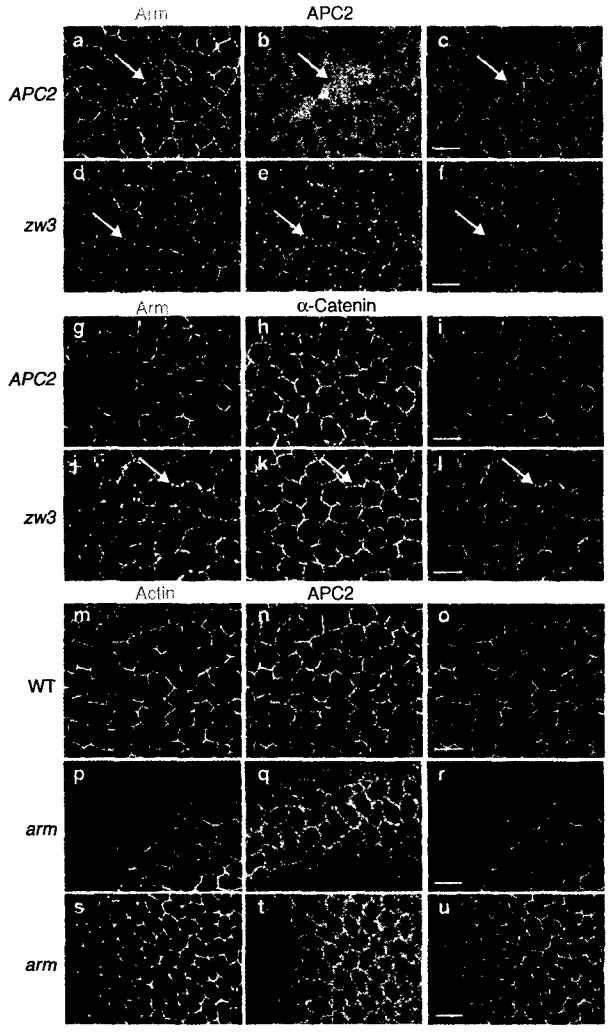

Figure 4 **Localization of APC2, Arm and α-catenin (α-cat) in *APC2*$^{\Delta S}$, *arm*^{XP33} and *zw3*$^{M1\text{-}1}$ mutants. a–f**, Embryos stained with anti-Arm (green) and anti-APC2 (red) antibodies. **a–c**, In *APC2*$^{\Delta S}$ mutants, APC2$^{\Delta S}$ protein (red) no longer localizes to the cortex during syncytial development but Arm localization is unaffected (**a**), even where nuclei are lost (arrows). **d–f**, In *zw3*$^{M1\text{-}1}$ mutants, APC2 (red) is nearly lost from the cortex and instead is found with Arm (green) in cytoplasmic and cortical puncta (arrow). A substantial amount of Arm remains at the cortex. **g–l**, Embryos stained with anti-Arm (green) and anti-α-cat (red) antibodies. **g–i**, Neither Arm nor α-cat localization is altered in *APC2*$^{\Delta S}$ mutants. **j–l**, In *zw3*$^{M1\text{-}1}$ mutants, Arm localizes to cytoplasmic and cortical puncta (arrows), whereas α-cat localization remains unchanged. **m–u**, Embryos stained with phalloidin to reveal F-actin (green) and with anti-APC2 antibody (red). **m–o**, In wild-type embryos, both actin and APC2 are tightly localized to pseudocleavage furrows. **p–u**, In *arm*^{XP33} mutants, tight localization of APC2 to the cortex is reduced or abolished. Scale bars (shown in merged images), 10 μm

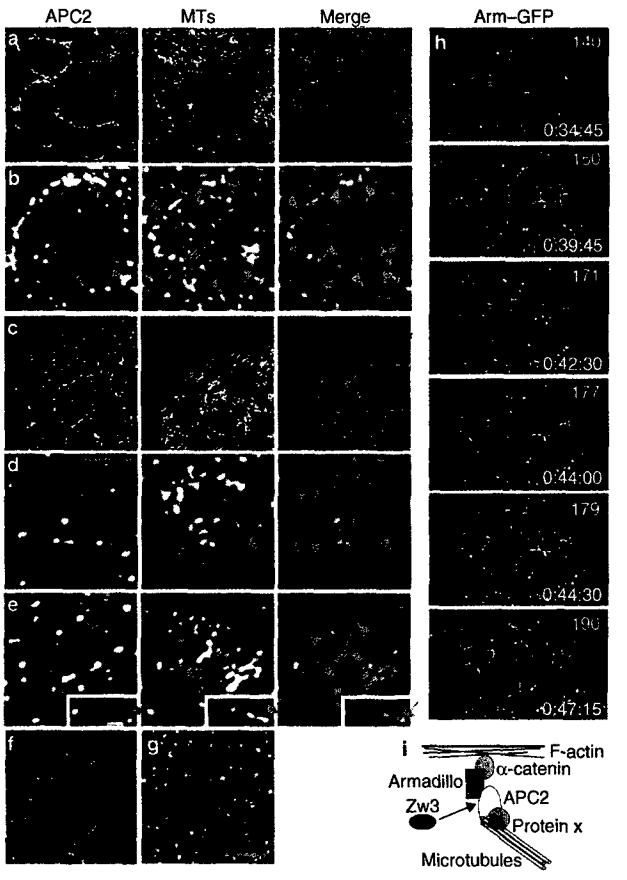

Figure 5 **APC2 puncta localize with microtubules (MTs). a–e**, Stage 9 embryos double-labelled with anti-APC2 (red) and anti-tubulin (green) antibodies. **a**, In wild-type embryos, APC2 localizes to the apical surface and the apical–lateral cortex near the adherens junctions (arrow). In this region, the microtubules form a dense, unoriented meshwork. **b**, Higher magnification image of wild-type embryo showing cortical and cytoplasmic APC2 puncta localizing with the ends of short microtubule segments (arrowheads). **c**, In *zw3*$^{M1\text{-}1}$ mutants, APC2 localizes to both cortically associated (arrow, left) and cytoplasmic (arrowhead, left) puncta. Microtubules form a dense web with only occasional long microtubules caught in a single plane of section (arrowheads, middle). **d,e**, Higher magnification images of a *zw3*$^{M1\text{-}1}$ mutant. Many APC2 puncta localize to the ends of short microtubule segments (arrowheads). Only occasional long microtubules are seen in single planes of section (arrow and inset), and these also localize to APC2 puncta. **f**, Arm (green) and APC2 (red) both localize to cortical and cytoplasmic puncta in stage 9 *zw3*$^{M1\text{-}1}$ mutants, as they do during syncytial stages. **g**, The Arm–green-fluorescent-protein fusion (Arm–GFP) is found in the puncta that accumulate in syncytial *zw3* mutants. **h**, Time-lapse series obtained from a stage 9 germ-band-extended *zw3*$^{M1\text{-}1}$ mutant paternally loaded with Arm–GFP. Blue arrowheads track a punctum that moves through the cytoplasm, is captured by the cortex and then appears to protrude into the neighbouring cell, pushing back the plasma membrane. Red arrowheads track a punctum that begins the series cortically attached and then moves into the cytoplasm. The numbers in the top right-hand corner of each frame correspond to movie frame numbers (see Supplementary Information) and numbers in the bottom right-hand corner the time elapsed in minutes. **i**, Hypothetical model of how APC2, Arm, and the α-cat might link microtubules to cortical actin. Scale bars, 5 μm (**a–e**), 10 μm (**f–h**).

microtubules *in vitro*[10]. Alternately, Zw3 might act on Arm; non-phosphorylatable β-catenin exhibits enhanced localization with mammalian APC (ref. 25). Zw3 might also regulate the association of APC2–Arm with α-cat, as suggested by the lack of α-cat in APC2–Arm puncta, disrupting anchoring to cortical actin. Finally, Zw3 could affect the microtubule cytoskeleton more directly. APC2–Arm–microtubule interactions, regulated by Zw3, could do more than just tether microtubules. For example, cortical APC2–Arm complexes could exert tension on spindles, which would be relaxed by releasing APC2–Arm from the cortex. Alternately, cortical microtubule tethering could allow cadherin–catenin complexes to influence microtubule dynamics[26,27]. These hypothetical roles can now be tested.

A recent study[28] suggests that the mechanism we propose for spindle attachment might also operate later in development. The disruption of adherens junctions in *Drosophila* epidermal cells led those cells to use spindle-orientation cues normally used only by neuroblasts. Blocking *APC2* or *EB1* function by double-stranded RNA interference had similar effects. This suggested that adherens junctions, acting via APC2 and EB1, influence spindle positioning[28].

Other recent work suggests a role for human APC in a different microtubule-anchoring event[29,30]. In mitotic cells, APC localizes to the kinetechore–microtubule junction, and mutations in *APC* affect the fidelity of chromosome segregation. APC could function at kinetechores in a manner analogous to that we suggest for spindle anchoring, joining microtubule plus ends to a cellular structure (in our case the actin cortex, in the other case the kinetechore). Although we did not observe high-frequency chromosome mis-segregation in *APC2* mutants, we cannot rule out a similar phenomenon in *Drosophila*. Together, these data suggest that APC family members might link the microtubule cytoskeleton to other cellular structures in many contexts. The details of these links, their regulation and their potential relevance to chromosome segregation and thus tumour progression must now be elucidated. □

Methods

Stocks and alleles.

The $zw3^{M1\,1}$, $zw3^{M27}$ and arm^{XP11} maternal and zygotic mutant embryos were generated as in ref. 31. $APC2^{\Delta 5}$ and $APC2^{q40}$ maternal and zygotic mutant embryos were derived from homozygous parents. Embryo collections were at 25 °C for *zw3*, arm^{XP11} and *y w* (wild type) and at 27 °C for $APC2^{\Delta 5}$ and $APC2^{q40}$. $APC2^{q40}$ was derived from a non-complementation screen for new maternal effect lethal mutations over $APC2^{\Delta 5}$ that will be described elsewhere. $APC2^{q40}$ and $APC2^{\Delta 5}$ have similar effects on embryonic pattern, resulting in most epidermal cells adopting posterior fates (data not shown). $APC2^{q40}$ results from the change of cysteine 677 to a stop codon, truncating the protein after the second 20 amino acid repeat. The lesion in $APC2^{\Delta 5}$ has been previously described[12].

Immunohistochemistry.

Fixation and staining of embryos was carried out as in ref. 12, with the following exceptions. Where specified, heat–methanol fixation was performed as in ref. 16. For anti-DE-cadherin labelling, embryos were fixed 1:1 in 4% formaldehyde in PEM:heptane (PEM contains 100 mM PIPES, 0.2 mM $MgSO_4$, 1 mM EGTA, 0.1% NP-40) for 1 h before blocking for 1 h in phosphate-buffered saline (PBS), 0.3% Triton X-100, 2% bovine serum albumin (BSA). Incubation in primary antibodies was overnight at 4 °C in PBS, 0.3% Triton X-100, 1% BSA. Antibodies and labels were: for DNA, anti-phosphohistone (1:500; Upstate Biotechnology); for actin, Alexa 488 phalloidin (1:1000; Molecular Probes) or anti-phosphotyrosine (1:1000; Upstate Biotechnology); for microtubules, anti-β-tubulin (1:1000; E7, Developmental Studies Hybridoma Bank (DSHB)); for centrosomes, anti-centrosomin (1:500; gift from E. Schejter); anti-APC2 (1:1000; ref. 12); anti-Armadillo (1:500; DSHB); anti-α-catenin (1:250) and anti-DE-cadherin (1:50; gifts from T. Uemura and M. Takeichi). Images in Figs 1–4 were generated with a Zeiss LSM 410 laser scanning microscope. The localization of APC2 and microtubules in Fig. 5 was done on a Perkin–Elmer Wallac Ultraview Spinning Disc Confocal Imaging System with a 0.2 μm step distance; data were deconvoluted using Deltavision software.

Time-lapse analysis.

Construction and characterization of the *Arm–GFP* transgene will be reported in detail elsewhere. For imaging, embryos derived from $zw3^{M1\,1}/ovo^{D}$; *Arm–GFP/+* × *FM7/Y*; *Arm–GFP* or $zw3^{M1\,1}/ovo^{D}$ × *y w/Y*; *Arm–GFP* parents were dechorionated and mounted in halocarbon oil (series 700, Halocarbon Products Corporation) between glass and a gas-permeable membrane (Petriperm, Sartorius Corporation). Images were captured using a Perkin-Elmer Wallac Ultraview Spinning Disc Confocal Imaging System and images analysed with NIH Image 1.62.

RECEIVED 13 FEBRUARY 2001; REVISED 29 MAY 2001; ACCEPTED 5 JULY 2001; PUBLISHED 2001.

1. Goode, B. L., Drubin, D. G. & Barnes, G. *Curr. Opin. Cell Biol.* **12**, 63–71 (2000).
2. Foe, V. E., Odell, G. M. & Edgar, B. A. in *The Development of Drosophila* Vol. I (eds Bate, M. & Martinez-Arias, A.) 149–300 (Cold Spring Harbor Press, Cold Spring Harbor, 1993).
3. Sullivan, W., Fogarty, P. & Theurkauf, W. *Development* **118**, 1245–1254 (1993).
4. Rothwell, W. F., Fogarty, P., Field, C. M. & Sullivan, W. *Development* **125**, 1295–1303 (1998).
5. Zhang, C. X., Lee, M. P., Chen, A. D., Brown, S. D. & Hsieh, T. *J. Cell Biol.* **134**, 923–934 (1996).
6. Stevenson, V. A., Kramer, J., Kuhn, J. & Theurkauf, W. E. *Nature Cell Biol.* **3**, 68–75 (2001).
7. Polakis, P. *Genes Dev.* **14**, 1837–1851 (2000).
8. McCartney, B. M. & Peifer, M. *Nature Cell Biol* **2**, E58–E60 (2000).
9. Nathke, I. S., Adams, C. L., Polakis, P., Sellin, J. H. & Nelson, W. J. *J. Cell Biol.* **134**, 165–180 (1996).
10. Zumbrunn, J., Kinoshita, K., Hyman, A. A. & Nathke, I. S. *Curr. Biol.* **11**, 44–49 (2001).
11. Mimori-Kiyosue, Y., Shiina, N. & Tsukita, S. *J. Cell Biol.* **148**, 505–518 (2000).
12. McCartney, B. M. *et al. J. Cell Biol.* **146**, 1303–1318 (1999).
13. Yu, X. & Bienz, M. *Mech. Dev.* **84**, 69–73 (1999).
14. Townsley, F. M. & Bienz, M. *Curr. Biol.* **10**, 1339–1348 (2000).
15. Reinacher-Schick, A. & Gumbiner, B. M. *J. Cell Biol.* **152**, 491–502 (2001).
16. Peifer, M. *J. Cell Sci.* **105**, 993–1000 (1993).
17. Yu, X., Waltzer, L. & Bienz, M. *Nature Cell Biol.* **1**, 144–151 (1999).
18. Siegfried, E., Chou, T.-B. & Perrimon, N. *Cell* **71**, 1167–1179 (1992).
19. Cox, R. T., Kirkpatrick, C. & Peifer, M. *J. Cell Biol.* **134**, 133–148 (1996).
20. Bloom, K. *Nature Cell Biol.* **2**, E96–E98 (2000).
21. Su, L.-K., Vogelstein, B. & Kinzler, K. W. *Science* **262**, 1734–1737 (1993).
22. Hulsken, J., Birchmeier, W. & Behrens, J. *J. Cell Biol.* **127**, 2061–2069 (1994).
23. Ahmed, Y., Hayashi, S., Levine, A. & Wieschaus, E. *Cell* **93**, 1171–1182 (1998).
24. Bacallao, R. *et al. J. Cell Biol.* **109**, 2817–2832 (1989).
25. Barth, A. I. M., Pollack, A. L., Altschuler, Y., Mostov, K. E. & Nelson, W. J. *J. Cell Biol.* **136**, 693–706 (1997).
26. Waterman-Storer, C. M., Salmon, W. C. & Salmon, E. D. *Mol. Biol. Cell* **11**, 2471–2483 (2000).
27. Chausovsky, A., Bershadsky, A. D. & Borisy, G. G. *Nature Cell Biol.* **2**, 797–804 (2000).
28. Lu, B., Roegiers, F., Jan, L. Y. & Jan, Y. N. *Nature* **409**, 522–525 (2001).
29. Kaplan, K. B. *et al. Nature Cell Biol.* **3**, 429–432 (2001).
30. Fodde, R. *et al. Nature Cell Biol.* **3**, 433–438 (2001).
31. Peifer, M., Sweeton, D., Casey, M. & Wieschaus, E. *Development* **120**, 369–380 (1994).

ACKNOWLEDGMENTS

We thank E. Schejter, T. Uemura, M. Takeichi, E. Siegfried and the Bloomington *Drosophila* Stock Center for fly stocks and antibodies, T. Salmon, K. Bloom and the three reviewers for helpful suggestions, and S. Whitfield for assistance with the figures. This work was supported by grants to M.P. from the Human Frontiers Science Program and the NIH (GM47857), and to A.B. from the NSF IBN97-34072. B.M. was supported by NIH NRSA 1F32CA79172, D.M. was supported by NIH NRSA 1F32GM19824, E.G. was supported by NIH 5T32CA71341, and M.P. was supported in part by a Career Development Award from the U.S. Army Breast Cancer Research Program.

Correspondence and requests for materials should be addressed to M.P.